monoclonal or affinity purified polyclonal antibody was incubated with 500 μg of cell lysate for 2 hours at 4°C, and then precipitated with protein G agarose for 1 hr at 4°C. Immunoprecipitates were extensively washed with PLC buffer, separated by SDS-PAGE, and immunoblotted. In some experiments, TrueBlot anti-rabbit IgG (eBioscience), which does not react to the denatured rabbit IgG, was used as the secondary antibody of the immunoblotting. For detection of MMP-8, rabbit polyclonal antibody was basically used in this study, however, almost the same results were obtained by using mouse monoclonal antibody.

RT-PCR

Total RNA was prepared from cultured cells by Isogen (Nippon Gene) according to the manufacturer's instructions and treated with DNase I. cDNA was synthesized from 2 μg of total RNA, and polymerase chain reactions (PCR) were performed in a 25 μl reaction volume at an annealing temperature of 55°C. The linear area of the PCR for each reaction was defined; 15 cycles for GAPDH and 25 cycles for MMP-8. Specific primers for MMP-8 and GAPDH have been described previously (Wahlgren et al., 2001; Woo et al., 2003); the expected PCR products were 352 bp and 300 bp, respectively. PCR products were subjected to electrophoresis on 2% agarose gels, and DNA was visualized by ethidium bromide staining.

Metabolic labeling

Cells cultured in 60 mm diameter dishes were preincubated in methionine-free DMEM (Sigma) for 1 hour, then cultured in 1.5 ml of methionine-free medium containing 0.15 mCi of [^{35}S]methionine (Amersham) for a further 4 hours. The cells were rinsed extensively and incubated in medium supplemented with EphB2-Fc or control Fc at 4 μg/ml for 2 hours. MMP-8 in the conditioned medium was purified by immunoprecipitation using an anti-MMP-8 polyclonal antibody and separated on SDS-PAGE. The gel was dried and subjected to autoradiography. The results were visualized with a Bio Imaging Analyzer (BAS1000; Fuji).

In vitro cleavage of ephrin-B1

Purified MMP-1 and MMP-8 were activated prior to use by treatment with 2 mM *p*-aminophenylmercuric acetate for 90 minutes at 37°C and dialyzed against 50 mM Tris-HCl (pH 7.5) containing 150 mM NaCl, 5 mM $CaCl_2$ and 50 μM $ZnCl_2$. Activated enzymes (10 nM, each) were incubated with ephrin-B1-Fc (2 μM) in 50 mM Tris-HCl (pH 7.5) containing 150 mM NaCl, 5 mM $CaCl_2$, 50 μM $ZnCl_2$ and 0.05% SDS at 37°C for 1 hour, separated by SDS-PAGE, and immunoblotted with anti-Fc of mouse IgG.

Arf1-GTP pull-down assay

To assess the amount of activated Arf1-GTP in cells, we performed a pull-down assay by using a GST-GGA3 construct (Dell's Angelica et al., 2000). Briefly, cells were left untreated or treated with EphB2-Fc (4 μg/ml) for 20 minutes. Cell lysates were prepared in lysis buffer [50 mM HEPES (pH 7.5), 150 mM NaCl, 10 mM $MgCl_2$, 10% glycerol, 100 mM NaF, 1 mM Na_3VO_4 and 1% Triton X-100], and then incubated with gluthathione-Sepharose beads containing a GST-GGA3 fusion protein for 45 minutes at 4°C. Precipitates were washed four times in the same buffer, and the precipitated Arf1 was detected by immunoblotting.

In vivo tumor invasion assay

The animal experimental protocols were approved by the Committee for Ethics of Animal Experimentation, and the experiments were conducted in accordance with the guidelines for Animal Experiments of the National Cancer Center. Peritoneal dissemination of tumors was tested by intraperitoneal injection of 1×10^7 PANC-1 cells suspended in 0.3 ml of RPMI1640 medium into 6-week-old BALB/c nude mice (CLEA Japan, Inc.). The mice were sacrificed 8 weeks after injection, and peritoneal dissemination was evaluated. To examine expression of Eph receptors in mesentery-derived cells, the mesenteric sheets were cut along the streak of arteries as described previously (Akedo et al., 1986). The cells were collected from dissected sheets by incubating at 37°C for about 20 minutes in 0.25% trypsin in PBS.

We thank D. B. Alexander (Department of Molecular Toxicology, Nagoya City University) for useful discussions and critical reading of this manuscript. We thank J. S. Bonifacino (National Institute of Child Health and Human Development, NIH) for donating Arf1 plasmids. This work was supported by the Program for the Promotion of Fundamental Studies in Health Science of the Organization for Pharmaceutical Safety and Research of Japan.

References

Akedo, H., Shinkai, K., Mukai, M., Mori, Y., Tateishi, R., Tanaka, K., Yamamoto, R. and Morishita, T. (1986). Interaction of rat ascites hepatoma cells with cultured mesothelial cell layers: a model for tumor invasion. *Cancer Res.* **46**, 2416-2422.

Amour, A., Knight, C. G., Webster, A., Slocombe, M., Stephens, P. E., Knauper, V., Docherty A. J. P. and Murphy, G. (2000). The in vitro activity of ADAM-10 is inhibited by TIMP-1 and TIMP-3. *FEBS Lett.* **473**, 275-279.

Batlle, E., Henderson, J. T., Beghtel, H., Van den Born, M., Sancho, E., Huls, G., Meeldijk, J., Robertson, J., Van de Wetering, M., Pawson, T. et al. (2002). Beta-catenin and TCF mediate cell positioning in the intestinal epithelium by controlling the expression of EphB/ephrinB. *Cell* **111**, 251-263.

Batlle, E., Bacani, J., Begthel, H., Jonkheer, S., Gregorieff, A., Van den Born, M., Malats, N., Sancho, E., Boon, E., Pawson, T. et al. (2005). EphB receptor activity suppresses colorectal cancer progression. *Nature* **435**, 1126-1130.

Blits-Huizinga, C., Nelersa, C., Malhotra, A. and Liebl, D. (2004). Ephrins and their receptors: binding versus biology. *IUBMB Life* **56**, 257-265.

Bong, Y. S., Park, Y. H., Lee, H. S., Mood, K., Ishimura, A. and Daar, I. O. (2004). Tyr-298 in ephrin-B1 is critical for an interaction with the Grb4 adaptor protein. *Biochem. J.* **377**, 499-507.

Brew, K., Dinakarpandian, D. and Nagase, H. (2000). Tissue inhibitors of metalloproteinases: evolution, structure and function. *Biochem. Biophys. Acta* **1477**, 267-283.

Castellvi, J., Garcia, A., De la Torre, J., Hernandez, J., Gil, A., Xercavins, J. and Cajal, S. R. (2006). EphrinB expression in epithelial ovarian neoplasms correlates with tumor differentiation and angiogenesis. *Hum. Pathol.* **37**, 883-889.

Chinni, S. R., Sivalogan, S., Dong, Z., Trindade Filho, J. C., Deng, X., Bonfil, R. D. and Cher, M. L. (2006). CXCL12/CXCR4 signaling activates Akt-1 and MMP-9 expression in prostate cancer cells: the role of Bone microenvironment-associated CXCL12. *Prostate* **66**, 32-48.

Cowan, C. A. and Henkemeyer, M. (2001). The SH2/SH3 adaptor Grb4 transduces B-ephrin reverse signals. *Nature* **413**, 174-179.

Dell'Angelica, E. C., Puertollano, R., Mullins, C., Aguilar, R. C., Vargas, J.D., Hartnell, L. M. and Bonifacino, J.S. (2000). GGAs: a family of ADP ribosylation factor-binding proteins related to adaptors and associated with the Golgi complex. *J. Cell Biol.* **149**, 81-93.

Donaldson, J. G. (2005). Arfs, phosphoinositides and membrane traffic. *Biochem. Soc. Trans.* **33**, 1276-1278.

Georgakopoulos, A., Litterst, C., Ghersi, E., Baki, L., Xu, C. J., Serban, G. and Robakis, N. K. (2006). Metalloproteinase/Presenilin1 processing of ephrinB regulates EphB-induced Src phosphorylation and signaling. *EMBO J.* **25**, 1242-1252.

Hashimoto, G., Aoki, T., Nakamura, H., Tanzawa, K. and Okada, Y. (2001). Inhibition of ADAMTS4 (aggrecanase-1) by tissue inhibitors of metalloproteinases (TIMP-1, 2, 3 and 4). *FEBS Lett.* **494**, 192-195.

Hattori, M., Osterfield, M. and Flanagan, J. G. (2000). Regulated cleavage of a contact-mediated axon repellent. *Science* **289**, 1360-1365.

Holmberg, J., Genander, M., Halford, M. M., Anneren, C., Sondell, M., Chumley, M. J., Silvany, R. E., Henkemeyer, M. and Frisen, J. (2006). EphB receptors coordinate migration and proliferation in the intestinal stem cell niche. *Cell* **125**, 1151-1263.

Huynh-Do, U., Vindis, C., Liu, H., Cerretti, D. P., McGrew, J. T., Enriquez, M., Chen, J. and Daniel, T. O. (2002). Ephrin-B1 transduces signals to active integrin-mediated migration, attachment and angiogenesis. *J. Cell Sci.* **115**, 3073-3081.

Janes, P. W., Saha, N., Barton, W. A., Kolev, M. V., Wimmer-Kleikamp, S. H., Nievergall, E., Blobel, C. P., Himanen, J. P., Lackmann, M. and Nikolov, D. B. (2005). Adam meets Eph: an ADAM substrate recognition module acts as a molecular switch for ephrin cleavage in trans. *Cell* **123**, 291-304.

Kataoka, H., Tanaka, M., Kanamori, M., Yoshii, S., Ihara, M., Wang, Y. J., Song, J. P., Li, Z. Y., Arai, H., Otuki, Y.et al. (2002). Expression profile of EFNB1, EFNB2, two ligands of EPHB2 in human gastric cancer. *J. Cancer Res. Clin. Oncol.* **128**, 343-348.

Kawano, K., Iwamura, T., Yamarari, H., Seo, Y., Suganuma, T. and Chijiiwa, K. (2004). Establishment and characterization of a novel human pancreatic cancer cell line (SUIT-4) metastasizing to lymph nodes and lungs in nude mice. *Oncology* **66**, 458-467.

Klein, R. (2004). Eph/ephrin signaling in morphogenesis, neural development and plasticity. *Curr. Opin. Cell Biol.* **16**, 580-589.

Lee, H. S., Bong, Y. S., Moore, K. B., Soria, K., Moody, S. A. and Daar, I. O. (2005). Dishevelled mediates ephrinB1 signalling in the eye field through the planar cell polarity pathway. *Nat. Cell Biol.* **8**, 55-63.

Lin, D., Gish, G. D., Songyang, Z. and Powson, T. (1999). The carboxyl terminus of B class ephrins constitutes a PDZ domain binding motif. *J. Biol. Chem.* **274**, 3726-3733.

Lint, P. V. and Libert, C. (2006). Matrix metalloproteinase-8: cleavage can be decisive. *Cytokine Growth Factor Rev.* **17**, 217-223.

Marston, D. J., Dickinson, S. and Nobes, C. D. (2003). Rac-dependent trans-endocytosis of ephrinBs regulates Eph-ephrin contact repulsion. *Nat. Cell Biol.* **5**, 879-888.

Meyer, S., Hafner, C., Guba, M., Flegel, S., Geissler, E. K., Becker, B., Koehl, G., Orso, E., Landthaler, M. and Vogt, T. (2005). Ephrin-B2 overexpression enhances integrin-mediated ECM-attachment and migration of B16 melanoma cells. *Int. J. Oncol.* **27**, 1197-1206.

Murai, K. K. and Pasquale, E. B. (2003). Ephective signaling: forward, reverse and crosstalk. *J. Cell Sci.* **116**, 2823-2832.

Nakada, M., Drake, K. L., Nakada, S., Niska, J. A. and Berens, M. E. (2006). Ephrin-B3 ligand promotes glioma invasion through activation of Rac1. *Cancer Res.* **66**, 8492-8500.

Niu, T. K., Pfeifer, A. C., Lippincott-Schwartz, J. and Jackson, C. L. (2005). Dynamics of GBF1, a Brefeldin A-sensitive Arf1 exchange factor at the Golgi. *Mol. Biol. Cell* **16**, 1213-1222.

Parker, M., Roberts, R., Enriquez, M., Zhao, X., Takahashi, T., Pat, C., Daniel, T. and Chen, J. (2004). Reverse endocytosis of transmembrane ephrin-B ligands via a clathrin-mediated pathway. *Biochem. Biophys. Res. Commun.* **323**, 17-23.

Pascall, J. C. and Brown, K. D. (2004). Intramembrane cleavage of ephrinB3 by the human rhomboid family protease, RHBDL2. *Biochem. Biophys. Res. Commun* **317**, 244-252.

Poliakov, A., Cotrina, M. and Wilkinson, D. G. (2004). Diverse roles of Eph receptors and ephrins in the regulation of cell migration and tissue assembly. *Dev. Cell* **7**, 465-480.

Raymond, I., Eck, S., Mollmark, J., Hays, E., Tomek, I., Kantor, S., Elliott, S. and Vincenti, M. (2006). Interleukin-1 beta induction of matrix metalloproteinase-1 transcription in chondrocytes requires ERK-dependent activation of CCAAT enhancer-binding protein-beta. *J. Cell. Physiol.* **207**, 683-688.

Reuben, P. M. and Cheung, H. S. (2006). Regulation of matrix metalloproteinase (MMP) gene expression by protein kinases. *Front. Biosci.* **11**, 1199-1215.

Sasaki, K., Sato, K., Akiyama, Y., Yanagihara, K., Oka, M. and Yamaguchi, K. (2002). Peptidomics-based approach reveals the secretion of the 29-residue COOH-terminal fragment of the putative tumor suppressor protein DMBT1 from pancreatic adenocarcinoma cell lines. *Cancer Res.* **62**, 4894-4898.

Sawicki, G., Leon, H., Sawicka, J., Sariahmetoglu, M., Schulze, C. J., Scott, P. G., Szczesna-Cordary, D. and Schulz, R. (2005). Degradation of myosin light chain in isolated rat hearts subjected to ischemia-reperfusion injury. *Circulation* **112**, 544-552.

Siller-Lopez, F., Garcia-Banuelos, J., Hasty, K. A., Segura, J., Ramos-Marquez, M., Qoronfleh, M. W., Aguilar-Cordova, E. and Armendariz-Borunda, J. (2000). Truncated active matrix metalloproteinase-8 gene expression in HepG2 cells is active against native type I collagen. *J. Hepatol.* **33**, 758-763.

Stadlemann, S., Pollheimer, J., Moser, P. L., Raggi, A., Amberger, A., Margreiter, R., Offner, F. A., Mikuz, G., Dirnhofer, S. and Moch, H. (2003). Cytokine-regulated expression of collagenase-2 (MMP-8) is involved in the progression of ovarian cancer. *Eur. J. Cancer* **39**, 2499-2505.

Sternlicht, M. D. and Werb, Z. (2001). How matrix metalloproteinases regulate cell behavior. *Annu. Rev. Cell Dev. Biol.* **17**, 463-516.

Tamaki, H. and Yamashina, S. (2002). The stack of the Golgi apparatus. *Arch. Histol. Cytol.* **65**, 209-218.

Tanaka, M., Kamo, T., Ota, S. and Sugimura, H. (2003). Association of dishevelled with Eph tyrosine kinase receptor and ephrin mediates cell repulsion. *EMBO J.* **22**, 847-858.

Tanaka, M., Ohashi, R., Nakamura, R., Shinmura, K., Kamo, T., Sakai, R. and Sugimura, H. (2004). Tiam1 mediates neurite outgrowth induced by ephrin-B1 and EphA2. *EMBO J.* **23**, 1075-1088.

Tanaka, M., Kamata, R. and Sakai, R. (2005). Phosphorylation of ephrin-B1 via the interaction with claudin following cell-cell contact formation. *EMBO J.* **24**, 3700-3711.

Tomita, T., Tanaka, S., Morohashi, Y. and Iwatsubo, T. (2006). Presenilin-dependent intramembrane cleavage of ephrin-B1. *Mol. Neurodegener.* **1**, 2.

Varelias, A., Koblar, S. A., Cowled, P. A., Carter, C. D. and Clayer, M. (2002). Human osteosarcoma express specific ephrin profiles: implications for tumorigenicity and prognosis. *Cancer* **95**, 862-869.

Wahlgren, J., Maisi, P., Sorsa, T., Sutinen, M., Tervahartiala, T., Pirila, E., Teronen, O., Hietanen, J., Tjaderhane, L. and Salo, T. (2001). Expression and induction of collagenases (MMP-8 and -13) in plasma cells and associated with bone-destructive lesions. *J. Pathol.* **194**, 217-224.

Woo, J. H., Park, J. W., Lee, S. H., Kim, Y. H., Lee, I. K., Gabrielson, E., Lee, S. H., Lee, H. J., Kho, Y. H. and Won, T. K. (2003). Dykellic acid inhibits phorbol myristate acetate-induced matrix metalloproteinase-9 expression by inhibiting nuclear factor kappa B transcriptional activity. *Cancer Res.* **63**, 3430-3434.

Yu, W. H., Woessner, J. F., McNeish, J. D. and Stamenkovic, I. (2007). CD44 anchors the assembly of matrilysin/MMP-7 with heparin-binding epidermal growth factor precursor and ErbB4 and regulates female reproductive organ remodeling. *Genes Dev.* **16**, 307-323.

Zeeh, J. C., Zeghouf, M., Grauffel, C., Guilbert, B., Martin, E., Dejaegere, A. and Cherfils, J. (2006). Dual specificity of the interfacial inhibitor Brefeldin A for Arf proteins and Sec7 domains. *J. Biol. Chem.* **281**, 11805-11814.

Zimmer, M., Palmer, A., Kohler, J. and Klein, R. (2003). EphB-ephrinB bi-directional endocytosis terminates adhesion allowing contact mediated repulsion. *Nat. Cell Biol.* **5**, 869-878.

Journal of Cell Science

The American Journal of Pathology, Vol. 171, No. 1, July 2007
Copyright © American Society for Investigative Pathology
DOI: 10.2353/ajpath.2007.070033

Growth Factors, Cytokines, Cell Cycle Molecules

Phosphorylation of Ephrin-B1 Regulates Dissemination of Gastric Scirrhous Carcinoma

Masamitsu Tanaka,* Reiko Kamata,* Misato Takigahira,† Kazuyoshi Yanagihara,† and Ryuichi Sakai*

From the Growth Factor Division, Central Animal Laboratory,† National Cancer Center Research Institute, Tokyo, Japan*

Interaction of the Eph family of receptor protein tyrosine kinase and its ligand ephrin family induces bidirectional signaling via cell-cell contacts. High expression of B-type ephrin is frequently found in various cancer cells, and their expression levels are associated with high invasion of tumors and poor prognosis. However, whether ephrin-B1 actually promotes invasion of cancer cells *in vivo* has not been shown. We investigated the involvement of ephrin-B1 in regulating the invasiveness of scirrhous gastric cancer, which is a diffusely infiltrative carcinoma with high invasion potential. Reduction of ephrin-B1 expression by short interfering RNA or overexpression of phosphorylation-defective mutant suppressed migration and invasion of scirrhous gastric cancer cells *in vitro* without affecting tumor cell proliferation and apoptosis. Blocking of tyrosine phosphorylation of ephrin-B1 attenuates not only dissemination of cancer cells injected intraperitoneally but also local invasion and dissemination of orthotopically implanted cancer cells in the gastric wall of nude mice. Furthermore, blocking of ephrin-B1 phosphorylation attenuated the activation of Rac1 GTPase in these invasive gastric cancer cells. Our results suggest that tyrosine phosphorylation of ephrin-B1 promotes invasion of cancer cells *in vivo* and is a potential therapeutic target in some types of gastrointestinal cancers. (Am J Pathol 2007, 171:68–78; DOI: 10.2353/ajpath.2007.070033)

Members of the Eph receptor family can be classified into two groups based on their sequence similarity and their preferential binding to the subset of ligands tethered to the cell surface either by a glycosylphosphatidyl inositol-anchor (ephrin-A) or a transmembrane domain (ephrin-B).[1–3] Interaction of the EphB family of receptor protein tyrosine kinases and its ligand ephrin-B family induces bidirectional signaling via cell-cell contacts.

The biological functions of Ephs and ephrins in epithelial cells and tumors have recently been highlighted.[4–9] For example, EphB receptors and ephrin-B ligands are expressed in normal intestinal epithelium, which contributes for the restriction of cell migration and positioning along the crypt-villus axis.[4] Overexpression of B-type ephrin in cancer cells correlates with poor prognosis characterized by high invasion and high vascularity of the tumors.[10–15] Expression of ephrin-B2 has been reported in invasive tumor cells and is often highly expressed in the peripheral region of the tumors especially at the front of the invasion.[11] Ephrin-B1 is frequently overexpressed in gastrointestinal tumors, especially in poorly differentiated invasive tumor cells.[15] Although an accumulating number of reports have suggested that expression of B-type ephrin is closely associated with tumor cell invasion, whether ephrin-B modifies tumor invasion *in vivo* has not been well established.

Ephrin-Bs are tyrosine phosphorylated via Src family kinases in response to the interaction with EphB receptors, which serves as a docking site for Src homology 2 domain of adaptor protein Grb4, and transduce intracellular signaling.[16,17] We have also demonstrated that ephrin-B1 is phosphorylated independently of Eph receptors through association with an intercellular adhesion molecule, which leads to attenuation of cell-cell adhesion.[7] In our recent observations, signaling mediated by ephrin-B1 promoted the process of intracellular transport and secretion of matrix metalloproteinase (M. Tanaka, K. Sasaki, R. Kamata, and R. Sakai, unpublished data), which led us to examine in this study whether disruption of ephrin-B1-mediated signaling, especially through the tyrosine phosphorylation of ephrin-B1, could suppress tumor cell invasion.

Supported by the Program for the Promotion of Fundamental Studies in Health Science of the Organization for Pharmaceutical Safety and Research of Japan.

Accepted for publication April 10, 2007.

Supplemental material for this article can be found on *http://ajp.amjpathol.org*.

Address reprint requests to Ryuichi Sakai, Growth Factor Division, Central Animal Laboratory, National Cancer Center Research Institute, 5-1-1 Tsukiji, Chuo-ku, Tokyo 104-0045. E-mail: rsakai@gan2.res.ncc.go.jp.

Scirrhous gastric carcinoma diffusely infiltrates a broad region of the stomach and frequently associates with metastasis to lymph nodes and peritoneal dissemination and, therefore, has the worst prognosis among various types of gastric cancers. We previously established two cell lines of human gastric scirrhous carcinoma possessing high infiltrative potential by repeating cycles of orthotopic transplantation in nude mice and collecting cancer cells from the ascitic fluid formed as a result of cancerous peritonitis.[18,19] In this study, we show that reduction of ephrin-B1 expression or blocking of tyrosine phosphorylation of ephrin-B1 inhibits tumor invasion of these highly invasive gastric cancer cells. Our results suggest that ephrin-B1 represents a rational therapeutic target and that suppression of its phosphorylation is a strategy for modulating the invasion of some types of cancers.

Materials and Methods

Plasmids, Antibodies, and Reagents

Plasmids encoding full-length cDNAs of human ephrin-B1 and ephrin-B1 with mutations of four tyrosine residues in the cytoplasmic domain (Y313, 317, 324, and 329) ephrin-B1 4YF have already been described.[7] To generate the recombinant retrovirus, cDNAs were subcloned into the vector pDON-AI (Takara, Kyoto, Japan). The rabbit polyclonal antibodies for ephrin-B1 (C18) and α-tubulin were purchased from Santa Cruz Biotechnology, Inc. (Santa Cruz, CA). Polyclonal antibody against tyrosine-phosphorylated ephrin-B1 (ephrin-B1 pY317, amino acids 314 to 321, which is identical to corresponding region of ephrin-B2, 301 to 308, and ephrin-B3, 308 to 315) was raised in rabbits and affinity-purified as described previously.[7] The monoclonal antibodies for phosphotyrosine (4G10) and Rac1 were from Upstate Biotechnology (Lake Placid, NY). The polyclonal antibodies for EphB2 and EphB4 were from R&D Systems (Minneapolis, MN). Fibronectin (bovine), collagen type I, and Matrigel basement membrane matrices were purchased from Sigma (St. Louis, MO), Nitta Gelatin, Inc. (Osaka, Japan), and BD Biosciences (San Jose, CA), respectively.

Cell Culture and Transfection

Gastric carcinoma cell lines were cultured in RPMI 1640 medium supplemented with 10% fetal bovine serum. Mouse fibroblast L cells were cultured in Dulbecco's modified Eagle's medium with 10% fetal bovine serum. L cells stably expressing EphB2 (L EphB2) were established through transfection of a plasmid encoding human ephrin-B1 in parent L cells, which do not express cognate receptors for ephrin-B1 as previously described,[7] and selection in medium containing hygromycin B at a concentration of 400 μg/ml. Recombinant retroviral plasmid pDON-AI was cotransfected with pCL-10A1 retrovirus packaging vector (Imgenex, San Diego, CA) into 293gp cells to allow the production of retroviral particles. Gastric cancer cells stably expressing ephrin-B1 4YF were established by infecting cancer cells with retroviruses and selected in the medium containing G418 at a concentration of 500 μg/ml for 3 weeks. The mixture of selected cells was used for the experiments.

In Vitro *Short Interfering RNA (siRNA) Treatment*

Two sets of Stealth siRNAs of ephrin-B1 were synthesized as follows (Invitrogen, Carlsbad, CA): ephrin-B1 sense 1, 5′-UAAGGGAAUGAUGAUGUCGCUGGGC-3′; ephrin-B1 antisense 1, 5′-GCCCAGCGACAUCAUCAUUCCCUUA-3′; ephrin-B1 sense 2, UAGUCCGUAAGGGAAUGAUGAUGUC-3′; and ephrin-B1 antisense 2, GACAUCAUCAUUCCCUUACGGACUA-3′. The control siRNA (scramble II duplex, 5′-GCGCGCUUUGUAGGAUUCGdTdT-3′) was purchased from Dharmacon (Lafayette, CO). siRNAs were incorporated into cells using Lipofectamine2000 according to the manufacturer's instructions (Invitrogen). Assays were performed 72 hours after treatment.

Immunoprecipitation

Cell lysates were prepared with protease inhibitors in PLC buffer [50 mmol/L 4-(2-hydroxyethyl)-1-piperazineethanesulfonic acid, pH 7.5, 150 mmol/L NaCl, 1.5 mmol/L $MgCl_2$, 1 mmol/L ethylene glycol bis(β-aminoethyl ether)-*N,N,N′,N′*-tetraacetic acid, 10% glycerol, 100 mmol/L NaF, 1 mmol/L Na_3VO_4, and 1% Triton X-100]. To precipitate the proteins, 1 μg of affinity-purified polyclonal antibody was incubated with 500 μg of cell lysate for 2 hours at 4°C and then precipitated with protein G agarose for 1 hour at 4°C. Immunoprecipitates were extensively washed with PLC buffer, separated by sodium dodecyl sulfate-polyacrylamide gel electrophoresis, and immunoblotted.

Affinity Precipitation

Affinity precipitation with GST-PBD (p21-binding domain of p21-activated kinase 1) was performed as described previously.[20] In brief, cells were lysed in the lysis buffer [50 mmol/L 4-(2-hydroxyethyl)-1-piperazineethanesulfonic acid, pH 7.5, 150 mmol/L NaCl, 10 mmol/L $MgCl_2$, 1 mmol/L ethylene glycol bis(β-aminoethyl ether)-*N,N,N′,N′*-tetraacetic acid, 10% glycerol, 100 mmol/L NaF, 1 mmol/L Na_3VO_4, and 1% Triton X-100] and incubated with GST-PBD on Sepharose for 1 hour at 4°C. Precipitants were washed three times in the same buffer, and endogenous Rac1 was detected by immunoblotting with anti-Rac1 antibody.

5-Bromo-2′-Deoxyuridine Incorporation

Cell proliferation was assessed by measurement of 5-bromo-2′-deoxyuridine (BrdU) incorporation into the DNA with Cell Proliferation enzyme-linked immunosorbent assay, BrdU (colorimetric) kit (Roche, Basel, Switzerland). In brief, gastric cancer cells were plated onto 96-well plates (1×10^4 cells/well) 48 hours after treatment of siRNAs and further incubated for 24 hours before the addition of BrdU. Cells were reincubated for 6 hours,

and incorporated BrdU was detected with peroxidase-labeled anti-BrdU antibody and developed with tetramethyl-benzidine as a chromogenic substrate according to the manufacturer's instructions (Roche). The absorbance of the samples was measured at the wavelength of 450 nm using a microplate reader (model 550; Bio-Rad, Hercules, CA).

Apoptosis Assays

Gastric cancer cells were plated in triplicate onto 96-well plates (1×10^4 cells) 48 hours after treatment of siRNAs and incubated for 24 hours. Cells were lysed to detect apoptosis by measurement of nucleosomes in the cytoplasm of apoptotic cells using a Cell Death enzyme-linked immunosorbent assay kit according to the manufacturer's instructions (Roche Molecular Biochemicals). In brief, nucleosomes in cell lysates were detected with peroxidase-labeled anti-DNA antibody and developed with 2,2'-azino-di[3-ethylbenzthiazolin-sulfonate] as a chromogenic substrate. The absorbance of the samples was measured at the wavelength of 405 nm using a microplate reader (model 550; Bio-Rad).

Cell Attachment Assay

Cancer cells were detached by phosphate-buffered saline(−) [PBS$^{(-)}$] containing ethylenediamine tetraacetic acid (2 mmol/L) and replated on the chamber slides coated with either collagen type I (100 μg/ml; Nitta Gelatin, Inc.), fibronectin (50 μg/ml; Sigma), or Matrigel (85 μg/ml; Asahi Techno Glass Co., Tokyo, Japan). After incubation for 30 minutes, unattached cells were removed by washing the slides in PBS$^{(-)}$ several times, and the remaining cells were stained with Giemsa's solution. The number of attached cells on each substrate was counted.

Cell Staining

Cells were fixed for 5 minutes at room temperature with 4% paraformaldehyde in PBS and permeabilized for 10 minutes with 0.2% Triton X-100. The cells were preincubated in 2% bovine serum albumin for 0.5 hour and incubated with Alexa546-conjugated phalloidin (Molecular Probes, Eugene, OR) for 1 hour at room temperature. Photos were taken with a Radiance 2100 confocal microscope (Bio-Rad).

Overlay Tumor Invasion Assay

Invasion of tumor cells into the monolayer of stromal cells was monitored basically as described previously.[20] Gastric cancer cells treated with ephrin-B1 siRNA or control siRNA were labeled with 2 mmol/L lipophilic tracer DiO (Molecular Probes) and then detached with Hanks' balanced salt solution$^-$ containing 2 mmol/L ethylenediamine tetraacetic acid and seeded on the confluent monolayer of parent L cells or L EphB2 cells. After being cultured in the medium with 10% fetal bovine serum for 15 hours, the cells were fixed with 4% paraformaldehyde in PBS, and the number of invasion foci of cancer cells was counted using fluorescence microscopy.

In Vivo *Tumor Cell Invasion Assay*

The animal experimental protocols were approved by the Committee for Ethics of Animal Experimentation, and the experiments were conducted in accordance with the guidelines for Animal Experiments in the National Cancer Center. Peritoneal dissemination of tumors was examined by intraperitoneal injection of 5×10^6 gastric cancer cells suspended in 0.3 ml of RPMI 1640 medium into 6-week-old BALB/c nude mice (CLEA Japan, Inc., Tokyo, Japan). The mice were sacrificed 2 weeks after injection, and peritoneal dissemination was evaluated. Orthotopic implantation of gastric cancer cells into BALB/c nude mice has been described previously.[18,19] In brief, 1×10^6 cells were inoculated into the middle wall of the greater curvature of the glandular stomach by using a 30-gauge needle. The mice were sacrificed at different time points after the orthotopic transplantation of the cancer cells and subjected to macroscopic and histopathological examination of the tumors.

Results

Reduction of Ephrin-B1 Expression Attenuates Tumor Invasion of Gastric Cancer Cells

To examine the involvement of ephrin-B1 for invasion of tumors, we analyzed cell lines of scirrhous gastric carcinoma, which is characterized as reduced cell-cell adhesion with high invasion potential. HSC-44PE and HSC-58 were originally established from the patients of scirrhous gastric carcinoma, and highly invasive sublines were further selected from these parent cells (44As3 from HSC-44PE; 58As1 and 58As9 from HSC-58[18,19]). Both expression and phosphorylation levels of ephrin-B1 were higher in cells of invasive sublines than in corresponding parent cell lines, whereas the expression level of control α-tubulin was not altered in these cell lines (Figure 1a). In addition, EphB2 was expressed in all of these cell lines, and HSC-44PE and 44As3 cells also expressed EphB4, showing the existence of cognate receptors (Figure 1a).

We next examined whether reduction of ephrin-B1 expression affects cell motility and proliferation of these gastric cancer cells. The treatment of cells with two independent siRNA of ephrin-B1 effectively reduced ephrin-B1 expression level in 58As9 cells and 44As3 cells (Figure 1b). In addition, phosphorylation of B class ephrin was greatly reduced by knocking down ephrin-B1, as judged by the antibody recognizing phosphorylation of all three members of ephrin-Bs at the tyrosine in the cytoplasmic region (Figure 1b). From the analysis of *in vitro* Transwell assay, reducing the amount of ephrin-B1 in 44As3 cells inhibited migration and invasion through the extracellular matrix (Figure 2a). Similar results were also observed in 58As9 cells (Figure 2a). On the other

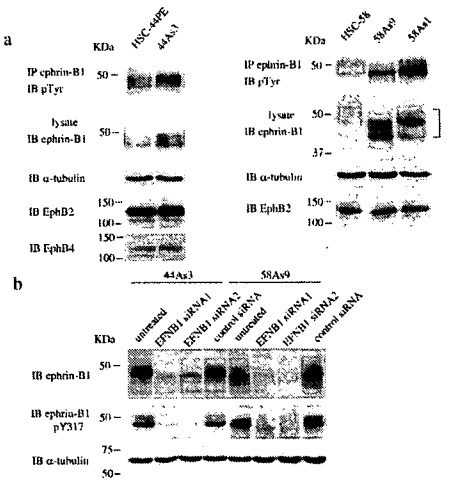

Figure 1. Tyrosine phosphorylation of ephrin-B1 is higher in invasive gastric cancer cell lines. **a:** As indicated, lysates from cells were subjected to immunoprecipitation (IP) with anti-ephrin-B1 antibody and immunoblotting (IB) with anti-phosphotyrosine antibody. The expression levels of ephrin-B1, α-tubulin, EphB2, and EphB4 in each cell lysate were confirmed by immunoblotting (bottom). When cell lysates were blotted with ephrin-B1 antibody, several ephrin-B1-reactive bands (blanket) were detected because of the glycosylation and difference in tyrosine phosphorylation as reported.[31] **b:** Cellular levels of ephrin-B1 were analyzed 72 hours after treatment with siRNAs by Western blotting using α-tubulin as a loading control. Expression of ephrin-B1 was reduced in cells treated with ephrin-B1 siRNA (EFNB1siRNA1, 2). The phosphorylation level of ephrin-Bs was assessed by the antibody recognizing phosphorylation of Tyr317 of ephrin-B1, which also detects phosphorylation of corresponding tyrosine of ephrin-B2 (Tyr304) and ephrin-B3 (Tyr311) as described in Materials and Methods.

hand, proliferation and apoptosis of these cells were not significantly affected (Figure 2b). In addition, reduction of ephrin-B1 expression did not cause remarkable change in the adhesion of 44As3 and 58As9 cells on different extracellular matrices, including type I collagen, fibronectin, and Matrigel (Figure 2c). We further examined whether overexpression of ephrin-B1 is sufficient to promote the migration and invasion of cancer cells by stably expressing ephrin-B1 in one parental cell line HSC-58. The migration and invasion through extracellular matrix was apparently increased by the overexpression of ephrin-B1 (Figure 2d).

Phosphorylation of Ephrin-B1 Promotes Migration and Invasion of Gastric Cancer Cells

Because the level of tyrosine phosphorylation of ephrin-B1 was higher in invasive sublines of gastric cancer cells, we next examined whether blocking of ephrin-B1 phosphorylation in these cells attenuates their migration and invasion. The stable expression of ephrin-B1 with mutations of four tyrosine residues in the cytoplasmic domain (Y313, 317, 324, and 329) ephrin-B1 4YF reduced the tyrosine phosphorylation level of ephrin-B1 in 44As3 and 58As9 cells, because overexpression of ephrin-B1 4YF prevents endogenous ephrin-B1 from association with EphB receptors expressed in these cells (Figure 3a). From the analysis of *in vitro* Transwell assay, migration and invasion of cancer cells stably expressing ephrin-B1 4YF mutant (44As3 4YF and 58As9 4YF cells) were decreased compared with the control cells expressing mock vector (44As3 mock and 58As9 mock cells) (Figure 3b). On the other hand, expression of ephrin-B1 4YF did not affect cell proliferation under usual two-dimensional cell culture condition (Figure 3c). When these cancer cells expressing mock vector or ephrin-B1 4YF were implanted subcutaneously in nude mice, the mean size and weight of the tumors were not significantly different (Figure 3d). To understand the mechanism by which ephrin-B1 4YF attenuates the cell migration, we examined activity of Rac1 GTPase, which is a critical molecule controlling the organization of actin cytoskeleton. The activation of Rac1 was examined by affinity precipitation of GTP-bound Rac1 with the GST-fusion protein of the p21-binding domain of p21-activated kinase 1.[21] The activated Rac1 was apparently reduced in 44As3 or 58s9 cells expressing ephrin-B1 4YF compared with the cells expressing mock vector (Figure 3e). When the appearance of cytoskeleton of these cancer cells was examined, formation of large lamellipodia was observed in most of the mock-containing 44As3 and 58As9 cells, whereas it was less frequently observed in 44As3 4YF and 58As9 4YF cells (Figure 3f), which may be consistent with the reduced Rac1 activity in cancer cells expressing ephrin-B1 4YF.

Gastric scirrhous carcinoma frequently associates with peritoneal dissemination through the process that cancer cells perforate gastric serosa and become exfoliated and free and then attached on the surface of the peritoneum and start to invade there. The effect of ephrin-B1 expression on tumor invasion was further monitored *in vitro* by overlay tumor cell invasion assay as a model system for stromal invasion of cancer cells. When 44As3 cells were plated onto the monolayer of fibroblasts, L cells, the formation of tumor cell islands was observed as tumor cells invaded and grew between the fibroblasts (Figure 4a). The formation of such tumor islands is the sign of penetration of tumor cells into the sheet of stromal cells, as used for the evaluation of cancer cell invasion through endothelial cells or mesothelial cells.[20,22,23] The invasion of 44As3 cells into the fibroblasts monolayer was more evident when the cancer cells were plated onto L cells stably expressing EphB2 (L EphB2) than on the parent L cells, which do not express receptors for ephrin-B1[7] (Figure 4b). The invasion foci of 44As3 in monolayer of L EphB2 cells were decreased in number and size when expression of ephrin-B1 in cancer cells was reduced (Figure 4a). In addition, the invasion of 44As3 4YF cells into the monolayer of L EphB2 cells was also decreased compared with 44As3 mock cells (Figure 4, a and b). These results indicate that activation of the signaling mediated by ephrin-B1 phosphorylation in cancer cells induced by the interaction with EphB2 receptor expressed in stromal cells enhanced the tumor invasion.

The effect of ephrin-B1 phosphorylation on tumor invasion was further examined *in vivo* using 44As3 and 58As9

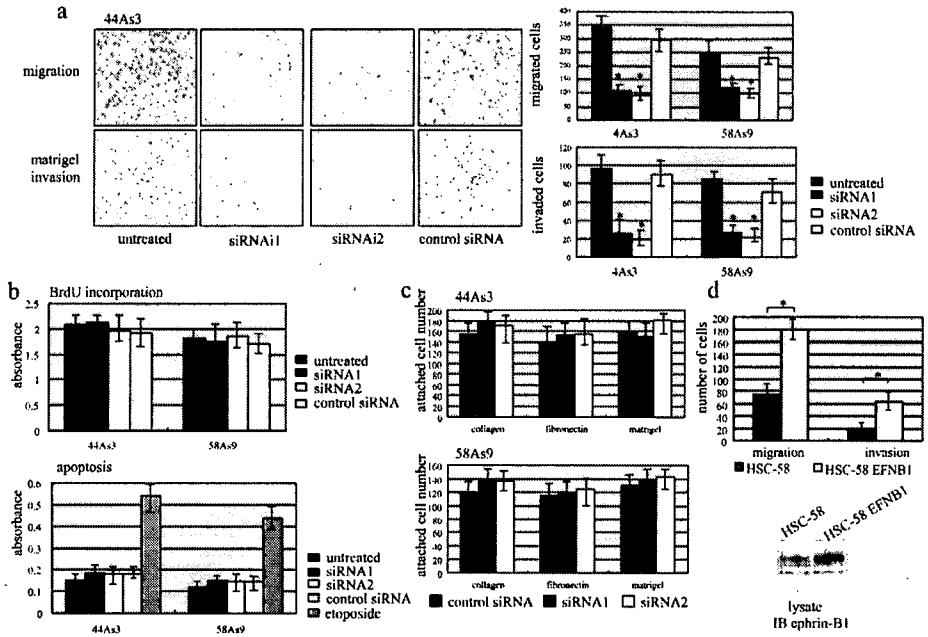

Figure 2. Reduction of ephrin-B1 expression suppressed cell motility and invasion in 44As3 and 58As9 cells. **a:** 44As3 and 58As9 cells treated with ephrin-B1 siRNA (siRNA1, 2) or control siRNA or left untreated were plated onto a Transwell membrane coated with Matrigel (bottom; 85 $\mu g/cm^2$) or uncoated (top) in serum-free medium. In the lower chamber, medium containing 5% fetal bovine serum was added as a chemoattractant. After 10 hours of incubation, the wells were harvested, and cells that migrated to the lower surface of the membrane were counted. Representative fields of 44As3 cells are shown. The results from three independent experiments, each in duplicate, are shown at the right as mean ± SD. The **asterisks** indicate differences from the cells treated with control siRNA. $^*P < 0.01$. **b:** Proliferation and apoptosis of cells were evaluated 72 hours after treatment of siRNAs. Top: Proliferation of the cells was evaluated by measurement of DNA synthesis through detection of BrdU incorporation by enzyme-linked immunosorbent assay (Roche). Bottom: Apoptosis of the cells was examined by measurement of nucleosomes through Cell death detection enzyme-linked immunosorbent assay kit (Roche). As a control, cells were treated with 50 μmol/L etoposide for 12 hours. The results from three independent experiments, each in duplicate, are shown as the mean ± SD. **c:** Reduction of ephrin-B1 expression did not significantly affect the cell adhesion to the extracellular matrix. 44As3 and 58As9 cells treated with ephrin-B1 siRNA (siRNA1, 2) or control siRNA were detached by ethylenediamine tetraacetic acid and replated on the chamber slides coated with collagen type I (100 μg/ml), fibronectin (50 μg/ml), or Matrigel (85 μg/ml). After incubation for 30 minutes, unattached cells were removed by washing the slides in PBS(−) several times, and the remaining cells were stained with Giemsa's solution. The number of attached cells on each substrate was counted, and the results from three independent experiments, each in duplicate, are shown as the mean ± SD. **d:** Expression of wild-type ephrin-B1 promotes migration and invasion of HSC-58 cells. Wild-type ephrin-B1 was stably expressed in HSC-58 cells by retrovirus-mediated gene transfer (HSC-58 EFNB1). The cells indicated were plated onto a Transwell membrane coated with Matrigel (invasion) or uncoated (migration) in serum-free medium and assayed as described in **a**. The results from three independent experiments, each in duplicate, are shown as mean ± SD. $^*P < 0.01$.

cells as a model system for peritoneal dissemination. When 58As9 or 44As3 cells expressing mock vector were injected intraperitoneally into nude mice, severe carcinomatous peritonitis was observed, as previously described (Figure 5a, top).[19] Innumerable whitish nodules were observed in the mesentery of almost all mice injected with 58As9 mock cells (Figure 5a, top left) and 44As3 mock cells (data not shown). In addition, many tumor nodules of 44As3 mock cells were observed in the peritoneal cavity, including the rectouterine region with invasion into the retroperitoneum (Figure 5a, top right). On the other hand, dissemination of cancer cells expressing ephrin-B1 4YF was apparently modest. Tumor nodules of 58As9 4YF cells in the mesentery were small in size and number compared with those of control 58As9 mock cells (Figure 5b; Table 1). Such reduction of tumor nodules in the mesentery was also observed in 44As3 cells expressing ephrin-B1 4YF (Table 1). In addition, the tumor volume involving the rectouterine region was reduced in the mice injected with 44As3 4YF cells (Figure 5c). These results suggest that ephrin-B1 promotes peritoneal dissemination of 58As9 and 44As3 gastric cancer cells through signaling mediated by its tyrosine phosphorylation.

Blocking of Tyrosine Phosphorylation of Ephrin-B1 Attenuates Tumor Invasion of Orthotopic Implanted Gastric Carcinoma

To further evaluate the effect of ephrin-B1 on the process of tumor invasion, we implanted gastric cancer cells orthotopically in the gastric submucosa of nude mice. At 15 days after implantation, 70% of 44As3 tumors expressing

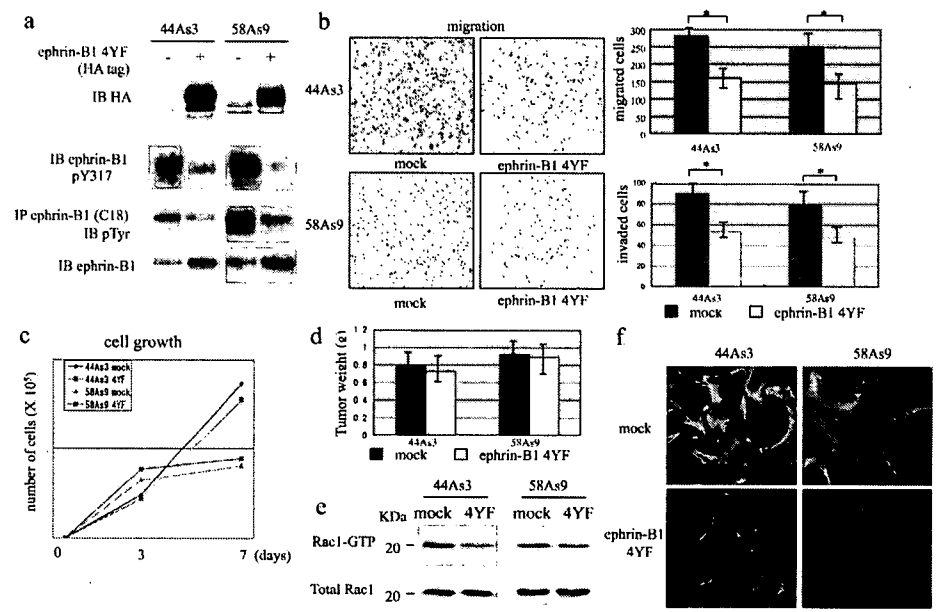

Figure 3. Blocking of ephrin-B1 phosphorylation suppressed cell migration *in vitro*. **a:** Lysates of cells stably expressing ephrin-B1 4YF tagged with HA at carboxyl terminus (+) or control mock vector (−) were subjected to immunoblotting with anti-HA antibody or tyrosine-phosphorylated ephrin-Bs (ephrin-B1 pY317) or immunoprecipitation of total ephrin-B1 and immunoblotting with anti-phosphotyrosine antibody (pTyr). The amount of immunoprecipitated ephrin-B1, which includes both endogenous ephrin-B1 and transfected ephrin-B1 4YF, is shown at the bottom. **b:** As indicated, the cells were seeded onto a Transwell membrane coated with Matrigel (invasion) or uncoated (migration) in serum-free medium as in Figure 2a. In the lower chamber, medium containing 5% fetal bovine serum was added. After 10 hours of incubation, the wells were harvested, and cells that migrated to the lower surface of the membrane were counted. Representative fields are shown. The results from three independent experiments, each in duplicate, are shown at the bottom as mean ± SD. $^*P < 0.01$. **c:** Proliferation of the cells under the culture in the medium containing 10% serum was evaluated by counting the cell number at different time points after being plated onto dishes. **d:** 44As3 and 58As9 cells (1×10^7 cells/mice) expressing either mock or ephrin-B1 4YF were implanted subcutaneously in the flank of nude mice, and the mice were sacrificed 5 weeks after implantation. The mean weight ± SD of eight subcutaneous tumors is shown. **e:** Activation of Rac1 was examined by affinity precipitation of GTP-bound Rac1 (Rac1-GTP) with GST-PBD as described in Materials and Methods. The precipitated Rac1-GTP and total Rac1 in each cell lysate were detected by immunoblotting with anti-Rac1 antibody. **f:** Morphology of gastric cancer cells was monitored. The cells were fixed around 12 hours after plating and stained with phalloidin as described in Materials and Methods for detection of F-actin.

the mock vector formed a large tumor mass involving the greater omentum because of the disruption of gastric serosa and invasion into the surrounding fat tissue (Figure 6a). On the other hand, such local invasion into the omentum was less frequently observed (18%) in mice implanted with 44As3 4YF cells, and most tumors remained within the gastric wall at day 15 (Figure 6a; Table 2). The dissemination of 44As3 mock cells was also observed in several tissues, including the liver surface and mesenteric sheets (Figure 6, b and c). However, we rarely observed cancer dissemination in the peritoneal cavity in mice implanted with 44As3 4YF cells (Figure 6, b and c; Table 2).

Histological examination revealed that expression of ephrin-B1 4YF did not greatly change the morphology of the tumor in the gastric wall (Figure 7, c, d, l, and m). However, invasion of control 44As3 mock cells into lymphatic vessels in subserosa and metastasis to the regional lymph nodes was more frequently observed than 44As3 4YF cells at day 10 after tumor implantation (70 and 18%, respectively; Figure 7, e–g; Table 3). Histological analysis also revealed that the tumor had already reached the outside of the serosal surface and invaded into the surrounding fat tissue in 80% of mice implanted with 44As3 mock cells, whereas it was of low frequency in mice implanted with 44As3 4YF cells (27%) (Figure 7, h and i; Table 3). These phenotypes, including lymphatic vessel invasion, lymph node metastasis, and perforation of gastric serosa, were developed in the same mice, and all three phenotypes are overlapped in 7 of 10 mice in the mock group and in 2 of 10 mice in the 4YF group, suggesting that these are sequential or correlated events. These results indicate that the disruption of signaling mediated by phosphorylation of ephrin-B1 suppressed the invasion and peritoneal dissemination of scirrhous gastric carcinomas.

Discussion

Ephrin-B1 plays pivotal roles in the migration and invasion of cancer cells. High invasion potential is one of the

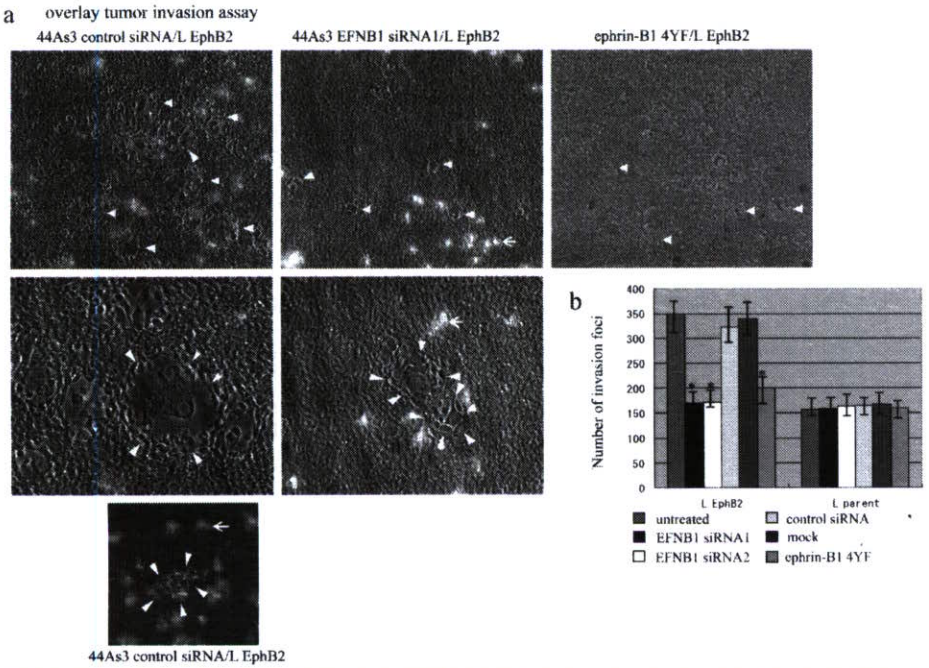

Figure 4. Invasion of ephrin-B1-expressing cells was promoted by interaction with EphB2 receptor. **a:** 44As3 cells were highly invasive into the monolayer of fibroblasts expressing EphB2, which was attenuated by reduction of ephrin-B1 expression. When L cells or L EphB2 cells grew to confluent state in 24-well plates, DiO-labeled 44As3 cells treated either with control or ephrin-B1 siRNA or with 44As3 mock or 44As3 4YF cells (1×10^4, each) were seeded onto the monolayer and incubated in a medium containing 10% fetal bovine serum for 15 hours. Representative fields of the co-culture are shown (top, ×100; bottom, ×200). **Arrowheads** indicate typical invasion foci of tumor cells. Bottom: Typical invasion focus of tumor cells is shown in the fluorescence field (×200). The nest of invaded tumor cells is surrounded by **arrowheads**. **b:** The number of invasion foci was counted as described in Materials and Methods, and the results from three independent experiments, each in duplicate, are shown as mean ± SD. The **asterisks** indicate differences from the cells treated with control siRNA or control cells expressing mock vector. $^*P < 0.01$. The **arrows** indicate unfocused DiO-labeled tumor cells, which did not invade but grew on the monolayer.

major characteristics of scirrhous carcinoma, which determines the poor prognosis of this type of cancer. Using two scirrhous gastric cancer cell lines with high invasion potential, we show for the first time that ephrin-B1 modifies cancer invasion *in vivo*. Blocking of the signaling mediated by tyrosine phosphorylation of ephrin-B1 suppressed the invasion and peritoneal dissemination of these scirrhous cancer cells. Notably, attenuation of phosphorylation of ephrin-B1 suppressed orthotopically implanted scirrhous cancer cells invading through the gastric wall and into the lymphatic vessels. The significance of ephrin-B1 in the invasive phenotype of cancer cells was further obtained from the result that stable expression of wild-type ephrin-B1 in HSC-58, the parental cell line of 58As9 cells, actually promoted the migration and invasion of this cell line *in vitro* (Figure 2d).

Association with EphB receptors triggers tyrosine phosphorylation of ephrin-B1, including Tyr317 (corresponding to Tyr298 of *Xenopus* ephrin-B1), by Src family kinases, which is a critical requirement for interaction with an Src homology 2/Src homology 3 adaptor, Grb4, to transduce signaling.[16] In the physiological conditions, phosphorylation of ephrin-B1 is induced by the contact of ephrin-B1-expressing cells with heterologous cells expressing EphB receptors. On the other hand, ephrin-B1 also promotes migration of cancer cells in a cell-autonomous mechanism as observed in Transwell assay (Figures 2 and 4b). Because EphB2 receptor was expressed in 44As3 and 58As9 cells and expression of EphB4 was also detected in 44As3 cells (Figure 1a), there is a possibility that ephrin-B1 in these cancer cells may be constitutively stimulated by EphB receptors coexpressed in the same cell surface or contacting neighboring cancer cells. This conclusion may be consistent with the observation that the basal phosphorylation level of ephrin-B1 is elevated in 44As3 and 58As9 cells under the usual two-dimensional culture condition *in vitro* (Figure 1a). Overexpression of ephrin-B1 4YF may suppress tumor invasion *in vivo* by blocking cell autonomous phosphorylation of ephrin-B1 in cancer cells and the induction of ephrin-B1 phosphorylation through the interaction with stromal cells. There is still the possibility that expression of eph-

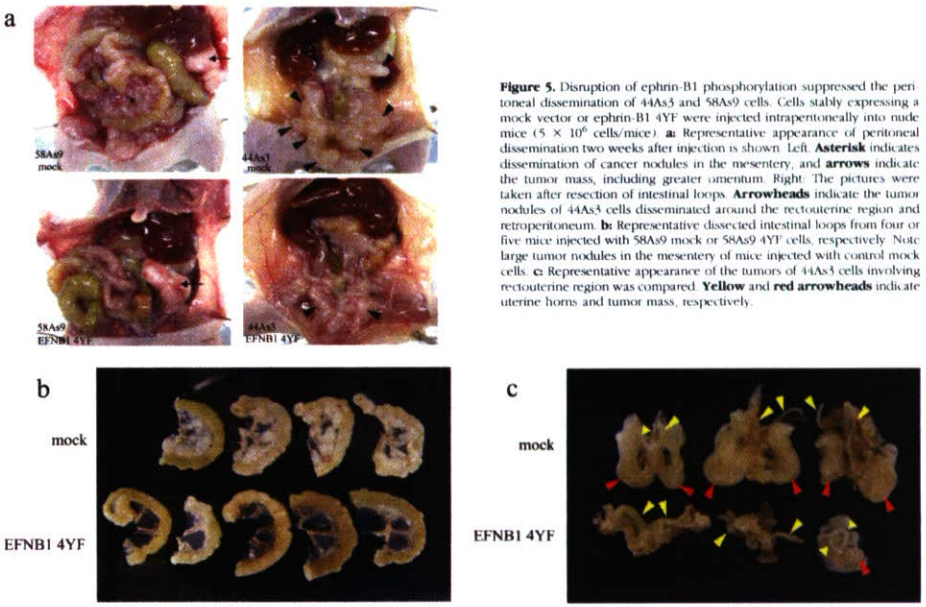

Figure 5. Disruption of ephrin-B1 phosphorylation suppressed the peritoneal dissemination of 44As3 and 58As9 cells. Cells stably expressing a mock vector or ephrin-B1 4YF were injected intraperitoneally into nude mice (5×10^6 cells/mice). **a:** Representative appearance of peritoneal dissemination two weeks after injection is shown. Left: **Asterisk** indicates dissemination of cancer nodules in the mesentery, and **arrows** indicate the tumor mass, including greater omentum. Right: The pictures were taken after resection of intestinal loops. **Arrowheads** indicate the tumor nodules of 44As3 cells disseminated around the rectouterine region and retroperitoneum. **b:** Representative dissected intestinal loops from four or five mice injected with 58As9 mock or 58As9 4YF cells, respectively. Note large tumor nodules in the mesentery of mice injected with control mock cells. **c:** Representative appearance of the tumors of 44As3 cells involving rectouterine region was compared. **Yellow** and **red arrowheads** indicate uterine horns and tumor mass, respectively.

rin-B1 4YF may also block the signaling mediated by other members of ephrin-Bs that also bind the similar group of EphB receptors. However, knocking down of ephrin-B1 by siRNA greatly reduced the phosphorylation of total ephrin-Bs (Figure 1b), suggesting that ephrin-B1, but not ephrin-B2 or ephrin-B3, is the major member of B-class ephrin, which is phosphorylated in these cells. Consistent with this conclusion, at least treatment of 44As3 and 58As9 cells with ephrin-B2 siRNA did not affect the phosphorylation level of the corresponding tyrosine residue of ephrin-Bs examined by anti-ephrin-B1 pY317 antibody (data not shown).

The ephrin/Eph interaction provides both ephrin-B1-mediated reverse signaling and EphB-mediated forward signaling. The expression of ephrin-B1 4YF may suppress the invasion of gastric cancer cells by stimulation of EphB receptor-mediated forward signaling in cancer cells through acting as a stimulator of EphB receptors,

Table 1. Mesenterial Dissemination after Intraperitoneal Inoculation of Gastric Cancer Cells

Cell	Number of nodules*		
	0 to 10	10 to 30	>30
44As3 mock	0	5	15
44As3 4YF	14	5	1
58As9 mock	0	2	18
58As9 4YF	16	3	1

Mice were sacrificed at 14 days after inoculation. Data are shown as the number of mice bearing tumors in the mesentery.
*Number of tumor nodules larger than 2 mm in the mesentery.

because EphB receptor-mediated forward signaling inhibited migration of colorectal tumors in a recent report.[24] However, cancer cell invasion was also inhibited by treatment with ephrin-B1 siRNA, which should cause reduction of forward signaling. Therefore, such inhibitory effect of forward signaling caused by the overexpression of the ligand, even if it exists, does not seem to be strong. In addition, we previously observed that overexpression of ephrin-B1 in Panc1 and Capan1 pancreas cancer cells, in which EphB2 is endogenously expressed, promoted the peritoneal dissemination of these cells by the similar experiment in this study (data not shown), which may also support this conclusion.

We observed that ephrin-B1-expressing cancer cells invaded more frequently into the monolayer of fibroblasts expressing EphB2 receptor than into the parent fibroblasts in overlay invasion assay. This result suggests that cancer cells expressing ephrin-B1 may actively invade into the stromal tissues that express EphB receptors, and such mechanism may also be involved in the process of peritoneal dissemination of ephrin-B1-expressing cancer cells *in vivo*. For example, stromal cells composed of mouse mesentery sheets actually expressed cognate receptors for ephrin-B1 (Supplemental Figure 1 at *http://ajp.amjpathol.org*). Again, there is a possibility that EphB2-mediated forward signaling in L EphB2 fibroblasts also contributes to the formation of invasion foci of cancer cells in this overlay assay. However, expression of ephrin-B1 4YF prevented the invasion of 44As3 cells into the monolayer of L EphB2 cells, suggesting that this invasion

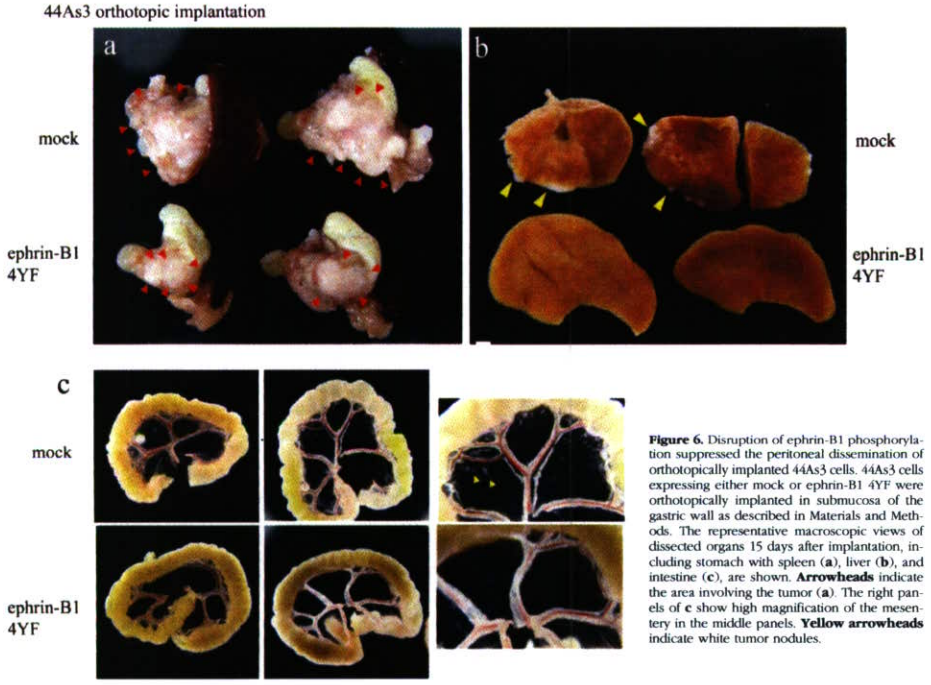

Figure 6. Disruption of ephrin-B1 phosphorylation suppressed the peritoneal dissemination of orthotopically implanted 44As3 cells. 44As3 cells expressing either mock or ephrin-B1 4YF were orthotopically implanted in submucosa of the gastric wall as described in Materials and Methods. The representative macroscopic views of dissected organs 15 days after implantation, including stomach with spleen (**a**), liver (**b**), and intestine (**c**), are shown. **Arrowheads** indicate the area involving the tumor (**a**). The right panels of **c** show high magnification of the mesentery in the middle panels. **Yellow arrowheads** indicate white tumor nodules.

is considered to depend predominantly on the ephrin-B1-mediated reverse signaling in cancer cells rather than the forward signaling in fibroblasts.

Tumor cells expressing ephrin-B1 may gain invasiveness in multiple steps of the cell invasion process. Phosphorylation of ephrin-B1 leads to the recruitment of scaffolding protein disheveled via Grb4, which results in aberrant activation of RhoA.[25,26] Ephrin-B1 makes a complex with Tiam1 to induce Rac1 activation,[20] and we showed blocking of tyrosine phosphorylation of ephrin-B1 decreased the Rac1 activity in this study. Ephrin-B1 is also phosphorylated on tyrosine residues through physical association with cell adhesion proteins such as claudin, which attenuates the cell-cell adhesion.[7] In addition, EphB2-induced phosphorylation of ephrin-B1 has been reported to modify the cell-to-substrate adhesion,[17] although reduction of ephrin-B1 with siRNA did not significantly affect cell adhesion to several substrates *in vitro* under the condition that ephrin-B1 was not stimulated with exogenous EphB2 receptor. Therefore, phosphorylation of ephrin-B1 may regulate cell motility also by affecting the cell adhesion to substrates in the process of stromal invasion of tumors *in vivo*. Blocking of ephrin-B1 phosphorylation by the ephrin-B1 4YF mutant may inhibit tumor invasion through blocking such multiple events.

We cannot exclude a possibility that phosphorylation-independent signaling of ephrin-B1 is also involved in the regulation of cancer cell invasion. For example, proteins containing PDZ domains make a stable complex with ephrin-B1 via PDZ domain-binding motif -YXV located at the carboxyl terminus of ephrin-B1.[27] It may be important to examine the phosphorylation state of ephrin-B1 *in vivo* in a wide range of cancers to estimate what types of cancers will be sensitive for blocking ephrin-B1 phosphorylation on tumor suppression. For example, phosphorylation of B-type ephrins in invading glioblastoma has been reported recently.[14]

We performed intraperitoneal inoculation of cancer cells into nude mice as a model of peritoneal dissemination of the tumor, as also reported by others.[28,29] Although many gastric cancer cell lines do not show typical histological appearance of human scirrhous carcinoma when inoculated into nude mice, our system of orthotopic transplantation of 44As3 cells is a highly reproducible animal model of peritoneal dissemination of human scirrhous gastric carcinoma.[18,19,30] Because early clinical diagnosis of scirrhous gastric carcinoma is difficult, peritoneal dissemination or metastasis to lymph nodes has frequently occurred by the time the diagnosis is made. We observed that expression of ephrin-B1 4YF suppressed not only local invasion of 44As3 cells in the gastric wall but also the infiltration of cancer cells into lymphatic vessels and lymph node metastasis. These results suggest that ephrin-B1 phosphorylation-mediated signaling may modulate the process of the invasion of cancer cells to lymphatic vessels. It may be useful to examine the expression and phosphorylation level of ephrin-B1 in a surgical specimen of scirrhous gastric carcinomas to predict lymphatic metastasis of tumors. Dissemination is a frequent form of the recurrence of scirrhous gastric carcinoma, which serves as a major factor determining the prognosis. Ephrin-B1 is considered to be a prognostic factor of gastric scirrhous carcinoma, and the inhibition of a specific cellular signal originating in ephrin-B1 phosphorylation may be a good candidate for regulating its invasion and dissemination.

Table 2. Dissemination at 15 Days after Orthotopic Implantation of 44As3 Gastric Cancer Cells

Cell	Omentum	Liver	Mesenterium
Mock	7/10 (70)	5/10 (50)	7/10 (70)
4YF	2/11 (18)	1/11 (9)	2/11 (18)

Number of mice bearing tumor at the site per total number of mice bearing tumor (%).

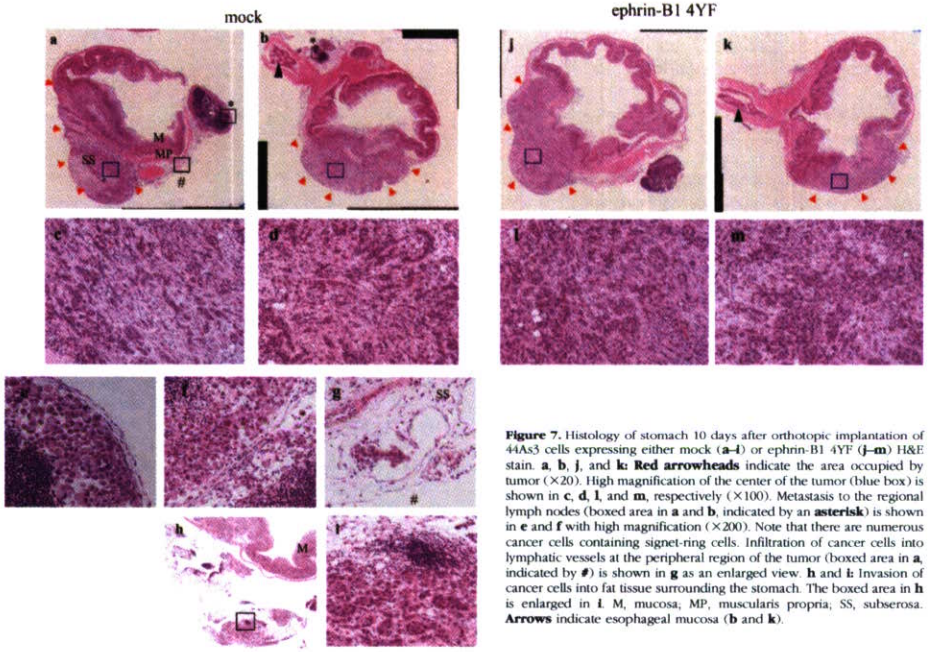

Figure 7. Histology of stomach 10 days after orthotopic implantation of 44As3 cells expressing either mock (**a–i**) or ephrin-B1 4YF (**j–m**) H&E stain. **a**, **b**, **j**, and **k**: **Red arrowheads** indicate the area occupied by tumor (×20). High magnification of the center of the tumor (blue box) is shown in **c**, **d**, **l**, and **m**, respectively (×100). Metastasis to the regional lymph nodes (boxed area in **a** and **b**, indicated by an **asterisk**) is shown in **e** and **f** with high magnification (×200). Note that there are numerous cancer cells containing signet-ring cells. Infiltration of cancer cells into lymphatic vessels at the peripheral region of the tumor (boxed area in **a**, indicated by **#**) is shown in **g** as an enlarged view. **h** and **i**: Invasion of cancer cells into fat tissue surrounding the stomach. The boxed area in **h** is enlarged in **i**. M, mucosa; MP, muscularis propria; SS, subserosa. **Arrows** indicate esophageal mucosa (**b** and **k**).

Table 3. Histological Analysis of the Stomach 10 Days after Orthotopic Implantation of 44As3 Cells

Cell	ly ves	Lymph node	Perforation
Mock	7/10 (70)	7/10 (70)	8/10 (80)
4YF	2/11 (18)	2/11 (18)	3/11 (27)

Data are shown as the number of mice bearing tumor with lymphatic vessel invasion (ly ves), metastasis to regional lymph nodes (lymph node), or perforation of the gastric serosa and infiltrating to the surrounding fat tissue (perforation) per total number of mice bearing tumor (%).

References

1. Blits-Huizinga C, Nelersa C, Malhotra A, Liebl D: Ephrins and their receptors: binding versus biology. IUBMB Life 2004, 56:257–265
2. Murai, KK, Pasquale EB: Ephective signaling: forward, reverse and crosstalk. J Cell Sci 2003, 116:2823–2832
3. Poliakov A, Cotrina M, Wilkinson DG: Diverse roles of Eph receptors and ephrins in the regulation of cell migration and tissue assembly. Dev Cell 2004, 7:465–480
4. Batlle E, Henderson JT, Beghtel H, Van den Born M, Sancho E, Huls G, Meeldijk J, Robertson J, Van de Wetering M, Pawson T, Clevers H: β-Catenin and TCF mediate cell positioning in the intestinal epithelium by controlling the expression of EphB/ephrinB. Cell 2002, 111:251–263
5. Batlle E, Bacani J, Begthel H, Jonkheer S, Gregorieff A, Van den Born M, Malats N, Sancho E, Boon E, Pawson T, Gallinger S, Pals S, Clevers H: EphB receptor activity suppresses colorectal cancer progression. Nature 2005, 435:1126–1130
6. Holmberg J, Genander M, Halford MM, Anneren C, Sondell M, Chumley MJ, Silvany RE, Henkemeyer M, Frisen J: ephB receptors coordinate migration and proliferation in the intestinal stem cell niche. Cell 2006, 125:1151–1263
7. Tanaka M, Kamata R, Sakai R: Phosphorylation of ephrin-B1 via the interaction with claudin following cell-cell contact formation. EMBO J 2005, 24:3700–3711
8. Tanaka M, Kamata R, Sakai R: EphA2 phosphorylates the cytoplas-

mic tail of claudin-4 and mediates paracellular permeability. J Biol Chem 2005, 280:42375–42382
9. Surawska H, Ma PC, Salgia R: The role of ephrins and Eph receptors in cancer. Cytokine Growth Factor Rev 2004, 15:419–433
10. Sawai Y, Tamura S, Fukui K, Ito N, Imanaka K, Saeki A, Sakuda S, Kiso S, Matsuzawa Y: expression of ephrin-B1 in hepatocellular carcinoma: possible involvement in neovascularization. J Hepatol 2003, 39:991–996
11. Meyer S, Hafner C, Guba M, Flegel S, Geissler EK, Becker B, Koehl G, Orso E, Landthaler M, Vogt T: Ephrin-B2 overexpression enhances integrin-mediated ECM-attachment and migration of B16 melanoma cells. Int J Oncol 2005, 27:1197–1206
12. Castellvi J, Garcia A, De la Torre J, Hernandez J, Gil A, Xercavins J, Cajal SR: EphrinB expression in epithelial ovarian neoplasms correlates with tumor differentiation and angiogenesis. Hum Pathol 2006, 37:883–889
13. Varelias A, Koblar SA, Cowled PA, Carter CD, Clayer M: Human osteosarcoma express specific ephrin profiles: implications for tumorigenicity and prognosis. Cancer 2002, 95:862–869
14. Nakada M, Drake KL, Nakada S, Niska JA, Berens ME: Ephrin-B3 ligand promotes glioma invasion through activation of Rac1. Cancer Res 2006, 66:8492–8500
15. Kataoka H, Tanaka M, Kanamori M, Yoshii S, Ihara M, Wang YJ, Song JP, Li ZY, Arai H, Otuki Y, Kobatashi T, Kohno H, Hanai H, Sugimura H: Expression profile of EFNB1, EFNB2, two ligands of EPHB2 in human gastric cancer. J Cancer Res Clin Oncol 2002, 128:343–348
16. Bong YS, Park YH, Lee HS, Mood K, Ishimura A, Daar IO: Tyr-298 in ephrin-B1 is critical for an interaction with the Grb4 adaptor protein. Biochem J 2004, 377:499–507
17. Cowan CA, Henkemeyer M: The SH2/SH3 adaptor Grb4 transduces B-ephrin reverse signals. Nature 2001, 413:174–179
18. Yanagihara K, Tanaka H, Takigahira M, Ino Y, Yamaguchi Y, Toge T, Sugano K, Hirohashi S: Establishment of two cell lines from human gastric scirrhous carcinoma that possess the potential to metastasize spontaneously in nude mice. Cancer Sci 2004, 95:575–582
19. Yanagihara K, Takigahira M, Tanaka H, Komatsu T, Fukumoto H, Koizumi F, Nishio K, Ochiya T, Ino Y, Hirohashi S: Development and biological analysis of peritoneal metastasis mouse models for human scirrhous stomach cancer. Cancer Sci 2005, 96:323–332
20. Akedo H, Shinkai K, Mukai M, Mori Y, Tateishi R, Tanaka K, Yamamoto R, Morishita T: Interaction of rat ascites hepatoma cells with cultured mesothelial cell layers: a model for tumor invasion. Cancer Res 1986, 46:2416–2422
21. Tanaka M, Ohashi R, Nakamura R, Shinmura K, Kamo T, Sakai R, Sugimura H: Tiam1 mediates neurite outgrowth induced by ephrin-B1 and EphA2. EMBO J 2004, 23:1075–1088
22. Kusama T, Mukai N, Tatsuta M, Nakamura H, Inoue M: Inhibition of transendothelial migration and invasion of human breast cancer cells by preventing geranylgeranylation of Rho. Int J Oncol 2006, 29:217–223
23. Blaheta RA, Daher FH, Michaelis M, Hasenberg C, Welch EM, Jonas D, Kotchetkov R, Doerr HW, Cinatl Jr J: Chemoresistance induces enhanced adhesion and transendothelial penetration of neuroblastoma cells by down-regulating NCAM surface expression. BMC Cancer 2006, 6:294
24. Guo DL, Zhang J, Yuen ST, Tsui WY, Chan ASY, Ho C, Ji J, Leung SY, Chen X: Reduced expression of EphB2 that parallels invasion and metastasis in colorectal tumors. Carcinogenesis 2006, 27:454–464
25. Tanaka M, Kamo T, Ota S, Sugimura H: Association of dishevelled with Eph tyrosine kinase receptor and ephrin mediates cell repulsion. EMBO J 2003, 22:847–858
26. Lee HS, Bong YS, Moore KB, Soria K, Moody SA, Daar IO: Dishevelled mediates ephrinB1 signalling in the eye field through the planar cell polarity pathway. Nat Cell Biol 2006, 8:55–63
27. Lin D, Gish GD, Songyang Z, Powson T: The carboxyl terminus of B class ephrins constitutes a PDZ domain binding motif. J Biol Chem 1999, 274:3726–3733
28. Li Z, Zhan W, Wang Z, Zhu B, He Y, Peng J, Cai S, Ma J: Inhibition of PRL-3 gene expression in gastric cancer cell line SGC7901 via micro RNA suppressed peritoneal metastasis. Biochem Biophys Res Commun 2006, 348:229–237
29. Arlt MJE, Novak-Hofer I, Gast D, Gschwend V, Moldenhauer G, Grunberg J, Honer M, Schubiger A, Altevogt P, Kruger A: Efficient inhibition of intra-peritoneal tumor growth and dissemination of human ovarian carcinoma cells in nude mice by anti-L1-cell adhesion molecule monoclonal antibody treatment. Cancer Res 2006, 66:936–943
30. Yanagihara K, Takigahira M, Takeshita F, Komatsu T, Nishio K, Hasegawa F, Ochiya T: A photon counting technique for quantitatively evaluating progression of peritoneal tumor dissemination. Cancer Res 2006, 66:7532–7539
31. Holland SJ, Gale NW, Mbamalu G, Yancopoulos GD, Henkemeyer M, Powson T: Bidirectional signaling through the EPH-family receptor Nuk and its transmembrane ligands. Nature 1996, 383:722–725

MOLECULAR AND CELLULAR BIOLOGY, Nov. 2007, p. 7649–7660 Vol. 27, No. 21
0270-7306/07/$08.00+0 doi:10.1128/MCB.01246-07

CUB Domain-Containing Protein 1 Is a Novel Regulator of Anoikis Resistance in Lung Adenocarcinoma▽†

Takamasa Uekita,[1] Lin Jia,[1] Mako Narisawa-Saito,[2] Jun Yokota,[3] Tohru Kiyono,[2] and Ryuichi Sakai[1]*

Growth Factor Division,[1] Virology Division,[2] and Biology Division,[3] National Cancer Center Research Institute, 5-1-1 Tsukiji, Chuo-ku, Tokyo 104-0045, Japan

Received 12 July 2007/Returned for modification 31 July 2007/Accepted 16 August 2007

Malignant tumor cells frequently achieve resistance to anoikis, a form of apoptosis induced by detachment from the basement membrane, which results in the anchorage-independent growth of these cells. Although the involvement of Src family kinases (SFKs) in this alteration has been reported, little is known about the signaling pathways involved in the regulation of anoikis under the control of SFKs. In this study, we identified a membrane protein, CUB-domain-containing protein 1 (CDCP1), as an SFK-binding phosphoprotein associated with the anchorage independence of human lung adenocarcinoma. Using RNA interference suppression and overexpression of CDCP1 mutants in lung cancer cells, we found that tyrosine-phosphorylated CDCP1 is required to overcome anoikis in lung cancer cells. An apoptosis-related molecule, protein kinase Cδ, was found to be phosphorylated by the CDCP1-SFK complex and was essential for anoikis resistance downstream of CDCP1. Loss of CDCP1 also inhibited the metastatic potential of the A549 cells in vivo. Our findings indicate that CDCP1 is a novel target for treating cancer-specific disorders, such as metastasis, by regulating anoikis in lung adenocarcinoma.

Src family kinases (SFKs) play important roles in various cell functions, including cell proliferation, cell adhesion, and cell migration, under the control of extracellular stimuli (26). Many studies have shown elevated activity of SFKs or increased protein expression in a variety of human cancers (31). The activities of SFKs often correlate with the malignant potential of cancer and poor prognosis (36). SFKs may contribute to various aspects of tumor progression, including uncontrolled proliferation and migration, disruption of cell-cell contacts, invasiveness, angiogenesis, and resistance to apoptosis.

Anoikis is a form of apoptosis triggered by the loss of cell survival signals generated from interaction with the extracellular matrix (10). Anoikis is considered to be physiologically important in the maintenance of homeostasis and tissue architecture (24). On the other hand, the resistance to anoikis acquired during carcinogenesis has been described as a core aspect of cancer cells for tumor progression and metastasis (12). This property indicates the existence of survival signals in tumor cells, which compensate for similar signals supported by cell-matrix interactions. Since they were originally described by Frisch and Francis (9), several previous reports have shown the crucial role of SFKs in the anoikis resistance of tumor cells. Viral Src oncoprotein abrogates anoikis in epithelial cells (13). Src activation is also important for resistance to anoikis in various cancers, such as colon tumor and lung adenocarcinoma cells (33, 35). However, the exact mechanism that is responsible for the anoikis resistance mediated by SFKs in human cancer cells has not been clearly elucidated.

The purpose of this study, therefore, was to identify the key molecules of anoikis resistance, which mediate signals from activated SFKs in human cancer cells. For that purpose, we analyzed proteins binding to SFKs with and without cell attachment in a number of human lung cancer cell lines. We found that tyrosine phosphorylation of a 135-kDa SFK-binding protein is associated with elevated anchorage independence in a group of lung cancer cell lines, especially in a cell suspension condition. This 135-kDa phosphoprotein was purified and identified as CUB-domain-containing protein 1 (CDCP1) by mass spectrometry. The protein CDCP1 is a type I transmembrane protein that has possible roles in cell-cell and cell-matrix adhesion (3, 5). The molecule has been reported to be highly expressed in lung, breast, and colon cancers (6, 28). Using an RNA interference (RNAi) technique, it was determined that CDCP1 is required for the survival of lung cancer cells both in suspension culture and in soft agar. This study identifies a novel modulator that sustains anoikis resistance under the control of SFKs in lung cancer cells.

MATERIALS AND METHODS

Plasmids, antibodies, and reagents. Full-length cDNA of human CDCP1 with a FLAG tag at the C terminus (wild type [WT]) was obtained by reverse transcription-PCR amplification from the mRNA of A549 human lung adenocarcinoma cells and cloned into pcDNA3.1 (Invitrogen). The cytoplasmic-domain mutants of CDCP1, Y734F (Tyr734 to Phe), Y762F (Tyr762 to Phe), and Y2F (Y734 and Y762 double mutant), were generated by PCR using the overlap extension method of Ho et al. (14). The C2 domain of protein kinase Cδ (PKCδ) corresponding to amino acids (1 to 160) with a hemagglutinin (HA) tag at the C terminus was obtained by PCR and cloned into pcDNA3.1 (Invitrogen). To express the Fyn Src homology 2 (SH2) domain fused with glutathione *S*-transferase (GST) protein (GST-FynSH2), a cDNA fragment of the Fyn SH2 domain corresponding to nucleotides 1018 to 1299 of the reported sequence (GenBank accession number NM 002037) was amplified by PCR and cloned into pGEX4T2 (Amersham Pharmacia).

Antiphosphotyrosine antibody (4G10) and anti-c-Src antibody (clone GD11) were purchased from Upstate Biotechnology. Anti-Akt antibody, anti-phospho-Akt (Ser473) antibody, anti-ERK1/2 antibody (p44/p42 mitogen-activated protein kinase [MAPK] antibody), anti-phospho-ERK1/2 antibody (phospho-p44/p42 MAPK [Thr202/Tyr204] antibody), anti-p38MAPK antibody, anti-phospho-

* Corresponding author. Mailing address: Growth Factor Division, National Cancer Center Research Institute, 5-1-1 Tsukiji, Chuo-ku, Tokyo 104-0045, Japan. Phone: 81-3-3547-5247. Fax: 81-3-3542-8170. E-mail: rsakai@gan2.res.ncc.go.jp.

† Supplemental material for this article may be found at http://mcb.asm.org/.

▽ Published ahead of print on 4 September 2007.

p38MAPK (Thr180/Tyr182) antibody, and anti-phospho-PKCδ (Tyr311) antibody were purchased from Cell Signaling. Anti-HA (Y-11), anti-PKCδ (C-20), and anti-Fyn (FYN3) antibodies were purchased from Santa Cruz Biotechnology. Anti-FLAG antibody (Anti-FLAG M2 peroxidase conjugate specific antibody) and antitubulin antibody (clone B-5-1-2) were purchased from Sigma. The anti-c-Yes antibody was purchased from Transduction Laboratories. An anti-CDCP1 antibody (ab1377) was purchased from Abcam Ltd. To generate the CDCP1 antibody, anti-CDCP1 and the anti-phospho-CDCP1 (Tyr734) antibody were obtained by rabbit immunization using the cytoplasmic domain of CDCP1 fused to GST, and the amino peptides NDSHV(pY^{734})AVIEC of CDCP1 were obtained from MBL Co., Ltd. Horseradish peroxidase (HRP)-conjugated anti-mouse and anti-rabbit antibodies were purchased from Amersham Pharmacia. The HRP-conjugated anti-goat immunoglobulin G (IgG) antibody was purchased from ZYMED. Mouse, rabbit, and goat IgGs were purchased from DakoCytomation. The SFK inhibitor PP2 and the structural analog PP3 were purchased from Calbiochem-Novabiochem Ltd. Etoposide and Rottlerin were purchased from Sigma-Aldrich.

Cell culture and transfection. The human lung adenocarcinoma cell lines A549, PC14, and H322 and human lung squamous carcinoma cell lines H520 and H157 were maintained in RPMI 1640 medium with 10% fetal bovine serum (FBS) at 37°C with 5% CO_2. For transfection, cells were seeded on a cell culture plate or a 2-methacryloyloxyethyl phosphorylcholine (MPC)-coated plate (Nunc) at 1.5×10^5 cells per six wells or 9.0×10^5 cells/10-cm plate, and transfection was performed after 14 h. Expression plasmids were transfected by Lipofectamine 2000 (Invitrogen) according to the manufacturer's instructions. To investigate the effect of PP2 treatment, cells were treated with 10 μM of PP2 or 10 μM of PP3.

Construction of dicer, stealth siRNAs, and miR RNAi vectors. Dicer small interfering RNAs (siRNAs) of human c-Src, Fyn, and c-Yes were generated using the BLOCK-iT RNAi TOPO transcription kit and BLOCK-iT complete dicer RNAi kit (Invitrogen) according to the manufacturer's instructions. In the generation of siRNA for Src, a 726-bp fragment from the initiation codon of human c-Src was chosen as the target sequence and amplified by PCR using the primers forward, 5′-ATGGGTAGCAACAAGAGCAAG-3′, and reverse, 5′-GTGGCACAGGCCATCGGCGTG-3′. As for Fyn and c-Yes, 999-bp and 857-bp fragments were chosen as the target sequences, respectively, and amplified with the following primers: Fyn forward, 5′-ATGGGCTGTGTGCAATGTAGG-3′, and reverse, 5′-CACCACTGCATAGAGCTGGAC-3′; c-Yes forward, 5′-CTGAAAATACTCCAGAGCCTG-3′, and reverse, 5′-CTTTGTCCTAGTTTAACCTCTAG-3′. Dicer siRNA of LacZ was generated by the same procedure as dicer siRNAs of c-Src, Fyn, and c-Yes and was used as a negative control. The stealth siRNAs of human CDCP1, PKCδ, and the negative control were ordered from Invitrogen. Specific primers were as follows: CDCP1 forward, 5′-GCUCUGCCACGAGAAAGCAACAUUA-3′, and reverse, 5′-UAAUGUUGCUUUCUCGUGGCAGAGC-3′; PKCδ forward, 5′-GGUGCAGAAGAAGCCGACCAUGUAU-3′, and reverse, 5′-AUACAUGGUCGGCUUCUUCUGCACC-3′. Transfection of both dicer and stealth siRNAs was performed with Lipofectamine 2000 (Invitrogen), and the effect was analyzed less than 48 h after the transfection.

A system stably expressing siRNA was generated using the BLOCK-iT Pol II miR RNAi expression vector kit (Invitrogen) according to the manufacturer's instructions. In the generation of the miR RNAi vector for humans, CDCP1 was chosen as the target sequence, using the forward primer 5′-TGCTGAATGTTGCTTTCTCGTGGCAGGTTTTGGCCACTGACTGACCTGCCACGAAAGCAACATT-3′ and the reverse primer 5′-CCTGAATGTTGCTTTCGTGGCAGGTCAGTCAGTGGCCAAAACCTGCCACGAGAAAGCAACATTC-3′. Cells stably expressing the miR RNAi vector for CDCP1 and LacZ were established and cultured in medium containing blasticidin (Invivogen) at a concentration of 10 μg/ml for 3 weeks. Two clones expressing the CDCP1 RNAi vector (miCDCP1-1 and -2) were selected by significant suppression of the CDCP1 protein (<10%), and two clones from the control LacZ vector were also selected (miLacZ-1 and -2).

Soft-agar colony assay. Six-well tissue culture plates were coated with a layer of RPMI 1640-10% FBS containing 0.5% ultrapure agarose (Invitrogen). Subconfluent A549 cells transfected with the dicer siRNA or miR RNAi vector-expressed clone were treated with EDTA, washed in phosphate-buffered saline twice, and resuspended in RPMI 1640-10% FBS at 6×10^3 cells/ml. Then, a 500-μl cell sample was added to 1 ml of RPMI 1640-10% FBS containing 0.5% ultrapure agarose (final concentration, 0.33%). The cells were plated on the coated tissue culture plates, allowed to solidify, and then placed in a 37°C incubator. After 30 days, colonies were scanned using a GS-800 calibrated densitometer (Bio-Rad), and the numbers of colonies per well were determined. Soft-agar assays were performed three times.

Immunoprecipitation and Western blotting. Cell lysates were prepared with protease inhibitors in PLC buffer (10 mM Tris-HCl, pH 7.5, 5 mM EGTA, 150 mM NaCl, 1% Triton X-100, 10% glycerol, 10 μg/ml aprotinin, 1 mM sodium orthovanadate [Na_3VO_4], and 100 μg/ml leupeptin). The protein concentration was measured by BCA protein assay (Pierce). For purification, 1 μg of monoclonal or affinity-purified polyclonal antibody was added to the proteins, which were then incubated with 500 μl (2 mg/ml) of cell lysate for 2 h at 4°C. Next, they were precipitated with protein A- or protein G-agarose for 1 h at 4°C. The immunoprecipitates were extensively washed with PLC buffer and prepared for Western blotting.

For Western blotting, samples were separated on sodium dodecyl sulfate-polyacrylamide gel electrophoresis and transferred to a polyvinylidene difluoride membrane (Immobilon-P; Millipore). After blocking of the membrane with blocking buffer (Blocking One; Nakarai Tesque), the membrane was probed with antibodies for detection. The membrane was further probed with HRP-conjugated anti-mouse, anti-rabbit, or anti-goat IgG (1:4,000) to visualize the reacted antibody.

Images were captured by a molecular imager (GS-800; Bio-Rad), and the density of each smear was quantified using Quantity One software (Bio-Rad).

Identification of CDCP1. Isolated GST-FynSH2 protein coupled with cyanogen bromide (CNBr) was used to purify the 135-kDa and 70-kDa proteins from the A549 cells cultured for 48 h on MPC-coated plates in growth medium. Briefly, ~3×10^7 suspended A549 cells in a total of 400 dishes (10-cm dish; 30 ml culture medium) were collected and lysed in PLC buffer. The cell lysate was rotated for 8 h at 4°C with GST-FynSH2 protein and washed four times using PLC buffer before being eluted with GST-FynSH2-coupled proteins using 8 M urea buffer (8 M urea, 10 mM Tris-HCl, pH 7.4, 150 mM NaCl, 1% Triton X-100). Secondly, the eluted sample was dialyzed three times against a 100-fold volume of dialysis buffer (10 mM Tris-HCl, pH 7.4, 150 mM NaCl, 1 mM Na_3VO_4), and then the sample was affinity purified with antiphosphotyrosine monoclonal antibody (4G10) coupled with CNBr. 4G10-coupled proteins were washed four times using PLC buffer and once using heptyl-glucoside buffer (10 mM Tris-HCl, pH 7.4, 150 mM NaCl, 0.1% heptyl-glucoside). Next, the samples were eluted using 0.1 M phenylphosphate in heptyl-glucoside buffer. The purified 135-kDa and 70-kDa proteins were concentrated, electrophoresed, and blotted onto a ProBlott membrane (Applied Biosystems). After visualization with colloidal gold total-protein stain (Bio-Rad), the isolated 135-kDa and 70-kDa bands were analyzed by mass spectrometry. Four sets of amino acid sequences determined from the 135-kDa band and an amino acid sequence determined from the 70-kDa band indicated that both the 135-kDa and 70-kDa proteins were CDCP1.

Apoptosis assay. Each cell was treated with EDTA, and 1×10^4 cells were reseeded onto normal or MPC-coated 96-well plates. After 24 h, the cells were lysed and used for the detection of apoptosis. Apoptosis levels were determined using a cell death ELISA kit (Roche Molecular Biochemicals), which detects the presence of nucleosomes in the cytoplasm of apoptotic cells. The absorbance of the samples was measured at a wavelength of 405 nm using a microplate reader model 550 (Bio-Rad).

BrdU incorporation assay. Cell proliferation was analyzed with the cell proliferation ELISA BrdU kit according to the manufacturer's instructions (Roche Molecular Biochemicals) based on the measurement of 5-bromo-2′-deoxyuridine (BrdU) incorporation during DNA synthesis of proliferating cells. Briefly, A549 cells were cultured in triplicate for 24 h in 96-well plates (1.0×10^4 cells/well) with or without cell attachment. The cells were subjected to BrdU incorporation for 6 h. The colorimetric change was measured at 450 nm on a microplate reader model 550 (Bio-Rad).

Infection of retroviral constructs. The retroviral vectors PQCXIN (Clontech) and pCMSCVbsd were used to express human CDCP1 (WT) and Y734F with a FLAG tag at the C terminus and full-length cDNA of Fyn kinase with a double HA tag at the C terminus (FynHA), respectively. pCMSCVbsd contains the blasticidin resistance gene in place of the puromycin resistance gene of pCMSCVpuro (20). These retrovirus vectors were converted into the destination vectors with a vector conversion kit (Invitrogen). The cDNA segments were first cloned into pDONR221 and then into the destination vector, pDEST-PQCXIN or pDEST-CMSCVbsd, according to the manufacturer's instructions (Invitrogen). The production of recombinant retroviruses was performed as described previously (25). Briefly, the retroviral vector and the packaging construct pCL-10A1 were cotransfected into 293T cells using TransIT-293 (Mirus Co., Madison, WI) according to the manufacturer's instructions, and culture fluid was harvested 48 to 72 h posttransfection. H322 cells were infected with the viral fluid in the presence of 4 mg/ml Polybrene, and the infected cells were selected in the presence of 800 μg/ml G418 or 5 μg/ml blasticidin. For combinations of retroviral infections, cells were first transduced with CDCP1 and then with Fyn kinase.

Experimental metastasis assay. Female BALB/cAJc1-nu/nu nude mice were purchased from CLEA Japan Inc. All of the mice used in these experiments were 6 to 8 weeks old. A549 clones generated by the miR RNAi system and H322 cells were evaluated by experimental metastasis assay, as described by Fidler et al. (8). Briefly, cells (5×10^5 cells/0.2 ml of medium without serum; $n = 6$) were injected into the tail veins of mice. The mice were sacrificed 100 days after cell inoculation for the counting of metastatic nodules. The numbers of lung metastases and nodule formations were determined.

To determine the effect of CDCP1 on tumor growth in nude mice, A549 clones (3×10^6 cells/0.2 ml of medium without serum) were subcutaneously injected into the right flanks of mice. The mice were killed at 30 days. The results are expressed as the mean weight of tumors from three mice ± standard error.

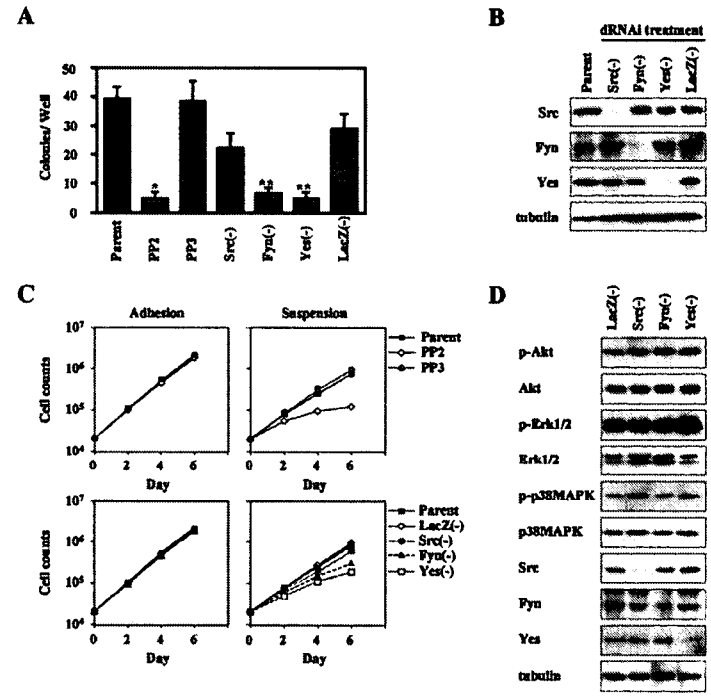

FIG. 1. Anchorage independence of lung adenocarcinoma cells requires SFK. (A) The effect of SFKs on anchorage independence was determined by soft-agar assay. A549 cells were treated with the SFK inhibitor PP2 (10 μM) and SFK dicer RNAi [bars Src(−), Fyn(−), and Yes(−)], and controls [bars Parent, PP3, and LacZ(−)] were seeded onto each soft-agar plate (3×10^3 cells). Colonies equal to and larger than 0.5 mm in diameter were counted after 30 days. The error bars represent standard deviations, and the asterisk indicates statistically significant differences ($P < 0.01$) between the parent and PP2 treatment cells, while the double asterisk indicates statistically significant differences ($P < 0.01$) between LacZ(−) and each of the SFK RNAi treatment cells. (B) A549 cells transiently transfected with c-Src, Fyn, c-Yes, or LacZ dicer RNAi (dRNAi) were incubated for 48 h in culture plates. The cells were lysed and subjected to immunoblotting with the indicated antibodies. (C) Cell growth in A549 cells was subjected to a determination of the number of cells, as described for panel A. Approximately 2×10^4 cells were seeded onto normal (Adhesion) or MPC-coated (Suspension) culture plates with medium. The growth medium was changed every 2 days. The total cell number on each plate was determined every 2 days by a Coulter particle counter z1 (Beckman). (D) SFKs did not affect the phosphorylation of Akt, Erk1/2, or p38MAPK. The lysate of suspended A549 cells transiently transfected with dicer RNAi for each of the SFKs was prepared and subjected to immunoblotting with the indicated antibodies.

RESULTS

The anchorage independence of lung cancer cells involves SFKs. We first examined the involvement of SFKs in the anchorage independence of A549 lung adenocarcinoma cells using the colony formation assay on soft agar with or without PP2, an SFK inhibitor (Fig. 1A). A549 cells and cells treated with PP3, an inactive derivative of PP2, formed a similar number of colonies in soft agar, while the addition of PP2 caused a significant decrease in the numbers of colonies. A similar effect of PP2 was observed in most lung cancer cells, such as the PC3, PC14, H520, and LK2 cell lines (data not shown).

To determine which member of the SFKs mainly contributes to the anchorage independence of A549 cells, individual expression of c-Src, Fyn, and c-Yes was downregulated using RNAi technology (Fig. 1B), and colony formation assays were performed on soft agar (Fig. 1A). A549 cells treated with Fyn or c-Yes siRNAs formed significantly fewer colonies than the control cells treated with LacZ siRNA, while cells treated with c-Src siRNA formed slightly fewer colonies. We also observed

a similar suppressive effect of Fyn and c-Yes RNAi in PC14 and H520 lung cancer cells (data not shown).

To further assess the significance of SFKs during the anchorage-independent growth, the effects of PP2 or RNAi for each SFK on cell growth were examined with or without cell attachment using a normal culture dish or MPC-coated dish, respectively. In adherent culture, no significant effect on cell numbers was observed by treatment with PP2 or by any siRNA for the SFKs (Fig. 1C, Adhesion). In suspension culture, however, A549 cells treated with PP2 or with siRNAs for Fyn or c-Yes showed a significant reduction of cell counts compared with untreated cells, while cells treated with c-Src siRNA showed only a slight reduction in cell numbers (Fig. 1C, Suspension). Neither control siRNA nor PP3 had a detectable effect on cell growth in suspension culture.

The phosphatidylinositol (PI) 3-kinase/Akt pathway and the MAPK pathway are the most significant pathways mediating growth factor signals during cell survival and cell proliferation. We therefore examined whether downstream signals of SFKs, which lead to anchorage independence of A549 cells, involve the activation of these two pathways. Suppression of the expression of c-Src, Fyn, or c-Yes by each RNAi had no significant effects on the phosphorylation of Akt and ERK in the suspension culture of A549 cells. These sets of siRNAs also had no effect on the phosphorylation of p38MAPK (Fig. 1D).

Taken together, these data suggest that Fyn and c-Yes are required for anchorage independence in A549 cells, and the cellular signals mediated by these kinases are independent of the Akt, ERK, and p38MAPK pathways.

Purification of 135-kDa and 70-kDa phosphotyrosine proteins associating with SFKs in suspension culture. To identify which molecules mediate the SFK signals specific for anchorage independence, we analyzed the phosphotyrosine-containing proteins that bind to SFKs. Among the proteins associated with SFKs, two proteins with molecular masses of 135 kDa and 70 kDa were prominently phosphorylated, even in suspension culture (Fig. 2A), and these proteins were also phosphorylated in PC14 and H520 cell lines, which also exhibit a high level of anchorage independence (Fig. 2A, High). In contrast, the H322 and H157 cell lines, which formed a small number of colonies in soft agar (Fig. 2A, Low), displayed rather lower levels of phosphorylation of these two proteins (Fig. 2A). Using these results, we sought to identify proteins that function as downstream mediators of SFKs in anchorage-independent growth.

As several antibodies against the known phosphoproteins failed to recognize the 135-kDa and 70-kDa proteins, we applied affinity purification. Using A549 cells cultured for 48 h with and without cell attachment, these 135-kDa and 70-kDa proteins were pulled down with the Fyn SH2 domain more efficiently under suspension conditions (Fig. 2B). A total of $\sim 1.2 \times 10^{10}$ cells in suspension culture were first purified with the Fyn SH2 domain. After purification by a second affinity column using a 4G10 antiphosphotyrosine antibody, samples were analyzed by Western blotting (Fig. 2C, WB) and colloidal gold total-protein stain (Fig. 2C, G). Bands corresponding to the two proteins were cut out and analyzed by mass spectrometry. Four peptides from the 135-kDa band and one peptide from the 70-kDa band were determined by mass spectrometry to be the recently identified membrane protein CDCP1 (Fig. 2C). The proteins at molecular masses of both 135 kDa and 70 kDa in the suspension culture appeared to contain the single protein CDCP1. The 70-kDa protein was estimated to be a cleaved product of 135-kDa CDCP1, as previously reported (5).

Identification of the major phosphoprotein of the 135-kDa and 70-kDa proteins as CDCP1 and its association with anchorage independence. Anti-CDCP1 antibody recognized proteins of exactly the same molecular masses as the 135-kDa and 70-kDa proteins both in the whole-cell lysate and in the sample pulled down by the Fyn SH2 domain (Fig. 3A, WCL and PD). CDCP1 was also clearly coimmunoprecipitated with each SFK molecule originally expressed in A549 cells, especially with Fyn and c-Yes, which is consistent with the original 135-kDa protein (Fig. 3A, IP). On the other hand, immunoprecipitation with anti-CDCP1 antibody revealed that CDCP1 was strongly associated with Fyn and c-Yes and very weakly with c-Src (Fig. 3B).

To confirm that the phosphorylation of CDCP1 in each lung cancer cell line is associated with high anchorage independence, we generated a phosphospecific antibody (p-CDCP1 [Tyr734]) against tyrosine 734 of CDCP1, which is reported to be a major phosphorylation site for SFK (1, 5), and analyzed the phosphorylation of CDCP1 in each cell line (Fig. 3C). Prominent phosphorylation of CDCP1 was observed in the A549, PC14, and H520 lung cancer cells with high anchorage independence (Fig. 3C, High), while the H322 and H157 cells, which have low anchorage independence (Fig. 3C, Low), exhibited rather low levels of phosphorylation of CDCP1. From these results, we concluded that the 135-kDa phosphoprotein detected in lung cancer cells is CDCP1, and its phosphorylation status appears to be associated with anchorage independence.

We examined whether the phosphorylation of CDCP1 is altered with or without cell attachment in the culture. After detachment of A549 cells with EDTA, the cells were either plated on a normal dish to cause readhesion or plated on an MPC-coated dish to grow in suspension for 48 h. Under either plating condition, the phosphorylation level of CDCP1 was continuously increased until 24 h; however, it exhibited a sudden decrease at 48 h in adhesion culture, while it increased further in suspension culture (Fig. 3D). Notably, these dynamic changes of phosphorylation during cell suspension and readhesion appear to partially reflect the change in the expression level of CDCP1.

CDCP1 is a regulator of anoikis resistance in lung adenocarcinoma. Next, we checked whether CDCP1 is involved in the regulation of the anchorage independence of A549 cells under the control of SFK activity. For this purpose, we obtained the stable A549 cell clones miCDCP1-1 and miCDCP1-2, which showed suppressed expression of the CDCP1 protein, by using the siRNA for CDCP1 with a BLOCK-iT Pol II miR RNAi expression vector system (Fig. 4A). Both of the clones formed significantly fewer colonies in the soft-agar assay than the LacZ clones (Fig. 4B), suggesting that CDCP1 is actually required for the anchorage independence of A549 lung adenocarcinoma.

Anchorage independence may reflect the persistence of growth and/or survival of cancer cells in suspension; therefore, the effects of CDCP1 expression in suspended cells on cell proliferation and on cell apoptosis were individually examined. Each miCDCP1 clone in suspension culture showed an increased level of apoptosis compared with miLacZ clones (Fig. 4C). In contrast, no significant change in the cell growth level was observed in each of the miCDCP1 and miLacZ clones compared with the parental A549 cells in suspension culture (Fig. 4D). Importantly, there was no significant change in either cell growth or apoptosis in the adhesion culture (Fig. 4C and D).

We also examined the effect of the expression of phosphorylated CDCP1 on cell proliferation and cell apoptosis using H322 lung adenocarcinoma cells with low anchorage independence. CDCP1 (WT) and/or Fyn kinase with double HA tags at the C terminus (FynHA) were expressed in H322 cells by retroviral vectors, and the expression was checked by Western blotting (Fig. 5A). Additionally, a CDCP1 mutant lacking a putative SFK-binding site (Y734F) was also expressed (2). An increased level of phosphorylation of CDCP1 was observed in H322 cells overexpressing both WT and Fyn kinase (Fig. 5A, WT+FynHA), which caused an inhibition of apoptosis in suspension culture (Fig. 5B). These changes were not observed with either Fyn kinase or WT CDCP1 alone. On the other hand, expression of Y734F alone increased the level of apoptosis in suspension culture, suggesting a dominant-negative effect of this CDCP1 mutant (Fig. 5B, Y734F). A slight enhancement of cell proliferation in suspension culture was observed by expressing Fyn kinase and either WT or mutant CDCP1, but this change was not significant (Fig. 5C).

These results suggest that phosphorylation of CDCP1 confers anchorage independence through the inhibition of apoptosis. In other words, phosphorylation of CDCP1 regulates resistance to anoikis in lung cancer cells.

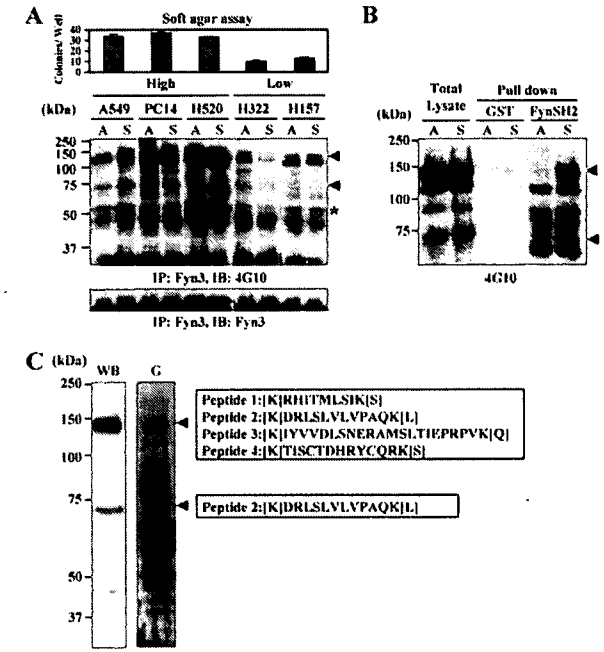

FIG. 2. Purification of phosphotyrosine-containing 135-kDa and 70-kDa protein-forming complexes with SFKs in suspension culture. (A) Anchorage independence in a series of lung cancer cell lines was examined by soft-agar assay (top). The large number of colonies formed in the lung cancer cell lines A549, PC14, and H520 (High) and the small number of colonies formed in the H322 and H157 cell lines (Low) cultured for 48 h under both adhesion and suspension conditions were collected and subjected to immunoprecipitation (IP) with anti-Fyn (Fyn3) antibody and immunoblotting (IB) with antiphosphotyrosine (4G10) antibody. Phosphotyrosine-containing proteins coimmunoprecipitated with Fyn at the molecular masses of 135 kDa and 70 kDa are indicated by arrowheads. The asterisk indicates phosphorylated Fyn. The expression of Fyn in each cell lysate was confirmed by immunoblotting (bottom). A, adhesion; S, suspension. The error bars represent standard deviations. (B) GST-FynSH2 protein generated by *Escherichia coli* was used to pull down the lysate of A549 cells cultured under adhesion or suspension conditions. The isolated samples were immunoblotted with antiphosphotyrosine (4G10) antibody. The arrowheads indicate the phosphotyrosine-containing 135-kDa and 70-kDa proteins. (C) Phosphotyrosine-containing proteins (135 kDa and 70 kDa) were purified according to the protocol described in Materials and Methods. Aliquots of the purified 135-kDa and 70-kDa phosphotyrosine-containing proteins were examined by Western blotting (WB) using antiphosphotyrosine (4G10) antibody, and the remaining samples were stained with colloidal gold total-protein stain (G). Four peptides determined by mass spectrometry (peptides 1 to 4) were identified within the sequence of CDCP1.

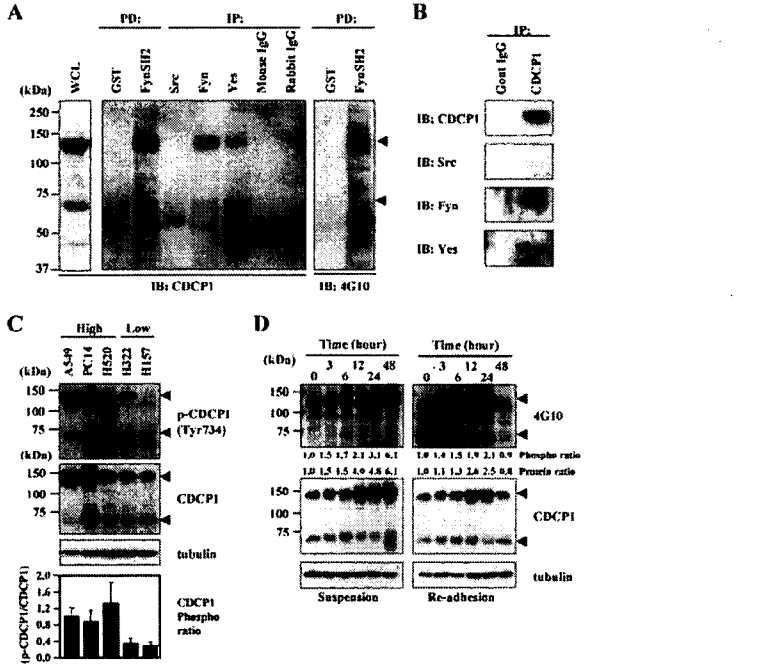

FIG. 3. Identification of the 135-kDa and 70-kDa proteins as CDCP1 and its phosphorylation associated with anchorage independence. (A) The lysate of A549 cells was subjected to whole-cell lysate (WCL) or pull-down assay with GST-FynSH2 protein (PD) or immunoprecipitated with anti-c-Src, anti-Fyn, and anti-c-Yes antibodies (IP) and immunoblotted (IB) with anti-CDCP1 antibody. The same blot was rehybridized with antiphosphotyrosine (4G10) antibody. (B) The lysate of A549 cells was immunoprecipitated with anti-CDCP1 antibody (ab1377) or goat IgG as indicated. The precipitates were subjected to immunoblotting with anti-c-Src, anti-Fyn, anti-c-Yes, and anti-CDCP1 antibodies. (C) The large number of colonies formed by the lung cancer cell lines A549, PC14, and H520 (High) and the small number of colonies formed by the H322 and H157 cell lines (Low) cultured for 48 h in the suspension condition were collected and subjected to immunoblotting with anti-phospho-CDCP1 (Tyr734) and CDCP1 antibodies. This experiment was performed three times. The ratio of the phosphorylation level in each lung adenocarcinoma cell was measured as described in Materials and Methods. The error bars represent standard deviations. (D) Time course analysis of CDCP1 expression and phosphorylation with or without cell attachment. A549 cells were reseeded on normal cell culture plates and an MPC-coated plate at a density of 1.5×10^5 cells per plate with complete medium. For the preparation of the reseeding cells, 2 mM EDTA/Hanks' balanced salt solution was used to detach the cells. For each time point, cells were collected and subjected to immunoblotting with the indicated antibody. The same membrane rehybridized with antitubulin antibody confirmed the concentration of total proteins in each lysate (tubulin). The arrowheads indicate CDCP1.

PKCδ is a signal molecule downstream of CDCP1 during anoikis resistance in lung adenocarcinoma. CDCP1 protein has been shown to bind PKCδ in a phosphorylation-dependent manner (2). PKCδ is a regulator of apoptosis, and it has been reported that the phosphorylation of PKCδ requires the activity of SFKs (37). By treatment with the SFK inhibitor PP2, both the association of PKCδ with CDCP1 and the phosphorylation of PKCδ at Tyr311 were clearly inhibited (Fig. 6A). CDCP1 (WT) and the CDCP1 protein with a point mutation at Tyr734 (Y734F) were C-terminally FLAG tagged and expressed in COS7 cells. After transfection with each plasmid, the association of the Fyn SH2 domain with WT and Y734F mutants was examined. The Fyn SH2 domain was able to pull down the WT but not the Y734F mutants (Fig. 6B, PD: Fyn SH2). The levels of tyrosine phosphorylation of Y734F mutants was much lower than that of the WT in A549 cells (Fig. 6B, IB: 4G10), suggesting that Tyr734 of CDCP1 directly binds to Fyn and that the association is essential for the phosphorylation of CDCP1. The association between CDCP1 and PKCδ was also impaired in the Y734F mutant compared with the WT, indicating that the phosphorylation of CDCP1 is required for the association.

Overexpression of Y734F in A549 cells also blocked the association between PKCδ and CDCP1 and the phosphorylation of PKCδ at Tyr311 (Fig. 6B). Moreover, treatment with CDCP1 siRNA also decreased the phosphorylation level of PKCδ (Fig. 6C). In addition, the phosphorylation level of PKCδ at Tyr311 was elevated in H322 cells by overexpressing both WT CDCP1 and Fyn kinase but not significantly with either the WT, the Y734F mutant, or Fyn kinase alone (see the supplemental material). Therefore, CDCP1 might be required for the phosphorylation of PKCδ by linking PKCδ to SFKs in a phosphorylation-dependent manner.

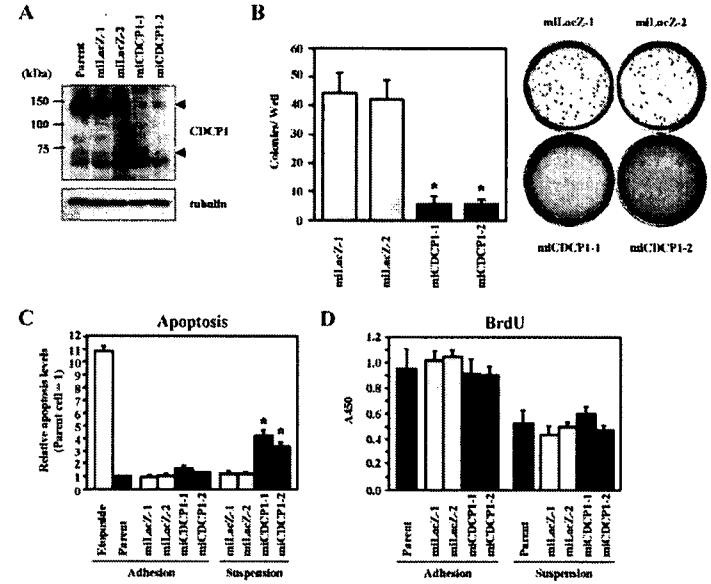

FIG. 4. CDCP1 confers anchorage independence by inhibiting apoptosis in suspended lung adenocarcinoma. (A) CDCP1-defective A549 cell clones (miCDCP1-1 and miCDCP1-2) were generated by an miR RNAi expression vector kit (Invitrogen). miLacZ-1 and miLacZ-2 were control clones. The expression of CDCP1 in each clone (1.5×10^5 cells) cultured for 24 h in an MPC-coated plate was examined by Western blotting using CDCP1 antibody. The concentration of total protein in each clone was confirmed by the same membrane rehybridized with antitubulin antibody (bottom). The arrowheads indicate CDCP1. (B) Each CDCP1-defective clone and control clone was seeded onto soft-agar plates (3×10^3 cells) (right). Colonies equal to and larger than 0.5 mm in diameter were counted after 30 days. The error bars represent standard deviations, and the asterisks indicate statistically significant differences ($P < 0.01$) (left). (C) CDCP1-defective A549 cell clones (miCDCP1-1 and -2) and control miLacZ clones (1.0×10^4 cells) were cultured in normal and MPC-coated 96-well plates. After 24 h, the cells were lysed and apoptosis was examined using a cell death ELISA kit (Roche). The total apoptotic level of A549 cells was examined by treatment with etoposide (25 μM). The relative apoptosis levels are shown as the levels of apoptosis in each clone compared with those of parental cells. In suspension culture, miCDCP1 clones exhibited an increased level of apoptosis compared with that of miLacZ clones. The error bars represent standard deviations, and the asterisks indicate statistically significant differences ($P < 0.01$). (D) Cell proliferation was determined with a cell proliferation ELISA BrdU kit (Roche). Each clone (1.0×10^4 cells) was cultured on normal and MPC-coated 96-well plates. No significant change in cell proliferation was observed in the miCDCP1 or in miLacZ clones compared with parental A549 cells with or without cell attachment. The error bars represent standard deviations.

To check whether PKCδ can regulate anoikis in lung adenocarcinoma cells, cell apoptosis caused by the suspension of miCDCP1 and miLacZ clones was examined with or without PKCδ RNAi. As shown in Fig. 6D, PKCδ RNAi increased the level of apoptosis in the control A549 cells (miLacZ) to a degree similar to that achieved by the suppression of CDCP1 expression (miCDCP1); however, no additive effect on cell apoptosis was observed by the suppression of both CDCP1 and PKCδ. Similar results were obtained from two other independent sets of siRNAs for PKCδ (data not shown). Moreover, treatment with the PKC inhibitor Rottlerin increased the level of apoptosis compared with the parental A549 cells (Fig. 6E). We also examined whether the blocking of the CDCP1-PKCδ signal pathway affects anoikis resistance in A549 cells by overexpressing the C2 domain of PKCδ, which has been shown to be responsible for the association with tyrosine-phosphorylated CDCP1 (2). The HA-tagged C2 domain of PKCδ (C2HA) expressed in A549 cells was actually associated with phosphorylated CDCP1 (Fig. 6F, upper panel) and suppressed the tyrosine phosphorylation levels of PKCδ (Fig. 6F, bottom). At the same time, overexpression of C2HA resulted in a significant increase in the level of apoptosis in suspension culture compared with a mock-transfected control, while it had no significant effect on adherent culture (Fig. 6G).

These results suggest that the CDCP1-SFK complex is required for the phosphorylation of PKCδ under suspension conditions and that PKCδ is a signal molecule for regulating anoikis resistance downstream of CDCP1 signaling.

CDCP1 affects the metastatic potential of A549 lung adenocarcinoma in vivo. Anchorage independence is thought to be an important characteristic of cancer cells that acquire metastatic potential. In order to determine the effect of CDCP1 for in vivo metastasis, miCDCP1 and miLacZ cells were injected

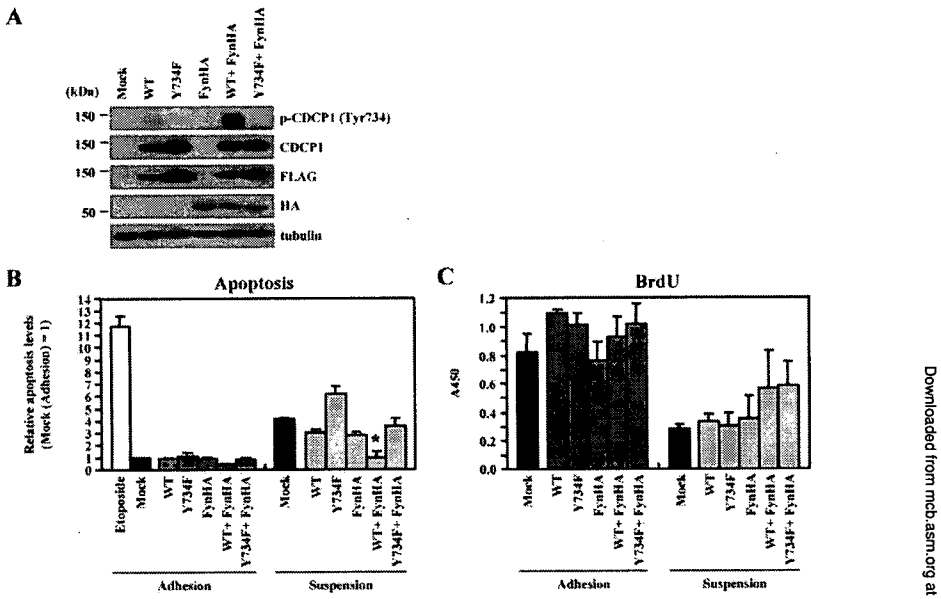

FIG. 5. Anoikis resistance was recovered by phosphorylated CDCP1 in H322 cells with low anchorage independence. (A) H322 cells that overexpressed CDCP1 (WT), a CDCP1 mutant (Y734F), and/or Fyn kinase tagged with HA (FynHA) was incubated for 24 h in MPC-coated plates. The cells were lysed and subjected to immunoblotting with the indicated antibodies. (B) Cells, as indicated (1.0×10^4 cells), were cultured in normal and MPC-coated 96-well plates. After 24 h, the cells were lysed and apoptosis was examined using a cell death ELISA kit (Roche). The total apoptotic level of mock-infected cells was examined by treatment with etoposide (25 μM). The relative apoptosis levels are shown as the levels of apoptosis in each of the cells compared with mock-infected cells in adhesion culture. The error bars represent standard deviations, and the asterisk indicates a statistically significant difference ($P < 0.05$) between mock-transfected cells and other cells in suspension culture. (C) Cell proliferation was determined with a cell proliferation ELISA BrdU kit (Roche). Each of the cells (1.0×10^4 cells) was cultured on normal and MPC-coated 96-well plates. No significant change in cell proliferation was observed in each of the cells compared with mock-infected cells with or without cell attachment (BrdU). The error bars represent standard deviations.

into the tail veins of mice and raised for 100 days. The metastatic capacity was assessed from the number of metastatic cell nodules in mouse lungs. The frequency and number of the metastatic nodules observed in the lungs of each miCDCP1 clone were much less than those found in A549 miLacZ (Fig. 7B). Additionally, H322 cells that belong to the group with low anchorage independence displayed metastasis in only one out of six mice. The average of each of the metastatic nodules and the results of metastasis for each mouse are shown in Table 1. Interestingly, no significant change in tumor growth in nude mice was observed in the miCDCP1-1 clone compared with the A549 miLacZ-1 clone (Fig. 7A). Since the metastatic assay mimics only the middle and late processes of metastasis, these results indicate that CDCP1 affects the later process in the metastasis of lung adenocarcinoma in vivo, possibly through the regulation of anchorage independence.

DISCUSSION

This study has identified CDCP1 as a crucial regulatory molecule of anoikis resistance in lung cancer cells. The signal mediated by the CDCP1-SFK complex appears to play the principal role in overcoming anoikis. CDCP1 has previously been identified as a novel epithelial tumor antigen (28) and as a tumor-associated protein preferentially expressed by highly metastatic epidermoid carcinoma (15), although little is known about the function of CDCP1 in tumor cells. Some putative functions have been suggested, such as the hypothesis that CDCP1 is a mitotic substrate of SFKs under cell cycle regulation in MDA-468 breast cancer cells (3). In this study, we found a distinct novel function of CDCP1 in tumor cells that occurs through phosphorylation by SFKs.

We found that the disruption of CDCP1 expression in A549 cells resulted in defective colony formation in soft agar, suggesting that CDCP1 affects anchorage independence (Fig. 4B). Anchorage independence is an outstanding characteristic of tumor cells, which confers the ability to grow without attachment to the extracellular matrix. Anchorage independence may come from either persistent cell growth or resistance to apoptosis in a suspension condition. As found in this study, CDCP1 does not significantly affect cell growth. A key finding here is that the loss of CDCP1 induces the apoptosis of lung

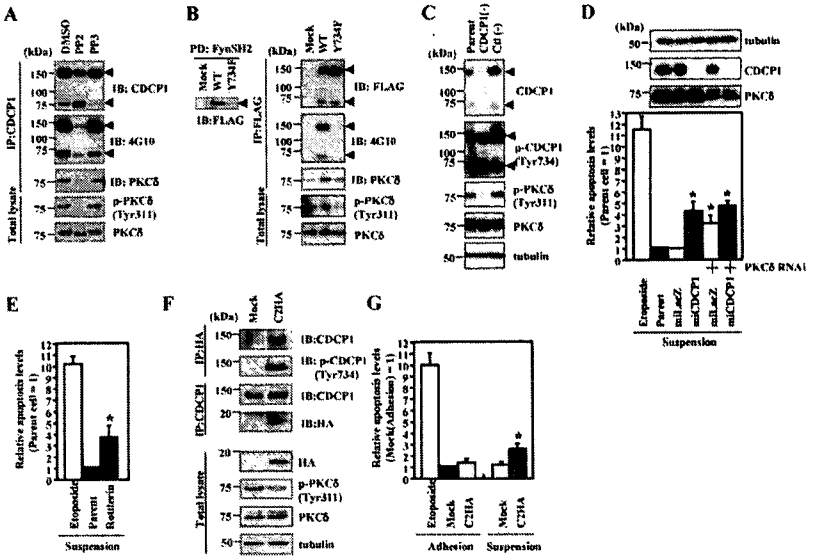

FIG. 6. PKCδ is a signaling molecule downstream of CDCP1 during anoikis resistance. (A) Treatment with the SFK inhibitor PP2 blocked the physical association between PKCδ and CDCP1 and at the same time suppressed phosphorylation of PKCδ at Tyr311. A549 cells treated with 10 μM of PP2 and 10 μM of PP3 in suspension culture were collected and subjected to immunoprecipitation with anti-CDCP1 antibody (ab1377) and immunoblotting (IB) with the indicated antibodies. The phospho-specific antibody against PKCδ (p-PKCδ [Tyr311]) total cell lysate was used to detect the phosphorylation of PKCδ, and the expression of PKCδ was also confirmed. (B) CDCP1 mutants were expressed in COS7 cells and pulled down (PD) with GST-FynSH2 protein. The samples pulled down were immunoblotted with FLAGM2 antibody (left). CDCP1 mutants were transiently transfected in A549 cells. After 24 h, cells were collected and subjected to immunoprecipitation (IP) with anti-FLAGM2 antibody. The immunoprecipitates were subjected to immunoblotting with the indicated antibodies. Each total cell lysate was used to detect the phosphorylation and the expression of PKCδ. (C) A549 cells treated with CDCP1 stealth siRNA and control siRNA were collected and subjected to immunoblotting with the indicated antibodies. (D) The effect of PKCδ on apoptosis was determined by apoptosis assay. PKCδ stealth siRNA was transiently transfected into CDCP1-defective A549 cell clones and control miLacZ clones. After 48 h, each cell clone (1.0×10^4 cells) was reseeded onto MPC-coated 96-well plates and cultured for 24 h. The cells were lysed and examined for apoptosis using a cell death ELISA kit (Roche). The total apoptotic level of A549 cells was examined by treatment with etoposide (25 μM). The relative apoptosis levels are shown as the level of apoptosis compared with the parent cells. The error bars represent standard deviations, and the asterisks indicate statistically significant differences ($P < 0.01$) between the parent and each of the other cells. Expression of CDCP1 and PKCδ was determined by Western blotting with the indicated antibodies (top). (E) The effect of PKCδ activation on apoptosis was determined by apoptosis assay. A549 cells (1.0×10^4 cells) were seeded onto MPC-coated 96-well plates and treated or not with Rottlerin (5 μM). The relative apoptosis levels after culture for 24 h are shown as the level of apoptosis compared with parent cells. The error bars represent standard deviations, and the asterisk indicates a statistically significant difference ($P < 0.01$) between the parent and Rottlerin-treated cells. (F) The C2 domain of PKCδ with the HA tag (C2HA) was expressed in A549 cells. After 24 h, cells were collected and subjected to immunoprecipitation with anti-CDCP1 (ab1377) or anti-HA antibody. Immunoprecipitates were subjected to immunoblotting with the indicated antibodies. Total cell lysate was used to detect the expression of C2HA and the phosphorylation level of endogenous PKCδ in A549 cells. (G) The cells transiently transfected with C2HA or mock vector, as indicated (1.0×10^4 cells), were cultured in normal and MPC-coated 96-well plates. After 24 h, the cells were lysed and apoptosis was examined using a cell death ELISA kit (Roche). The relative apoptosis levels are shown as the level of apoptosis in each of the cells compared with the control mock cells in adhesion culture. The error bars represent standard deviations, and the asterisk indicates a statistically significant difference ($P < 0.05$) between the mock cells and each of the other cells in suspension culture.

adenocarcinoma cells in a suspended condition but not in an adherent condition (Fig. 4C). This phenomenon strongly suggests that CDCP1 is involved in the suppression of anoikis, a form of apoptosis triggered by disruption of cell-matrix interactions.

The molecules and signaling pathways in the anoikis resistance of human cancer cells are not sufficiently understood. Previous reports have shown that oncogenes encoding, e.g., Ras, Src, and their downstream signaling molecules, such as PI 3-kinase/Akt and MAPK, are critical players in compensating for the cell survival signals derived from matrix attachment via integrins (9, 16). Inhibition of PI 3-kinase/Akt and Erk1/2 does not induce apoptosis in lung cancer cells, while SFK inhibitor causes apoptosis in these cells (32, 33). This study has revealed that the inhibition of SFKs blocked anchorage independence in lung cancer cells without affecting the phosphorylation state of PI 3-kinase/Akt, Erk1/2, or p38MAPK (Fig. 1D). These results suggest that SFKs are critical regulators of anoikis in cancer cells. On the other hand, the inhibition of SFKs was effected independently of the PI 3-kinase/Akt pathway.

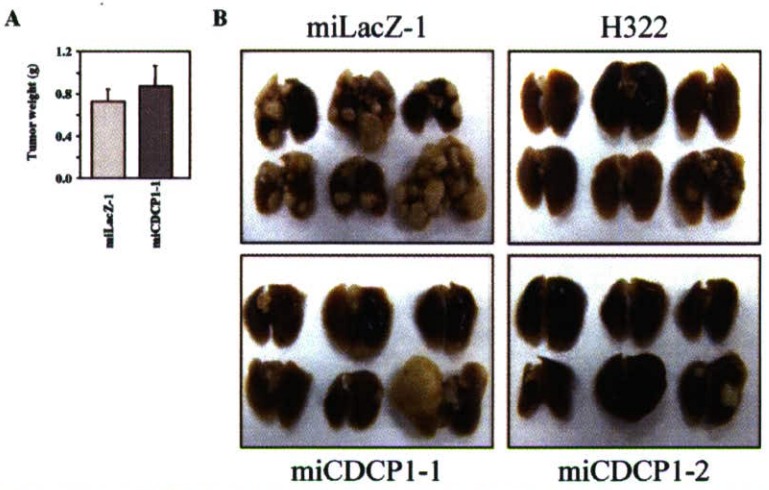

FIG. 7. Metastatic capacity of CDCP1-defective lung adenocarcinoma cells. (A) The effect of CDCP1 on tumor growth in nude mice was determined as described in Materials and Methods. The data represent the weights of tumors from the miCDCP1-1 clone or the miLacZ-1 clone ($n = 3$). The error bars indicate standard deviations. (B) The metastatic potential was evaluated from the number of metastatic cell nodules in mouse lungs after injection of tumor cells from the tail vein ($n = 6$). Lung tissues were fixed with 10% formaldehyde solution. Many metastatic nodules were observed in the control A549 miLacZ-1 clone, while fewer nodules were observed in the miCDCP1-1 and miCDCP1-2 clones and H322 cells. The number of mice with obvious lung metastasis and the average number of metastatic nodules per mouse for each cell clone are shown in Table 1.

CDCP1 is a potent substrate of SFKs within cells, and its function is likely modulated by phosphorylation of the tyrosine residues in the cytoplasmic domain (2, 3, 5). In our study, the SFK inhibitor PP2 inhibited phosphorylation of CDCP1, and at the same time, soft-agar colony formation of A549 cells was also inhibited (Fig. 1A, PP2). In fact, the level of tyrosine phosphorylation of CDCP1 is associated with the capacity for anchorage independence in lung cancer cells (Fig. 3C). Together with the observation that apoptosis of H322 cells in suspension culture was inhibited by overexpression of CDCP1 and Fyn kinase together but not CDCP1 or Fyn kinase alone, or by the Y734F mutant of CDCP1, this suggested that active SFKs confer anoikis resistance through tyrosine phosphorylation of CDCP1.

Among the SFKs, the expression of c-Src, Fyn, and c-Yes is commonly observed in human solid tumors (31). In this study, we detected the expression of c-Src, Fyn, and c-Yes in the suspension culture of A549 cells (Fig. 1B, Parent). Among these kinases, Fyn and c-Yes may regulate CDCP1-mediated cell survival in A549 cells, since these kinases are associated with CDCP1 (Fig. 3A and B), and downregulation of Fyn or c-Yes inhibits soft-agar colony formation in A549 cells (Fig. 1A). On the other hand, the amount of phosphorylated CDCP1 was either partially or remarkably reduced by Fyn or c-Yes dicer siRNA, respectively (data not shown), supporting the claim that these two members of the SFKs have a considerable effect on the phosphorylation of CDCP1. A dynamic balance of active SFK and protein tyrosine phosphatase activities regulates the phosphorylation of CDCP1 during cell attachment (5). This balance may shift when integrin signaling is shut off by cell detachment. As shown in Fig. 3D, dynamic changes in the amount of tyrosine-phosphorylated CDCP1 were also caused by changes in the expression level of CDCP1, although it is not yet clearly understood how the expression of CDCP1 is regulated by the cell detachment/attachment signal.

Benes et al. (2) recently reported that the C2 domain of PKCδ associates with phosphorylated CDCP1. Several studies have also reported on the phosphorylation of PKCδ by SFKs (19, 30), but the regulatory mechanism of PKCδ phosphorylation remains unclear. Our study found that PKCδ was remarkably phosphorylated in suspended A549 cells and also confirmed a physical association through the regulation of the phosphorylation state of CDCP1 in A549 lung adenocarcinoma cells (Fig. 6A, B, and C). Both the expression of CDCP1 and the association of CDCP1 with SFKs are required for the phosphorylation of PKCδ, which suggests that CDCP1 mediates the phosphorylation of PKCδ by SFKs. We found that an increased level of apoptosis was observed with the treatment of siRNA for PKCδ or with the PKC inhibitor Rottlerin in A549 cells in a suspension condition (Fig. 6D and E). Moreover, inhibition of the association between CDCP1 and PKCδ, by expressing the C2 domain of PKCδ, suppressed the tyrosine phosphorylation of PKCδ and increased the level of apoptosis in A549 cells in a suspension condition at the same time (Fig. 6F and G). It is speculated that CDCP1-mediated tyrosine phosphorylation and the activation of PKCδ lead to the suppression of apoptosis in A549 cells.

Tyrosine phosphorylation of PKCδ is a critical regulatory factor for PKCδ activity and results in the elevation of both tyrosine phosphorylation and the activity of PKCδ in various cells stimulated with substances such as phorbol esters, growth factors, and hormones (21, 22, 23, 27, 29). It was also reported that tyrosine phosphorylation of PKCδ by Src actually increased PKCδ activity (1, 11). On the other hand, several reports have shown that active PKCδ possesses an antiapoptotic function. For example, the activation of PKCδ by fibroblast growth factor has an antiapoptotic effect in PC12 cells (34) and a reduction of PKCδ activity by using a kinase-dead mutant of PKCδ induced apoptosis in lung cancer cells (7). Further evidence that supports PKCδ as a suppressor of apoptosis includes the requirement for active PKCδ during cell transformation mediated by insulin-like growth factor I receptor (23) and the induction of anchorage-independent growth and increased metastatic potential of breast cancer cells overexpressing PKCδ (17, 18). Our observation that tyrosine-phosphorylated PKCδ serves an antiapoptotic function in lung cancer cells supports these reports, although it appears that PKCδ has both proapoptotic and antiapoptotic functions, which are dependent on the specific circumstances and modes of action (4).

Taken together, it is strongly suggested that CDCP1 is a docking protein between SFKs and PKCδ and that CDCP1-SFK complex-dependent PKCδ phosphorylation plays a significant role in the control of anoikis resistance in lung adenocarcinoma cells. Further study is required to identify the signal downstream of tyrosine-phosphorylated PKCδ.

Finally, this study suggests that CDCP1 is a novel regulator of anoikis resistance under the control of SFKs in lung adenocarcinoma cells and that PKCδ, which is associated with and conditionally phosphorylated by the CDCP1-SFK complex, is a good candidate as a signal mediator of anoikis resistance. It was found that CDCP1 is essential in vivo for lung cancer metastasis in the mouse model (Fig. 7), indicating that CDCP1 is actually a modulator of the later processes of cancer metastasis through the regulation of anoikis. Further investigation of the specific functions of CDCP1 in normal cells and its disorders in cancer may yield important information that will help determine a clinical target for lung cancer metastasis.

TABLE 1. Effects of CDCP1 downregulation on lung cancer metastasis in vivo[a]

Cells	Metastasis[b]	No. of nodules in lung[c]
A549 miLacZ	6/6	12.8
H322	1/6	1.3
A549 miCDCP1-1	1/6	0.2
A549 miCDCP1-2	1/6	0.5

[a] Mice were sacrificed 100 days after inoculation.
[b] Data are shown as the number of mice bearing tumors in the lung/total number of mice.
[c] Average number of metastatic tumor nodules larger than 2 mm in the lung per mouse.

This work was supported by a Grant-in-Aid for Cancer Research and a Grant-in-Aid for Young Scientists by the Ministry of Education, Culture, Sports, Science and Technology of Japan, and in part by a Grant-in-Aid from the Ministry of Health, Labor and Welfare of Japan for the third-term Comprehensive 10-year Strategy for Cancer Control.

ACKNOWLEDGMENTS

We thank M. Iigo for technical assistance with the in vivo metastasis model and M. Tanaka for useful discussions (National Cancer Center Research Institute, Tokyo, Japan).

REFERENCES

1. **Benes, C., and S. P. Soltoff.** 2001. Modulation of PKCδ tyrosine phosphorylation and activity in salivary and PC-12 cells by Src kinases. Am. J. Physiol. Cell Physiol. **280:**C1498–C1510.
2. **Benes, C. H., N. Wu, A. H. Elia, T. Dharia, L. C. Cantley, and S. P. Soltoff.** 2005. The C2 domain of PKCδ is a phosphotyrosine binding domain. Cell **121:**271–280.
3. **Bhatt, A. S., H. Erdjument-Bromage, P. Tempst, C. S. Craik, and M. M. Moasser.** 2005. Adhesion signaling by a novel mitotic substrate of Src kinases. Oncogene **24:**5333–5343.
4. **Brodie, C., and P. M. Blumberg.** 2003. Regulation of cell apoptosis by protein kinase C δ. Apoptosis **8:**19–27.
5. **Brown, T. A., T. M. Yang, T. Zaitsevskaia, Y. Xia, C. A. Dunn, R. O. Sigle, B. Kundsen, and W. G. Carter.** 2004. Adhesion or plasmin regulates tyrosine phosphorylation of a novel membrane glycoprotein p80/gp140/CUB domain-containing protein 1 in epithelia. J. Biol. Chem. **279:**14772–14783.
6. **Buhring, H. J., S. Kuci, T. Conze, G. Rathke, K. Bartolovic, F. Grunebach, M. Scherl-Mostageer, T. H. Brummendorf, N. Schweifer, and R. Lammers.** 2004. CDCP1 identifies a broad spectrum of normal and malignant stem/progenitor cell subsets of hematopoietic and nonhematopoietic origin. Stem Cells **22:**334–343.
7. **Clark, A. S., K. A. West, P. M. Blumberg, and P. A. Dennis.** 2003. Altered protein kinase C (PKC) isoforms in non-small cell lung cancer cells: PKCδ promotes cellular survival and chemotherapeutic resistance. Cancer Res. **63:**780–786.
8. **Fidler, I. J., E. Gruys, M. A. Cifone, Z. Banes, and C. Bucana.** 1981. Demonstration of multiple phenotypic diversity in a murine melanoma of recent origin. J. Natl. Cancer Inst. **67:**947–956.
9. **Frisch, S. M., and H. Francis.** 1994. Disruption of epithelial cell-matrix interactions induces apoptosis. J. Cell Biol. **124:**619–626.
10. **Frisch, S. M., and R. A. Screaton.** 2001. Anoikis mechanisms. Curr. Opin. Cell Biol. **13:**555–562.
11. **Gschwendt, M., K. Kielbassa, W. Kittstein, and F. Marks.** 1994. Tyrosine phosphorylation and stimulation of protein kinase C δ from porcine spleen by src in vitro. Dependence on the activated state of protein kinase C δ. FEBS Lett. **347:**85–89.
12. **Hanahan, D., and R. A. Weiberg.** 2000. The hallmarks of cancer. Cell **100:**57–70.
13. **Hisano, C., R. Tanaka, H. Fujishima, H. Ariyama, T. Tsuchiya, T. Tatsumoto, K. Mitsugi, M. Nakamura, and S. Nakano.** 2003. Suppression of anoikis by v-Src but not by activated c-H-ras in human gallbladder epithelial cells. Cell Biol. Int. **27:**415–421.
14. **Ho, S. N., H. D. Hunt, R. M. Horton, J. K. Pullen, and L. R. Pease.** 1989. Site-direct mutagenesis by overlap extension using the polymerase chain reaction. Gene **77:**51–59.
15. **Hooper, J. D., A. Zijlstra, R. T. Aimes, H. Liang, G. F. Claassen, D. Tarin, J. E. Testa, and J. P. Quigley.** 2003. Subtractive immunization using highly metastatic human tumor cells identifies SIMA135/CDCP1, a 135 kDa cell surface phosphorylated glycoprotein antigen. Oncogene **22:**1783–1794.
16. **Khwaja, A., P. Rodriguez-Viciana, S. Wennstrom, P. H. Warne, and J. Downward.** 1997. Matrix adhesion and Ras transformation both activate a phosphoinositide 3-OH kinase and protein kinase B/Akt cellular survival pathway. EMBO J. **16:**2783–2793.
17. **Kiley, S. C., K. J. Clark, S. K. Duddy, R. D. Welch, and S. Jaken.** 1999. Increased protein kinase C δ in mammary tumor cell: relationship to transformation and metastatic progression. Oncogene **18:**6748–6757.
18. **Kiley, S. C., K. J. Clark, M. Goodnough, D. R. Welch, and S. Jaken.** 1999. Protein kinase C δ involvement in mammary tumor cell metastasis. Cancer Res. **59:**3230–3238.
19. **Kronfeld, I., G. Kazimirsky, P. S. Lorenzo, S. H. Garfield, P. M. Blumberg, and C. Brodie.** 2000. Phosphorylation of PKCδ on distinct tyrosine residues regulates specific cellular functions. J. Biol. Chem. **275:**35491–35498.
20. **Kyo, S., M. Nakamura, T. Kiyono, Y. Maida, T. Kanaya, M. Tanaka, N. Yatabe, and M. Inoue.** 2003. Successful immortalization of endometrial glandular cells with normal structural and functional characteristics. Am. J. Pathol. **163:**2259–2269.
21. **Li, W., H. Mischak, J. C. Yu, L. M. Wang, J. F. Mushinski, M. A. Heidaran, and J. H. Pierce.** 1994. Tyrosine phosphorylation of protein kinase C-delta in response to its activation. J. Biol. Chem. **269:**2349–2352.
22. **Li, W., J. C. Yu, P. Michieli, J. F. Beeler, N. Ellmore, M. A. Heidaran, and J. H. Pierce.** 1994. Stimulation of the platelet-derived growth factor beta receptor signaling pathway activates protein kinase C-delta. Mol. Cell. Biol. **14:**6727–6735.
23. **Li, W., Y. X. Jiang, J. Zhang, L. Soon, L. Flechner, V. Kapoor, J. H. Pierce,**

and L. H. Wang. 1998. Protein kinase C-δ is an important signaling molecule in insulin-like growth factor I receptor-mediated cell transformation. Mol. Cell. Biol. 18:5888–5898.
24. Michel, J. B. 2003. Anoikis in the cardiovascular system: known and unknown extracellular mediators. Arterioscler. Thromb. Vasc. Biol. 23:2146–2154.
25. Naviaux, R. K., E. Costanzi, M. Haas, and I. M. Verma. 1996. The pCL vector system: rapid production of helper-free, high-titer, recombinant retroviruses. J. Virol. 70:5701–5705.
26. Payford, M. P., and M. D. Schaller. 2004. The interplay between Src and integrins in normal and tumor biology. Oncogene 23:7928–7946.
27. Popoff, I. J., and J. P. Dean. 1999. Activation and tyrosine phosphorylation of protein kinase C delta in response to B cell antigen receptor stimulation. Mol. Immunol. 36:1005–1016.
28. Scherl-Mostageer, M., W. Sommergruber, R. Abseher, R. Hauptmann, P. Ambros, and N. Schweifer. 2001. Identification of a novel gene, CDCP1, overexpressed in human colorectal cancer. Oncogene 20:4402–4408.
29. Soltoff, S. P., and A. Toker. 1995. Carbachol, substance P, and phorbol ester promote the tyrosine phosphorylation of protein kinase C δ in salivary gland epithelial cells. J. Biol. Chem. 270:13490–13495.
30. Song, J. S., P. G. Swann, Z. Szallasi, U. Blank, P. M. Blumberg, and J. Rivera. 1998. Tyrosine phosphorylation-dependent and -independent associations of protein kinase C-δ with Src family kinase in the RBL-2H3 mast cell line: regulation of Src family kinase activity by protein kinase C-δ. Oncogene 16:3357–3368.
31. Summy, J. M., and G. E. Gallick. 2003. Src family kinases in tumor progression and metastasis. Cancer Metastasis Rev. 22:337–358.
32. Wei, L., Y. Yang, and Q. Yu. 2001. Tyrosine kinase-dependent, phosphatidylinositol 3'-kinase, and mitogen-activated protein kinase-independent signaling pathways prevent lung adenocarcinoma cells from anoikis. Cancer Res. 61:2439–2444.
33. Wei, L., Y. Yang, X. Zhang, and Q. Yu. 2004. Altered regulation of Src upon cell detachment protects human lung adenocarcinoma cells from anoikis. Oncogene 23:9052–9061.
34. Wert, M. M., and H. C. Palfrey. 2000. Divergence in the anti-apoptotic signaling pathways used by nerve growth factor and basic fibroblast growth factor (bFGF) in PC12 cells: rescue by bFGF involves protein kinase Cδ. Biochem. J. 352:175–182.
35. Windham, T. C., N. U. Parikh, D. R. Siwak, J. M. Summy, D. J. McConkey, A. J. Kraker, and G. E. Gallick. 2002. Src activation regulates anoikis in human colon tumor cell lines. Oncogene 21:7797–7807.
36. Yeatman, T. J. 2004. A renaissance for Src. Nat. Rev. Cancer 4:470–480.
37. Zhong, M., Z. Lu, and D. A. Foster. 2002. Downregulation PKCδ provides a PI3K/Akt-independent survival signal that overcomes apoptotic signals generated by c-Src overexpression. Oncogene 21:1071–1078.

Functional analysis of Src homology 3-encoding exon (exon 2) of p130Cas in primary fibroblasts derived from exon 2-specific knockout mice

Tatsuya Tazaki[1,2], Kazuko Miyazaki[1], Eiso Hiyama[3], Tetsuya Nakamoto[4], Ryuichi Sakai[5], Norimasa Yamasaki[1], Zen-ichiro Honda[6], Masaki Noda[7], Nobuyuki Miyasaka[4], Taijiro Sueda[2] and Hiroaki Honda[1,*]

[1]*Department of Developmental Biology, Research Institute for Radiation Biology and Medicine, Hiroshima University, Hiroshima 734-8553, Japan*
[2]*Department of Surgery, Graduate School of Biomedical Sciences, Hiroshima University, Hiroshima 734-8553, Japan*
[3]*Natural Science Center for Basic Research and Development, Hiroshima University, Hiroshima 734-8553, Japan*
[4]*Department of Medicine and Rheumatology, Tokyo Medical and Dental University, Tokyo, 113-8519, Japan*
[5]*Growth Factor Division, National Cancer Center Research Institute, Tokyo, 104-0045, Japan*
[6]*Department of Allergy and Rheumatology, Faculty of Medicine, Graduate School of Medicine, University of Tokyo, Tokyo 113-8655, Japan*
[7]*Department of Molecular Pharmacology, Medical Research Institute, Tokyo Medical and Dental University, Tokyo, 113-8519, Japan*

p130Cas (Cas, Crk-associated substrate) is an adaptor molecule composed of a Src homology 3 (SH3) domain, a substrate domain (SD) and a Src binding domain (SBD). The SH3 domain of Cas associates with focal adhesion kinase (FAK), but its role in cellular function has not fully been understood. To address this issue, we established and analyzed primary fibroblasts derived from mice expressing a truncated Cas lacking exon 2, which encodes the SH3 domain (Cas Δexon 2). In comparison to wild-type cells, Cas exon $2^{\Delta/\Delta}$ cells showed reduced motility, which could be due to impaired tyrosine-phosphorylation of FAK and Cas, reduced FAK/Cas/Src/CrkII binding, and also impaired localization of Cas Δexon 2 to focal adhesions on fibronectin. In addition, to analyze downstream signaling pathways regulated by Cas exon 2, we performed microarray analyses. Interestingly, we found that a deficiency of Cas exon 2 up-regulated expression of CXC Chemokine Receptor-4 and CC Chemokine Receptor-5, which may be regulated by IκBα phosphorylation. These results indicate that the SH3-encoding exon of Cas participates in cell motility, tyrosine-phosphorylation of FAK and Cas, FAK/Cas/Src/CrkII complex formation, recruitment of Cas to focal adhesions and regulation of cell motility-associated gene expression in primary fibroblasts.

Introduction

Cas is composed of an N-terminal Src homology 3 (SH3) domain, a substrate domain (SD) that consists of a cluster of Tyr-Xaa-Xaa-Pro (YXXP) motifs (one YLVP, four YQXPs, nine YDXPs and one YAVP), a C-terminal Src binding domain (SBD) and other regions (Sakai *et al.* 1994). The SH3 domain binds to the proline-rich region of various signaling molecules, such as focal adhesion kinase (FAK) (Polte & Hanks 1995), PTP-1B (Liu *et al.* 1996), PTP-PEST (Garton *et al.* 1997), C3G (Kirsch *et al.* 1998) and CIZ (Nakamoto *et al.* 2000). The SD offers docking sites for the SH2 domain of several molecules including CrkII, Nck and an inositol 5'-phophatase, SHIP2 (SH2-containing inositol 5-phosphatase) in a tyrosine-phosphorylation-dependent manner (Mayer *et al.* 1995; Schlaepfer *et al.* 1997; Prasad *et al.* 2001). The SBD is rich in proline and serves as a binding site for the SH2 and SH3 domains of Src kinase (Nakamoto *et al.* 1996).

Communicated by: Kohei Miyazono
**Correspondence:* E-mail: hhonda@hiroshima-u.ac.jp

DOI: 10.1111/j.1365-2443.2007.01156.x

Physiologically, Cas becomes tyrosine phosphorylated in response to various extracellular stimuli, such as integrin engagement (Nojima *et al.* 1995; Vuori & Ruoslahti 1995), which recruits Cas from cytoplasm to focal adhesions (Nakamoto *et al.* 1997). Tyrosine-phosphorylated Cas binds to CrkII, forming a Cas/CrkII complex (Vuori *et al.* 1996), which subsequently leads to the activation of the Rac–JNK pathway (Dolfi *et al.* 1998; Kiyokawa *et al.* 1998a). In addition, over-expression of Cas promotes cell motility, depending on its association with FAK and CrkII (Cary *et al.* 1998; Klemke *et al.* 1998).

To clarify biological roles of Cas, we generated Cas-deficient mice (Honda *et al.* 1998). Cas-deficient embryos died *in utero* at 12.5 dpc showing marked systemic congestion and growth retardation (Honda *et al.* 1998). Histologically, the heart was poorly developed and blood vessels were prominently dilated. Electron microscope analysis of the heart revealed disorganization of myofibrils and disruption of Z-disks (Honda *et al.* 1998). Cas-deficient fibroblasts showed impaired actin stress fiber formation, defects in cell migration, delayed cell spreading and resistance to Src-induced transformation (Honda *et al.* 1998, 1999). These results demonstrated that Cas is an actin-assembly molecule, which plays an essential role in embryonic development, cytoskeletal organization and Src-induced cellular transformation. Subsequently, to examine the role of each domain of Cas in these processes, we performed a compensation assay by expressing a series of Cas mutants in Cas-deficient fibroblasts (Huang *et al.* 2002). The results showed that motifs containing YDXP were indispensable for actin cytoskeleton organization and cell migration, suggesting that CrkII-mediated signaling regulates these biological processes (Huang *et al.* 2002). In contrast, C-terminal SBD was essential for cell migration, Src-induced transformation and membrane localization of Cas, but was dispensable for the organization of actin stress fibers (Huang *et al.* 2002). Although the above results provided insights in the roles of SD and SBD, the role of the SH3 domain of Cas, which has been shown to associate with various signaling molecules, remains unclear.

To address this issue, we generated mice deficient in Cas exon 2, which produce a truncated Cas protein lacking the SH3 domain. Heterozygous (Cas exon $2^{+/\Delta}$) mice, which were apparently normal, were intercrossed to produce homozygous (Cas exon $2^{\Delta/\Delta}$) mutants. Cas exon $2^{\Delta/\Delta}$ mice died *in utero* at 12.5–13.5 dpc and the detailed analysis of the embryonic lethality of the Cas exon $2^{\Delta/\Delta}$ mice is underway and will be published elsewhere. In this report, we established primary fibroblasts from Cas exon 2-deficient embryos and investigated the roles of Cas exon 2 in cellular functions.

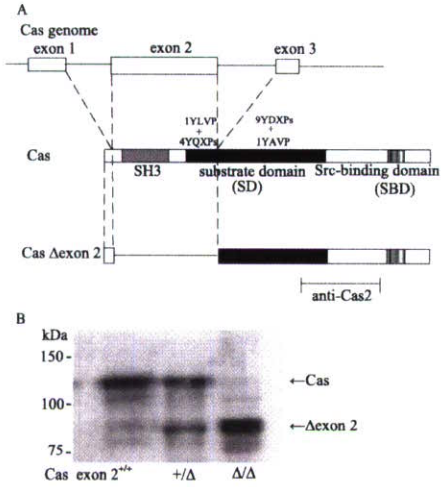

Figure 1 (A) Schematic illustration of Cas genome, Cas full-length product (Cas) and a truncated Cas protein lacking the exon 2-derived region (Cas Δexon 2). As compared to Cas, Cas Δexon 2 is deficient in the whole SH3 domain and one YLVP and four YQXP motifs. The position of the peptides for generating anti-Cas2 is also shown. (B) Western blot to detect Cas Δexon 2 protein. Thirty micrograms of cell lysates extracted from the wild-type (Cas exon $2^{+/+}$), heterozygous (Cas exon $2^{+/\Delta}$) and homozygous (Cas exon $2^{\Delta/\Delta}$) fibroblasts were separated by 7.5% SDS-PAGE, blotted to a nitrocellulose membrane and probed with 1:2000 diluted an anti-Cas antibody. Molecular weight markers are shown on the left.

Results

Cas exon $2^{\Delta/\Delta}$ cells are slower to initiate migration in the wound healing assay

To investigate functional defects caused by Cas exon 2-deficiency, we established primary fibroblasts from Cas exon 2-deficient (Cas exon $2^{\Delta/\Delta}$) embryos. Figure 1A shows the schematic diagram representing Cas Δexon 2. Cas exon 2 contains the entire SH3 domain and a part of the SD domain containing one YLVP and four YQXP motifs. It encodes 211 amino acids and the predicted molecular weight of Cas exon 2 is about 23 kDa. The expression of Cas Δexon 2 protein in Cas exon $2^{\Delta/\Delta}$ fibroblasts was detected almost as the expected size by Western blotting using an antibody against Cas, anti-Cas2 (Sakai *et al.* 1994) (Fig. 1B). Using the fibroblasts, we first performed wound healing cell migration assays. Migratory processes were assessed at 0, 3, 6, 9 and 12 h after wounding (Fig. 2A). Mean percentages of the filled area at each time points are shown in Fig. 2B. Three hours after wounding, Cas exon $2^{+/+}$ cells had filled over 30% of the gap and the cells migrating from both ends of the wound had achieved cell–cell contact. In contrast, only 10% of the area was filled by Cas exon $2^{\Delta/\Delta}$ cells. After 6 and 9 h, the migration deficit in Cas exon $2^{\Delta/\Delta}$ cells was less apparent but still present, and at 12 h the gap was almost filled in both types of the cells. This result demonstrated that Cas exon $2^{\Delta/\Delta}$ cells were deficient in ability to migrate, especially in the early phase of the response.

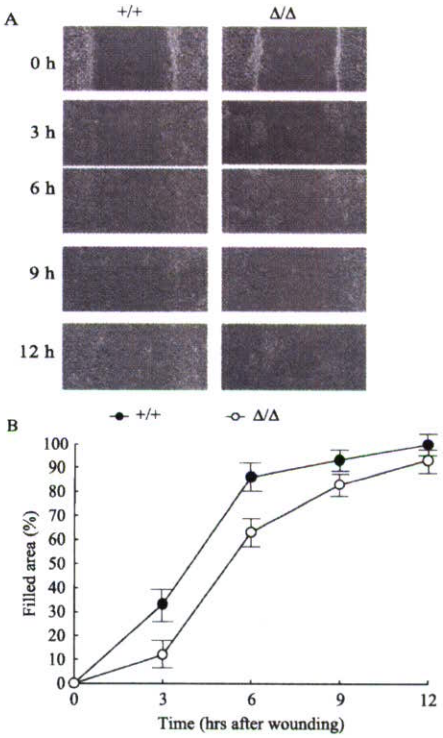

Figure 2 Delayed migration of Cas exon $2^{\Delta/\Delta}$ cells in the initial phase in the wound healing assay. (A) Photographs of Cas exon $2^{+/+}$ cells and Cas exon $2^{\Delta/\Delta}$ cells at 0, 3, 6, 9 and 12 h after wounding. Cells were first grown to confluence in plastic culture dishes, and a wound was made in the cell monolayer using a sterile micropipette tip. Cell movement was assessed 0, 3, 6, 9 and 12 h after wounding. Photographs were taken under a microscope with an objective of 100×. (B) The percentage of reduced distance between the nuclei of cells at each time period relative to the distance between two rims in the cleared field at the beginning was taken as the index (*error bars* show the standard deviation). Results presented here are representative mean values of three independent experiments.

Cas exon $2^{\Delta/\Delta}$ cells show reduced spreading activity on fibronectin (FN)

We next examined the roles of Cas exon 2 in cell attachment, cell adhesion and cell spreading on FN. The morphological changes in Cas exon $2^{+/+}$ and Cas exon $2^{\Delta/\Delta}$ cells were observed at 30, 60 and 120 min after plating on FN-coated dishes (Fig. 3A). The mean percentages of flattened cells at each time point are shown in Fig. 3B. The disparity in cell spreading was most apparent 30 min after plating, when more than 70% of the Cas exon $2^{+/+}$ cells had already flattened, while only 37% of Cas exon $2^{\Delta/\Delta}$ cells showed a flattened phenotype. The spreading delay in Cas exon $2^{\Delta/\Delta}$ cells continued and was still observed at 120 min. These results demonstrated that Cas exon $2^{\Delta/\Delta}$ cells had a reduced ability to spread on FN.

The deficiency of Cas exon 2 impaired formation of the FAK/Cas/CrkII complex, tyrosine-phosphorylation of FAK and Cas, and FAK/Src binding on FN

Upon FN stimulation, integrin clustering promotes FAK autophosphorylation at Tyr397, which creates a binding site for the SH2 domain of Src (Mitra *et al.* 2005). FAK/Src binding leads to the conformational activation of Src and results in an activated FAK/Src signaling complex (Schlaepfer *et al.* 2004), which enhances tyrosine-phosphorylation of Cas (Sakai *et al.* 1994; Mitra *et al.* 2005) Tyrosine-phosphorylated Cas binds to CrkII through the SD domain with preference for YDXP motifs (Songyang *et al.* 1993), which subsequently leads to activate downstream small GTP-binding proteins through C3G (Kiyokawa *et al.* 1998a,b; Klemke *et al.* 1998) and plays a key role in cell migration (Fig. 8A).

We then investigated whether the deficiency of Cas exon 2 might affect Cas' association with its major signaling molecules, FAK (Polte & Hanks 1995), Src (Nakamoto *et al.* 1996) and CrkII (Mayer *et al.* 1995) to which Cas binds through its SH3, SBD and SD, respectively. Protein aliquots extracted from Cas exon $2^{+/+}$ and

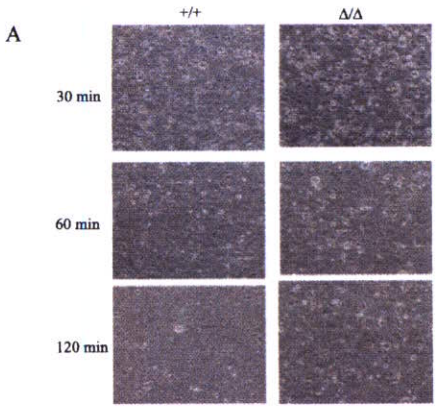

Figure 3 Reduced spreading ability of Cas exon $2^{\Delta/\Delta}$ cells on FN. (A) Photographs of Cas exon $2^{+/+}$ cells and Cas exon $2^{\Delta/\Delta}$ cells at 30, 60 and 120 min after plating on FN-coated dishes. Cells were added to FN-coated dishes and incubated at 37 °C for indicated times. Photographs were taken under a microscope with an objective of 100×. (B) Cell spreading was quantitated by calculating the percentages of spread cells (*error bars* show the standard deviation). Single cells that were phase-bright with rounded morphology were scored non-spread, whereas those that possessed a flattened shape and looked phase-dark were scored as spread. Results presented here are representative mean values of eight independent fields of three experiments.

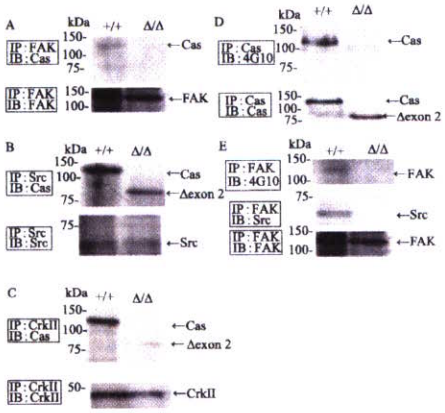

Figure 4 Impaired FAK/Cas/CrkII complex formation, tyrosine-phosphorylation of FAK and Cas, and FAK/Src binding upon FN stimulation in Cas exon $2^{\Delta/\Delta}$ cells. Serum-starved Cas exon $2^{+/+}$ cells and Cas exon $2^{\Delta/\Delta}$ cells were cultured on FN-coated dishes for 1 h, harvested and lysed with 1% Triton lysis buffer. (A) FAK immunoprecipitates (IP : FAK) were probed with anti-Cas (IB : Cas) or anti-FAK (IB : FAK). (B) Src immunoprecipitates (IP : Src) were probed with anti-Cas (IB : Cas) or anti-Src (IB : Src). (C) CrkII immunoprecipitates (IP : CrkII) were probed with anti-Cas (IB : Cas) or anti-CrkII (IB : CrkII). (D) Cas immunoprecipitates (IP : Cas) were probed with 4G10 (IB : 4G10) or anti-Cas (IB : Cas). (E) FAK immunoprecipitates (IP : FAK) were probed with 4G10 (IB : 4G10), anti-Src (IB : Src) or anti-FAK (IB : FAK).

Cas exon $2^{\Delta/\Delta}$ cells plated on FN were immunoprecipitated with antibodies against either FAK, Src or CrkII and immunoprecipitated proteins were blotted with anti-Cas2. As shown in Fig. 4A, wild-type Cas was associated with FAK, whereas Cas Δexon 2 could not bind to FAK. By contrast, Fig. 4B shows that Src bound to both Cas and Cas Δexon 2 at similar levels. We then analyzed possible alteration in CrkII binding to Cas in Cas exon $2^{\Delta/\Delta}$ cells. As shown in Fig. 4C, in Cas exon $2^{+/+}$ cells, stable complex formation of Cas and CrkII was detected, whereas in Cas exon $2^{\Delta/\Delta}$ cells, the binding activity of CrkII to Cas Δexon 2 was significantly reduced. We then analyzed whether the deficiency of Cas exon 2 might affect tyrosine-phosphorylation of Cas. As shown in Fig. 4D, Cas Δexon 2 was not tyrosine-phosphorylated upon FN stimulation. In addition, we could not detect FAK tyrosine-phosphorylation and FAK/Src binding (Fig. 4E). These results indicated that Cas exon 2-deficiency impaired formation of the FAK/Cas/CrkII complex, tyrosine-phosphorylation of FAK and Cas, and FAK/Src binding upon FN stimulation.

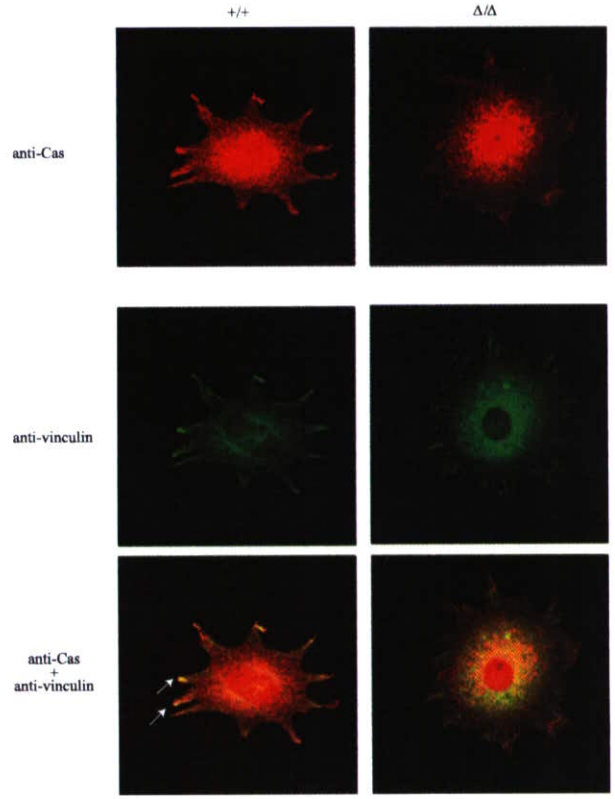

Figure 5 Cas exon 2 is required for the localization of Cas to focal adhesions upon FN stimulation. Cas exon $2^{+/+}$ and Cas exon $2^{\Delta/\Delta}$ cells grown on FN-coated coverslips were stained with anti-Cas and anti-vinculin (hVIN-1) antibodies. Texas red-labeled secondary antibody targeted the anti-Cas antibody and Fluorescein-labeled secondary antibody labeled the anti-vinculin antibody. Following FN stimulation, wild-type Cas was recruited to focal adhesions, as demonstrated by the yellow double staining pattern (left lower panel, indicated by *arrows*), whereas Cas Δexon 2 remained in the cytoplasm and did not concentrate at focal adhesions (right lower panel).

Cas exon 2 is required for the localization of Cas to focal adhesions upon FN stimulation

We compared the subcellular localization of wild-type Cas and Cas Δexon 2 in primary fibroblasts stimulated by FN. Cas exon $2^{+/+}$ and Cas exon $2^{\Delta/\Delta}$ cells grown on FN-coated coverslips were stained with an anti-Cas2. Anti-vinculin (hVIN-1) staining was also performed to identify focal adhesions. As shown in Fig. 5, following FN stimulation, wild-type Cas was recruited to focal adhesions as previously reported (Nakamoto *et al.* 1997), as demonstrated by the yellow double staining pattern (Fig. 5, left lower panel, indicated by *arrows*), whereas Cas Δexon 2 was retained mainly in the cytoplasm and was not concentrated at focal adhesions (Fig. 5, right lower panel). The results indicated that Cas exon 2 is required for the localization of Cas to focal adhesions upon FN stimulation.

The deficiency of Cas exon 2 up-regulated cell adhesion-associated genes including CXC Chemokine Receptor-4 (CXCR4), CC Chemokine Receptor-5 (CCR5) and thrombospondin 4 in primary fibroblasts

To further characterize the role of Cas exon 2 in intracellular signaling, we performed microarray analyses to investigate alterations in gene expression caused by Cas exon 2-deficiency. RNA samples extracted from Cas exon $2^{+/+}$, Cas exon $2^{\Delta/\Delta}$ and Cas exon $2^{\Delta/\Delta}$ fibroblasts

(12.5 dpc, two embryos for each genotype) were subjected to microarray analysis as described in Experimental procedures. Gene expression patterns of Cas exon $2^{\Delta/\Delta}$ fibroblasts were compared with those of Cas exon $2^{+/+}$ and Cas exon $2^{+/\Delta}$ cells. The complete microarray data set is available from the gene expression omnibus (GEO) database (accession no. GSE8357). Expressed sequence tags were excluded and genes that showed more than a 3.0-fold change in expression are presented in Table 1. One interesting aspect of the result is that cell migration- and cell adhesion-associated genes, such as chemokine ligands/receptors and thrombospondin, were listed among the genes up-regulated by Cas exon 2-deficiency. We thus confirmed the up-regulation of these genes in Cas exon $2^{\Delta/\Delta}$ fibroblasts by quantitative real-time RT-PCR analysis. The results showed that the expression levels of three genes, CXCR4, CCR5 and thrombospondin 4, were significantly enhanced by Cas exon 2-deficiency. The changes in expression measured by microarray analysis correlated well with data from quantitative real-time RT-PCR analyses (Fig. 6). These results demonstrated that the loss of Cas exon 2 induced expression of CXCR4, CCR5 and thrombospondin 4, genes involved in cell motility in primary fibroblasts.

Phospho-IκBα level was augmented in Cas exon $2^{\Delta/\Delta}$ fibroblasts

We then examined the underlying molecular mechanism for the up-regulated expression of CXCR4 and CCR5 in Cas exon $2^{\Delta/\Delta}$ fibroblasts. It is already demonstrated that the extracellular signal-activated transcription factor nuclear factor-κB (NF-κB) regulates the expression of some chemokine ligands/receptors, including CXCR4 (Helbig *et al.* 2003; Kukreja *et al.* 2005) and CCR5 (Kim *et al.* 2006). Activation of NF-κB requires phosphorylation of IκBα. Thus, we compared phospho-IκBα levels between Cas exon $2^{+/+}$ and Cas exon $2^{\Delta/\Delta}$ fibroblasts. As shown in Fig. 7, the phosphorylation level of IκBα was significantly augmented in Cas exon $2^{\Delta/\Delta}$ cells as compared to Cas exon $2^{+/+}$ cells. These results indicated that that the NF-κB signaling pathway was activated by Cas exon 2 deficiency, which would play a role in up-regulated expression of CXCR4 and CCR5 in Cas exon $2^{\Delta/\Delta}$ fibroblasts.

Discussion

Cas is an adaptor molecule implicated in various biological processes, such as cell adhesion, cell migration, cell apoptosis, cell transformation and bacterial infection (Defilippi *et al.* 2006). Structurally, Cas is an adaptor

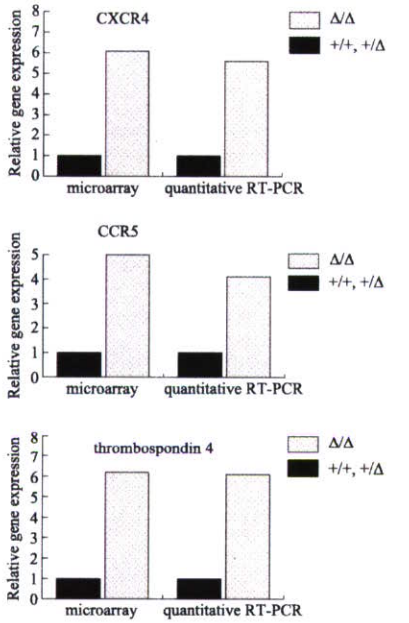

Figure 6 Up-regulated expression of CXCR4, CCR5 and thrombospondin 4 in Cas exon $2^{\Delta/\Delta}$ fibroblasts. RNA samples extracted from Cas exon $2^{+/+}$, Cas exon $2^{+/\Delta}$ and Cas exon $2^{\Delta/\Delta}$ fibroblasts (12.5 dpc, three embryos for each genotype) were used. The changes in expression levels determined by microarray (left) or quantitative real-time RT-PCR (right) are shown.

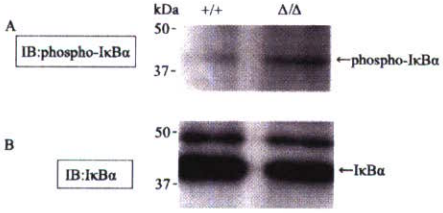

Figure 7 Increased phosphorylation of IκBα in Cas exon $2^{\Delta/\Delta}$ fibroblasts. Cas exon $2^{+/+}$ cells and Cas exon $2^{\Delta/\Delta}$ cells were harvested and lysed with 1% Triton lysis buffer. Equal amounts of total cell lysates were blotted with anti-phospho-IκBα (A) or an anti-IκBα (B).

Table 1 (A) Genes up-regulated in Cas exon $2^{\Delta/\Delta}$ fibroblasts

Fold change	Description	UniGene
46.72	Jumonji, AT rich interactive domain 1D (Rbp2 like)	Mm.262676
12.8	Chemokine (C–C motif) ligand 12	Mm.867
11.2	Killer cell lectin-like receptor, subfamily A, member 2	Mm.4783
7.812	SPARC-like 1 (mast9, hevin)	Mm.29027
6.172	Thrombospondin 4	Mm.20865
6.06	Chemokine (C–C motif) receptor 5	Mm.14302
5.988	Astrotactin 1	Mm.329586
5.714	EGF-like-domain, multiple 6	Mm.37707
5.263	Chemokine (C–C motif) ligand 3	Mm.1282
5.102	Chemokine (C–C motif) ligand 9	Mm.2271
5.025	Chemokine (C–X–C motif) receptor 4	Mm.1401
4.484	Lipoprotein lipase	Mm.1514
4.444	Carbonic anhydrase 2	Mm.1186
4.405	SLAM family member 7	Mm.164642
4.405	RAS-like, estrogen-regulated, growth-inhibitor	Mm.46233
4.149	Macrophage scavenger receptor 1	Mm.239291
4	Odd-skipped related 2 (*Drosophila*)	Mm.46336
3.984	X-linked lymphocyte-regulated 3a	Mm.195091
3.921	C-type lectin domain family 14, member a	Mm.280563
3.831	Schlafen 8	Mm.347694
3.802	Interferon activated gene 203	Mm.261270
3.623	G-protein coupled receptor 65	Mm.378924
3.584	Hepatitis A virus cellular receptor 2	Mm.72168
3.571	Sciellin	Mm.244003
3.333	Adrenomedullin receptor	Mm.2857
3.257	Matrix metalloproteinase 12	Mm.2055
3.236	Cytochrome b-245, β polypeptide	Mm.200362
3.205	Interferon, α-inducible protein 27	Mm.271275
3.195	Prostaglandin E receptor 2 (subtype EP2)	Mm.4630
3.185	Mannose receptor, C type 1	Mm.2019
3.175	Complement component 2 (within H-2S)	Mm.283217
3.155	C-type lectin domain family 4, member d	Mm.299633
3.115	Disabled homolog 2 (*Drosophila*)	Mm.240830

(B) Genes down-regulated in Cas exon $2^{\Delta/\Delta}$ fibroblasts

Fold change	Description	UniGene
−14.19	Xlr-related, meiosis regulated	Mm.14300
−14.17	Kallikrein 24	Mm.378954
−8.397	RIKEN cDNA E130012A19 gene	Mm.24506
−7.892	Vomeronasal 1 receptor, D7	Mm.160377
−7.051	RIKEN cDNA 4933413N12 gene	Mm.158581
−6.949	Probasin	Mm.8034
−6.489	Fibroblast growth factor 16	Mm.154768
−6.432	Phosphatidylinositol glycan, class H	Mm.281044
−5.785	Interleukin-1 receptor-associated kinase 4	Mm.279655
−5.717	RIKEN cDNA 4921517J23 gene	Mm.291129
−5.645	Forkhead box A1	Mm.4578
−5.54	RIKEN cDNA 4931406I20 gene	Mm.318331
−5.344	Phosphatase, orphan 1	Mm.133075
−5.058	RIKEN cDNA 1700020N01 gene	Mm.54306
−5.029	myosin, heavy polypeptide 1, skeletal muscle	Mm.340118

Continued overleaf

Table 1 *Continued*

Fold change	Description	UniGene
−4.676	Thyrotropin releasing hormone receptor	Mm.309350
−4.635	Elongation protein 4 homolog (*S. cerevisiae*)	Mm.33870
−4.213	Leukotriene A4 hydrolase	Mm.271071
−4.191	Serine dehydratase-like	Mm.5162
−4.171	Actin related protein M2	Mm.30958
−4.135	Component of Sp100-rs	Mm.362648
−4.058	RIKEN cDNA C230093N12 gene	Mm.4065
−3.843	Procollagen, type II, α1	Mm.2423
−3.734	Calcitonin receptor-like	Mm.75467
−3.528	SRY-box containing gene 10	Mm.276739
−3.46	Profilin 3	Mm.348015
−3.436	Defensin β7	Mm.207067
−3.329	Titin-cap	Mm.10762
−3.329	Melanocortin 3 receptor	Mm.57183
−3.311	Flavin containing monooxygenase 1	Mm.976
−3.271	RIKEN cDNA 2410017P07 gene	Mm.338605
−3.231	Transketolase-like 1	Mm.25057
−3.216	Expressed sequence AU041707	Mm.200898
−3.211	Chromobox homolog 1 (*Drosophila* HP1 β)	Mm.29055
−3.104	Deleted in azoospermia-like	Mm.280641
−3.045	Forkhead box G1	Mm.4704

molecule composed of SH3, SD and SBD (Fig. 1A), and exerts its biological function by interacting various intracellular molecules, such as FAK, CrkII and Src, through its different functional domains. In this paper, to primarily focus on the role of Cas SH3 in cellular function, we established and analyzed primary fibroblasts from mice that were engineered to produce truncated Cas lacking the exon 2-derived region containing the whole SH3 domain (Cas Δexon 2).

As expected from a previous study (Polte & Hanks 1995), we demonstrated that Cas Δexon 2 lost its ability to bind to FAK but retained the ability to bind to Src, irrespective of FN stimulation (Fig. 4A and B and data not shown). In addition, we found that upon FN stimulation, the binding activity of Cas Δexon 2 to CrkII was significantly reduced (Fig. 4C). This result seems curious since the YDXP motifs in the SD, that are the preferred binding site to the CrkII SH2 domain when phosphorylated (Songyang *et al.* 1993), are all conserved in Cas Δexon 2. To investigate the underlying mechanism, we analyzed tyrosine-phosphorylation of Cas between two types of cells. Upon FN stimulation, Cas was apparently tyrosine-phosphorylated in Cas exon $2^{+/+}$ cells as previously reported (Nojima *et al.* 1995), whereas we could not detect tyrosine-phosphorylation of Cas Δexon 2 in Cas exon $2^{\Delta/\Delta}$ cells (Fig. 4D). In addition, we examined tyrosine-phosphorylation of FAK, which is the primary event following integrin stimulation. Surprisingly, FAK was not tyrosine-phosphorylated in Cas exon $2^{\Delta/\Delta}$ cells (Fig. 4E). Furthermore, FAK/Src binding was not detected in Cas exon $2^{\Delta/\Delta}$ cells (Fig. 4E), probably owing to impaired tyrosine-phosphorylation of FAK. These results indicate that Cas exon 2 is essential for FAK auto-phosphorylation upon FN. This idea is in line with a previous study, in which Cas lacking SH3 failed to bind to CrkII, which subsequently abolished FAK/Cas/CrkII complex formation as well as FAK auto-phosphorylation by FN (Iwahara *et al.* 2004). The underlying mechanism for impaired tyrosine-phosphorylation of FAK in Cas exon $2^{\Delta/\Delta}$ cells remains unclear. One possibility is that the constitutive FAK/Cas binding might be essential for conformational change of FAK tyrosine-phosphorylation. Alternatively, the FAK/Cas complex formation might be required for FAK to keep the tyrosine-phosphorylated state. A previous study showed that CrkII knockdown reduces integrin-stimulated FAK Tyr397 autophosphorylation (Iwahara *et al.* 2004). Therefore, the Cas/CrkII complex may also affect tyrosine-phosphorylation of FAK as an upstream regulator in reverse (Iwahara *et al.* 2004).

We also compared the intracellular localization of Cas and Cas Δexon 2 upon FN stimulation. In contrast to Cas to be localized to focal adhesions as previously reported (Nakamoto *et al.* 1997), no clear localization of

Cas Δexon 2 at focal adhesions was found (Fig. 5). Impaired recruitment of Cas to focal adhesions following FN stimulation was reported in Src-deficient cells (Nakamoto *et al.* 1997), and Src can be regarded as a recruiting molecule of Cas to focal adhesions (Kaplan *et al.* 1995; Honda *et al.* 1999). Although Cas Δexon 2 and wild-type Cas have comparable binding abilities to bind Src (Fig. 4B), Cas Δexon 2 was not found in focal adhesions (Fig. 5), indicating that Cas exon 2 plays an essential role in the localization of Cas to focal adhesions upon FN stimulation. This idea is supported by our previous finding that Cas lacking SH3 failed to localize at focal adhesions on FN stimulation when expressed in COS-7 cells (Nakamoto *et al.* 1997). While the mechanism is not clear, one possibility is that when Cas Δexon 2 is recruited to focal adhesions by Src, FAK is not tyrosine-phosphorylated and cannot bind to Cas Δexon 2 and Src, which in turn would allow release of Cas Δexon 2 from focal adhesions. Another possibility is that the impaired FAK/Src complex leads to reduced activation of Src, which could not recruit Cas Δexon 2 to focal adhesions. It is possible that impaired tyrosine-phosphorylation of FAK and Cas leads to incomplete formation of FAK/Cas/Src/CrkII complex and impaired localization of Cas to focal adhesions, which resulted in delayed cell migration (Fig. 2) and spreading on FN (Fig. 3). A previous study using the Cas SD mutants and examining their ability to heal the wound revealed that the effective wound healing was achieved by Cas variants containing at least four of the YDXP/YAVP motifs, the major phosphorylation sites of Cas SD (Shin *et al.* 2004). Since YDXP/YAVP motifs, which serve main binding sites to CrkII, are all conserved in Cas exon $2^{\Delta/\Delta}$ cells (see Fig. 1A), it would be unlikely that the reduced motility is due to the lack of YLVP/YQXP motifs existing in exon 2. In addition, we found that the defects observed in Cas exon $2^{\Delta/\Delta}$ cells were less apparent than those in $Cas^{-/-}$ cells (Honda *et al.* 1999). The reason might be that since Cas exon $2^{\Delta/\Delta}$ cells retain the YDXP/YAVP motifs and the SBD as compared to $Cas^{-/-}$ cells, these domains would partly participate in downstream signaling. In fact, a slight amount of CrkII could bind to Cas upon FN stimulation (Fig. 4C).

To identify downstream molecules regulated by Cas exon 2, we investigated the expression profile of Cas exon $2^{\Delta/\Delta}$ fibroblasts using microarray methods (Table 1). Interestingly, we found that cell migration- and cell adhesion-associated genes, such as chemokine ligands/receptors and thrombospondin, were up-regulated by Cas exon 2 deficiency. We previously compared the expression profile of $Cas^{-/-}$ fibroblasts with that in Cas-re-expressing fibroblasts using the same methods (Nakamoto *et al.* 2002), but could not detect changes in expression of chemokine ligands/receptors and thrombospondins. Thus, the expression changes in these genes (chemokine ligands/receptors and thrombospondins) may be specifically regulated by Cas exon 2-mediated signals.

We also demonstrated that the phospho-IκBα level was augmented in Cas exon $2^{\Delta/\Delta}$ cells, indicating that the NF-κB signaling pathway was activated by Cas exon 2 deficiency (Fig. 7). Based on this result, it is conceivable that up-regulated expression of CXCR4 and CCR5 in Cas exon $2^{\Delta/\Delta}$ fibroblasts is, at least in part, dependent on IκBα phosphorylation. The mechanism underlying the activation of NF-κB signaling and up-regulated expression of CXCR4 and CCR5 is not clear. One possibility is that since the 5′-promoter region of FAK contains NF-κB binding sites, the NF-κB transcription factor might play a role in regulating FAK transcription (Golubovskaya *et al.* 2004). It would also be possible that NF-κB is activated to compensate for the impaired tyrosine-phosphorylation of FAK and FAK/Cas binding in Cas exon $2^{\Delta/\Delta}$ cells.

In summary, we demonstrated that Cas exon 2 plays an essential role in cell migration, cell spreading on FN, tyrosine-phosphorylation of FAK and Cas, FAK/Cas/Src/CrkII complex formation and recruitment of Cas to focal adhesions in primary fibroblasts. In addition, we showed that Cas exon 2-deficiency significantly up-regulated expression of CXCR4 and CCR5, molecules implicated in cell motility (Fig. 8). Our findings define the biological roles of Cas exon 2 and provide novel insights into Cas SH3 function in intracellular signaling.

Experimental procedures

Antibodies

A polyclonal antibody against Cas, anti-Cas2, was generated as previously described (Sakai *et al.* 1994). Antibodies against FAK, Src and CrkII were from Santa Cruz Biotechnology, Santa Cruz, CA. anti-phosphotyrosine antibody 4G10 was from Upstate Biotechnology, Lake Placid, NY and hVIN-1 was from Sigma, St. Louis, MO. Anti-IκBα and anti-phospho-IκBα were from Cell Signaling Technology, Danvers, MA. Anti-Fluorescein-labeled and Texas red-labeled secondary antibodies were from Invitrogen, Carlsbad, CA.

Cultivation of primary fibroblasts

Cas exon $2^{+/\Delta}$ mice were intercrossed and embryos at 12.5 dpc were collected. Heads and internal organs were used for genotyping and primary embryonic fibroblasts were isolated from the remaining of embryos and cultured in Dulbecco's modified Eagle's

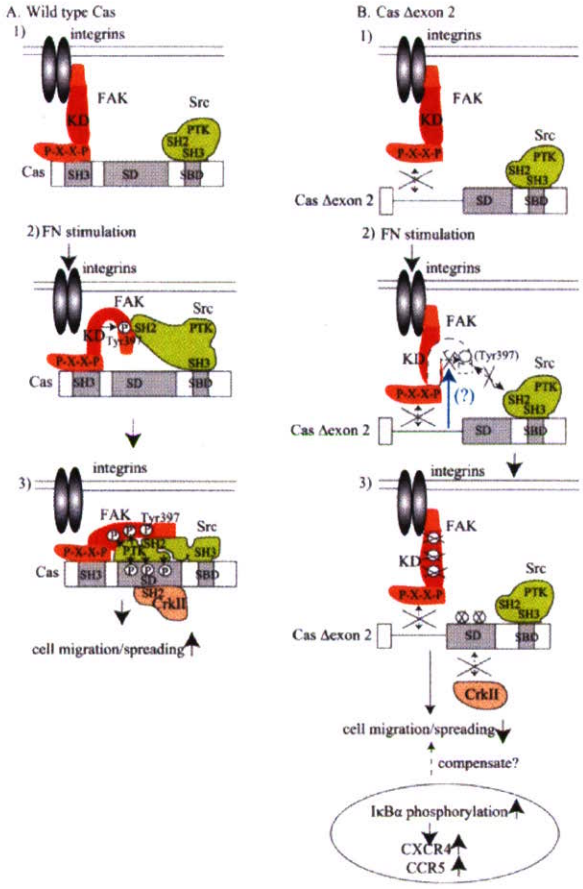

Figure 8 (A) Models for a signaling network involving wild-type Cas. (1) Cas binds to the proline-rich region of FAK through its SH3 domain and binds to the SH3 domain of Src through its Src binding domain (SBD) in unstimulated cells. (2) Upon FN stimulation, integrin clustering promotes FAK autophosphorylation at Tyr397, which creates a binding site for the SH2 domain of Src. (3) FAK/Src binding leads to the conformational activation of Src and results in an activated FAK/Src signaling complex. FAK/Cas binding and activated Src are linked to enhanced tyrosine-phosphorylation of Cas. Tyrosine-phosphorylated Cas binds to CrkII SH2 domain through the SD domain with preference for YDXP motifs and the Cas/CrkII complex plays a key role in cell migration/spreading. (B) Models for a signaling network involving Cas Δexon 2. (1) Cas Δexon 2 binds to Src but cannot bind to FAK in unstimulated cells because Cas binds to proline-rich region of FAK through its SH3 domain, which is missing from Cas Δexon 2. (2) Upon FN stimulation, FAK cannot be auto-phosphorylated by an unknown mechanism (possibly involving Cas SH3) and fails to bind to the SH2 domain of Src. Impaired FAK/Src complex leads to reduced activation of the FAK/Src signaling complex. (3) Because FAK is not tyrosine-phosphorylated and Src is not activated, Cas Δexon 2 cannot be tyrosine-phosphorylated and binding of CrkII to Cas Δexon 2 is impaired. Owing to impaired FAK/Cas/Src/CrkII complex, Cas exon 2-deficiency results in delay in cell migration/spreading. Cas exon 2-deficiency also enhances the expression of CXCR4 and CCR5, which may be dependent on IκBα phosphorylation. These factors may be up-regulated to compensate for the cellular functions affected by Cas exon 2-deficiency.

medium (DMEM) with 10% fetal bovine serum (FBS), penicillin (100 U/mL) and streptomycin (100 μg/mL) at 37 °C with 5% CO_2. Experiments were performed between three and five passages.

Immunoblotting and immunoprecipitation

Immunoblotting and immunoprecipitation were performed essentially as previously described (Huang *et al.* 2002). Proteins were extracted by lysing cells in ice-cold 1% Triton lysis buffer [50 mM Tris–HCl PH 8.0, 150 mM NaCl, 1% Triton X-100, 100 mM NaF, 1 mM Na_3VO_4]. For Western blotting, samples were separated by SDS-PAGE and probed with indicated antibodies. Positive signals were visualized with an enhanced chemiluminescence system (Amersham, Uppsala, Sweden). For immunoprecipitation, 500 μg protein aliquots were incubated with the indicated antibodies for 2 h at 4 °C and subsequently with Protein A-Sepharose (Invitrogen) for 1 h at 4 °C. Beads were washed 4 times with 1% Triton lysis buffer and boiled in sample buffer prior to SDS-PAGE analysis.

Cell stimulation with FN

Serum-starved cells were removed from the culture dishes by 0.05% trypsin treatment and were resuspended in DMEM. Culture dishes were coated overnight with 10 μg/mL FN (Chemicon, Temecula, CA) at 4 °C. The suspended cells were then plated on FN-coated dishes and incubated at 37 °C for various periods of time as described previously (Iwahara *et al.* 2004).

Wound healing cell migration assay

The wound healing cell migration assay was performed according to a method used previously (Honda *et al.* 1999). In brief, cells were first grown to confluence in plastic culture dishes, and a wound was made in the cell monolayer using a sterile micropipette tip. Then cells were washed 3 times with PBS and cultured at 37 °C in DMEM containing 10% FBS. Cell movement was assessed 3, 6, 9 and 12 h after wounding. The percentage of reduced distance between the nuclei of cells at each time period relative to the distance between two rims in the cleared field at the beginning was taken as the index.

Cell spreading assay

The cell spreading assay was performed as previously described (Honda *et al.* 1999). In brief, serum-starved cells were removed from the culture dishes by exposure to 0.05% trypsin–EDTA, and 2×10^5 cells in a volume of 1 mL DMEM were added to 35 mm tissue culture dishes coated with 10 μg/mL FN. The dishes were incubated at 37 °C for the indicated periods of time. Single cells that were phase-bright with rounded morphology were scored as non-spread, whereas those that possessed a flattened shape and looked phase-dark were scored as spread. The number of spread cells was calculated as percentage of the total cells in eight independent fields.

Immunofluorescence

Immunofluorescence was performed as previously described (Nakamoto *et al.* 1997). Cells were grown on FN-coated coverslips (Matsunami, Osaka, Japan) for 90 min. They were washed 3 times with phosphate-buffered saline (PBS) and fixed with 3.7% formaldehyde in PBS. The fixed cells were washed twice with PBS and permealized with 0.2% Triton-X in PBS. The cells were rinsed and then blocked in PBS plus 3% bovine serum albumin (Sigma). Primary antibodies were used at the following dilutions for 3 h at room temperature in a humidified chamber: 1 : 200 for anti-Cas2, and 1 : 200 for hVIN-1. The coverslips were washed 3 times with PBS and treated with secondary antibodies at the recommended dilutions. After three washes with PBS, the coverslips were mounted in a 1 : 2 mixture of glycerol and PBS. The cells were examined with a LSM5 PASCAL confocal microscopic system (Carl Zeiss, Germany).

Microarray analysis

Total RNA was extracted from primary fibroblasts using TRIzol Reagent (Invitrogen) according to the manufacturer's protocol. Two micrograms of total RNA from each sample were labeled using One-cycle Target Labeling and Control Reagents (Affymetrix, Santa Clara, CA) and hybridized with a GeneChip slide (Mouse Genome 430 2.0 Array, Affymetrix). Hybridization was performed at 45 °C for 16 h. After hybridization, slides were washed, dried and scanned using the GeneChip Scanner 3000 (Affymetrix). The array results were analyzed using GeneSpring (Agilent Technologies, Santa Clara, CA).

Quantitative real-time RT-PCR analysis

To confirm the differences in expression levels of the genes identified, we used fluorescent-based quantitative real-time RT-PCR with a TaqMan probe. RT-PCR was performed in 20 μL reaction mixtures containing 4 μL of 5 × LightCycler Taqman Master (Roche), 200 nM each primer and 100 nM Universal Probe-Library probe (Roche, Basel, Switzerland). Amplification reaction was carried out in a 384-well reaction plate in a spectrofluorimetric thermal cycler (ABI PRISM 7900 Sequence Detector, Applied Biosystems, Foster City, CA). A threshold cycle (Ct) for each sample was calculated by the point in which the fluorescence exceeded the threshold limit. To normalize the samples for loading total RNA equivalent, the second real-time PCR assay was performed targeting the 18S ribosomal RNA gene.

Acknowledgements

We thank Ikuko Fukuba for technical assistance regarding microarray and quantitative real-time RT-PCR analyses.

This work was in part supported by Grants-in Aids from the Ministry of Education, Culture, Sports, Science and Technology of Japan, from Tsuchiya Foundation, from the Astellas Foundation for Research on Metabolic Disorders, from the Ichiro Kanehara Foundation, and from Hiroshima University 21st Century Center of Excellence Program for Radiation Casualty Medical Research.

References

Cary, L.A., Han, D.C., Polte, T.R., Hanks, S.K. & Guan, J.L. (1998) Identification of p130Cas as a mediator of focal adhesion kinase-promoted cell migration. *J. Cell Biol.* **140**, 211–221.

Defilippi, P., Di Stefano, P. & Cabodi, S. (2006) p130Cas: a versatile scaffold in signaling networks. *Trends Cell Biol.* **16**, 257–263.

Dolfi, F., Garcia-Guzman, M., Ojaniemi, M., Nakamura, H., Matsuda, M. & Vuori, K. (1998) The adaptor protein Crk connects multiple cellular stimuli to the JNK signaling pathway. *Proc. Natl. Acad. Sci. USA* **95**, 15394–15399.

Garton, A.J., Burnham, M.R., Bouton, A.H. & Tonks, N.K. (1997) Association of PTP-PEST with the SH3 domain of p130cas; a novel mechanism of protein tyrosine phosphatase substrate recognition. *Oncogene* **15**, 877–885.

Golubovskaya, V., Kaur, A. & Cance, W. (2004) Cloning and characterization of the promoter region of human focal adhesion kinase gene: nuclear factor κB and p53 binding sites. *Biochim. Biophys. Acta* **1678**, 111–125.

Helbig, G., Christopherson, K.W., 2nd, Bhat-Nakshatri, P., Kumar, S., Kishimoto, H., Miller, K.D., Broxmeyer, H.E. & Nakshatri, H. (2003) NF-κB promotes breast cancer cell migration and metastasis by inducing the expression of the chemokine receptor CXCR4. *J. Biol. Chem.* **278**, 21631–21638.

Honda, H., Nakamoto, T., Sakai, R. & Hirai, H. (1999) p130Cas, an assembling molecule of actin filaments, promotes cell movement, cell migration, and cell spreading in fibroblasts. *Biochem. Biophys. Res. Commun.* **262**, 25–30.

Honda, H., Oda, H., Nakamoto, T., Honda, Z., Sakai, R., Suzuki, T., Saito, T., Nakamura, K., Nakao, K., Ishikawa, T., Katsuki, M., Yazaki, Y. & Hirai, H. (1998) Cardiovascular anomaly, impaired actin bundling and resistance to Src-induced transformation in mice lacking p130Cas. *Nat. Genet.* **19**, 361–365.

Huang, J., Hamasaki, H., Nakamoto, T., Honda, H., Hirai, H., Saito, M., Takato, T. & Sakai, R. (2002) Differential regulation of cell migration, actin stress fiber organization, and cell transformation by functional domains of Crk-associated substrate. *J. Biol. Chem.* **277**, 27265–27272.

Iwahara, T., Akagi, T., Fujitsuka, Y. & Hanafusa, H. (2004) Crk11 regulates focal adhesion kinase activation by making a complex with Crk-associated substrate, p130Cas. *Proc. Natl. Acad. Sci. USA* **101**, 17693–17698.

Kaplan, K.B., Swedlow, J.R., Morgan, D.O. & Varmus, H.E. (1995) c-Src enhances the spreading of $src^{-/-}$ fibroblasts on fibronectin by a kinase-independent mechanism. *Genes Dev.* **9**, 1505–1517.

Kim, H.K., Park, H.R., Sul, K.H., Chung, H.Y. & Chung, J. (2006) Induction of RANTES and CCR5 through NF-κB activation via MAPK pathway in aged rat gingival tissues. *Biotechnol. Lett.* **28**, 17–23.

Kirsch, K.H., Georgescu, M.M. & Hanafusa, H. (1998) Direct binding of p130Cas to the guanine nucleotide exchange factor C3G. *J. Biol. Chem.* **273**, 25673–25679.

Kiyokawa, E., Hashimoto, Y., Kobayashi, S., Sugimura, H., Kurata, T. & Matsuda, M. (1998a) Activation of Rac1 by a Crk SH3-binding protein, DOCK180. *Genes Dev.* **12**, 3331–3336.

Kiyokawa, E., Hashimoto, Y., Kurata, T., Sugimura, H. & Matsuda, M. (1998b) Evidence that DOCK180 up-regulates signals from the CrkII-p130Cas complex. *J. Biol. Chem.* **273**, 24479–24484.

Klemke, R.L., Leng, J., Molander, R., Brooks, P.C., Vuori, K. & Cheresh, D.A. (1998) CAS/Crk coupling serves as a "molecular switch" for induction of cell migration. *J. Cell Biol.* **140**, 961–972.

Kukreja, P., Abdel-Mageed, A.B., Mondal, D., Liu, K. & Agrawal, K.C. (2005) Up-regulation of CXCR4 expression in PC-3 cells by stromal-derived factor-1α (CXCL12) increases endothelial adhesion and transendothelial migration: role of MEK/ERK signaling pathway-dependent NF-κB activation. *Cancer Res.* **65**, 9891–9898.

Liu, F., Hill, D.E. & Chernoff, J. (1996) Direct binding of the proline-rich region of protein tyrosine phosphatase 1B to the Src homology 3 domain of p130Cas. *J. Biol. Chem.* **271**, 31290–31295.

Mayer, B.J., Hirai, H. & Sakai, R. (1995) Evidence that SH2 domains promote processive phosphorylation by protein-tyrosine kinases. *Curr. Biol.* **5**, 296–305.

Mitra, S.K., Hanson, D.A. & Schlaepfer, D.D. (2005) Focal adhesion kinase: in command and control of cell motility. *Nat. Rev. Mol. Cell. Biol.* **6**, 56–68.

Nakamoto, T., Sakai, R., Honda, H., Ogawa, S., Ueno, H., Suzuki, T., Aizawa, S., Yazaki, Y. & Hirai, H. (1997) Requirements for localization of p130cas to focal adhesions. *Mol. Cell. Biol.* **17**, 3884–3897.

Nakamoto, T., Sakai, R., Ozawa, K., Yazaki, Y. & Hirai, H. (1996) Direct binding of C-terminal region of p130Cas to SH2 and SH3 domains of Src kinase. *J. Biol. Chem.* **271**, 8959–8965.

Nakamoto, T., Suzuki, T., Huang, J., Matsumura, T., Seo, S., Honda, H., Sakai, R. & Hirai, H. (2002) Analysis of gene expression profile in p130Cas-deficient fibroblasts. *Biochem. Biophys. Res. Commun.* **294**, 635–641.

Nakamoto, T., Yamagata, T., Sakai, R., Ogawa, S., Honda, H., Ueno, H., Hirano, N., Yazaki, Y. & Hirai, H. (2000) CIZ, a zinc finger protein that interacts with p130cas and activates the expression of matrix metalloproteinases. *Mol. Cell. Biol.* **20**, 1649–1658.

Nojima, Y., Morino, N., Mimura, T., *et al.* (1995) Integrin-mediated cell adhesion promotes tyrosine phosphorylation of p130Cas, a Src homology 3-containing molecule having multiple Src homology 2-binding motifs. *J. Biol. Chem.* **270**, 15398–15402.

Polte, T.R. & Hanks, S.K. (1995) Interaction between focal adhesion kinase and Crk-associated tyrosine kinase substrate p130Cas. *Proc. Natl. Acad. Sci. USA* **92**, 10678–10682.

Prasad, N., Topping, R.S. & Decker, S.J. (2001) SH2-containing inositol 5′-phosphatase SHIP2 associates with the p130Cas adapter protein and regulates cellular adhesion and spreading. *Mol. Cell. Biol.* **21**, 1416–1428.

Sakai, R., Iwamatsu, A., Hirano, N., Ogawa, S., Tanaka, T., Mano, H., Yazaki, Y. & Hirai, H. (1994) A novel signaling molecule, p130, forms stable complexes *in vivo* with v-Crk and v-Src in a tyrosine phosphorylation-dependent manner. *EMBO J.* **13**, 3748–3756.

Schlaepfer, D.D., Broome, M.A. & Hunter, T. (1997) Fibronectin-stimulated signaling from a focal adhesion kinase-c-Src complex: involvement of the Grb2, p130cas, and Nck adaptor proteins. *Mol. Cell. Biol.* **17**, 1702–1713.

Schlaepfer, D.D., Mitra, S.K. & Ilic, D. (2004) Control of motile and invasive cell phenotypes by focal adhesion kinase. *Biochim. Biophys. Acta* **1692**, 77–102.

Shin, N.Y., Dise, R.S., Schneider-Mergener, J., Ritchie, M.D., Kilkenny, D.M. & Hanks, S.K. (2004) Subsets of the major tyrosine phosphorylation sites in Crk-associated substrate (CAS) are sufficient to promote cell migration. *J. Biol. Chem.* **279**, 38331–38337.

Songyang, Z., Shoelson, S.E., Chaudhuri, M., *et al.* (1993) SH2 domains recognize specific phosphopeptide sequences. *Cell* **72**, 767–778.

Vuori, K., Hirai, H., Aizawa, S. & Ruoslahti, E. (1996) Introduction of p130cas signaling complex formation upon integrin-mediated cell adhesion: a role for Src family kinases. *Mol. Cell. Biol.* **16**, 2606–2613.

Vuori, K. & Ruoslahti, E. (1995) Tyrosine phosphorylation of p130Cas and cortactin accompanies integrin-mediated cell adhesion to extracellular matrix. *J. Biol. Chem.* **270**, 22259–22262.

Received: 24 August 2007
Accepted: 6 November 2007

Mol Cancer Res (in press)

Hyperphosphorylated cortactin in cancer cells plays an inhibitory role in cell motility by regulating tyrosine phosphorylation of p130Cas

Running title: hyperphosphorylated cortactin inhibits cell motility

Lin Jia, Takamasa Uekita and Ryuichi Sakai*

Growth Factor Division, National Cancer Center Research Institute, Tokyo, Japan.

*Address correspondence to:
(To whom correspondence should be addressed):
Ryuichi Sakai
E-mail: rsakai@gan2.res.ncc.go.jp
Growth Factor Division
National Cancer Center Research Institute
5-1-1 Tsukiji, Chuo-ku, Tokyo, 104-0045, Japan
Tel: +81-3-3542-5247 Fax: +81-3-3542-8170

Abstract

Cortactin is frequently overexpressed in cancer cells, and changes of the levels of its tyrosine phosphorylation have been observed in several cancer cells. However, how the expression level and phosphorylation state of cortactin would influence the ultimate cellular function of cancer cells is unknown. In this study, we analyzed the role cortactin in gastric and breast cancer cell lines using RNA interference technique, and found that knockdown of cortactin inhibited cell migration in a subset of gastric cancer cells with a lower level of its tyrosine phosphorylation, whereas it greatly enhanced cell migration and increased tyrosine phosphorylation of p130Cas in other subsets of cells with hyperphosphorylated cortactin. Consistent results were obtained when hyperphosphorylation of cortactin was induced in MCF7 breast cancer cells by expressing Fyn tyrosine kinase. Additionally, immunostaining analysis demonstrated that knockdown of hyperphosphorylated cortactin resulted in recruitment of p130Cas to focal adhesions. These results suggest that cortactin hyperphosphorylation suppresses cell migration possibly through the inhibition of membrane localization and tyrosine phosphorylation of p130Cas.

Keywords: tyrosine phosphorylation, cortactin, p130Cas, small interfering RNA (siRNA), Fyn kinase and cell motility.

Introduction

Protein phosphorylation by tyrosine kinases functions as a major switch in cellular biological signaling events through modulating protein-protein interaction and protein conformation. Substrates of Src family kinases (SFKs) play essential roles in various cellular events by mediating tyrosine phosphorylation-dependent signals. Since cortactin was originally identified as a v-Src substrate, it has been shown to play a critical role in the organization of the cytoskeleton (1). The cortactin gene *EMS1* is located on chromosome 11q13, a region amplified in several cancers such as head and neck squamous carcinoma and breast cancer, (2-6). Cortactin is a modular protein that contains several motifs and domains involved in protein-protein interactions. An N-terminal acidic domain mediates its binding to Arp2/3, which regulates actin assembly, followed by an adjacency of six-and-a-half tandem repeats of 37 amino acids called cortactin repeats domain. There is a proline-rich domain immediately upstream of the SH3 domain, which also contains tyrosine residues phosphorylated by Src family kinases (7, 8). At the carboxyl terminus, there is a Src homology 3 (SH3) domain binding to several proteins including cortactin binding protein1 (CortBP1/Shank2) (9) and N-WASP (10). Cortactin is a substrate of tyrosine kinases including SFKs, Fer and Syk (11-13), and of serine/threonine kinases including Erk and PAK (14, 15). Among the Src family, Fyn kinase seems to play a specific role in the cortactin function in some tumors, since highly